ADVANCED MASTERS IN STRUCTURAL ANALYSIS
OF MONUMENTS AND HISTORICAL CONSTRUCTIONS

Master's Thesis

Larisa Garcia Ramonda

Dynamic procedures to estimate the axial force in historical ties

This Masters Course has been funded with support from the European Commission. This publication reflects the views only of the author, and the Commission cannot be held responsible for any use which may be made of the information contained therein.

Italy | 2015

DECLARATION

Name: Larisa Garcia Ramonda

Email: larisagarciar@gmail.com

Title of the Msc Dissertation: Dynamic procedures to estimate the axial force in historical ties

Supervisor(s): Francesca Da Porto

Elvis Cescatti

Year: 2015

I hereby declare that all information in this document has been obtained and presented in accordance with academic rules and ethical conduct. I also declare that, as required by these rules and conduct, I have fully cited and referenced all material and results that are not original to this work.

I hereby declare that the MSc Consortium responsible for the Advanced Masters in Structural Analysis of Monuments and Historical Constructions is allowed to store and make available electronically the present MSc Dissertation.

University: University of Padova

Date: 22nd of July 2015

Signature:

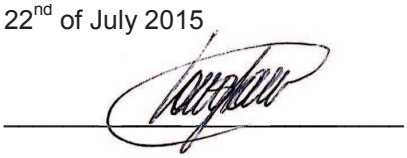

…para mamá y papá

sin ellos no hubiese sido posible

ACKNOWLEDGEMENTS

I would like to express my most sincere appreciation for all the people that help me and encourage me during the Master, specially, professor Pere Roca and Luca Pelà of University of Catalonia for all their guidance and support during the coursework and final project. I appreciate their time and patience to impart their knowledge and transmit me their passion for the conservation of our heritage. I am delight to have been able to spend my coursework learning from such remarkable professors.
To the professors from the University of Catalonia, University of Minho, University of Padova and Czech Technical University for their time and dedication during the different modules of the Master.

I would like to thanks my supervisor Prof. Eng. Francesca Da Porto for giving me the opportunity to work with her in this interesting topic and increase my interest in the field of historical preservation, and to Eng. Elvis Cescatti for all his help, guidance, support and encouragement, without him this thesis would not have been possible.

Also to the University of Padova for the facilities provided during the development of the Thesis, and the staff of the laboratory of the University for their help and suggestions during the performance of the tests. Moreover I would like to thanks Elisa Trovò for her constant presence and diligence regarding the organization of the Thesis.

I would like to thanks the Master Consortium for the scholarship, it meant a great opportunity for my personal and professional life to be able to pursuit this Master.

To all my colleagues and wonderful people I met in the SAHC Master, for their friendship, constant support and companion that made the Master one of the most rewarding experiences. I learnt a lot from all of you.

Finally, to my family without them and their support this would not have been possible at all. The biggest thanks are for my parents, Susana and Norberto, for allowing me to pursuit my dreams, for their support and affection from the distance during all this year away.

Larisa Garcia Ramonda

ABSTRACT

Tie-rods have been, for quite some time, one of the most used intervention technique to counteract the unbalanced thrust in masonry arches and vaults and also contribute to the equilibrium of the structure as a whole. In order to carry out a proper restoration, develop a monitoring plan or perform a structural strengthening of ancient buildings, it is of high importance the accurate identification of the tensile forces acting on these tie-rods.

The present work collects the research carried out until now on the field of conservation of historical ties by the University of Padova, and it summarizes the different dynamic methodologies developed in the last years. The principal aim of the thesis is the improvement of the non-destructive tests carried out on site, by means of dynamic tests, to determine the axial force on ties in a reliable and expeditious way. To achieve this goal several dynamic method were tested on the tie Database, in order to determine the analytical models that meet the requirements.

To validate such analytical model, in terms of accuracy and performance, a series of laboratory tests were planned and dynamic and statics approaches were performed. The test involved four load steps and six different boundary conditions. The results from both typologies of tests, static and dynamic, were used to calibrate a Finite Element Model, and have determined the accuracy of the method developed by Tullini & Laudiero, 2008. The static experimental campaign led to the calibration of the finite element regarding the boundary conditions, since it helps the identification of the stiffness of the end supports.

The work has a second aim that involves the study of a methodology for onsite tests that can be prove to be reliable and simple, reducing the equipment needed and time consumption of the test set up. From the case studies previously performed in the framework of this research and the experimental campaign carried out during the thesis, it is proposed a method based on the methodology suggested by Tullini & Laudiero but with the hypothesis of a symmetrical tie and boundary conditions. This methodology requires the set up of only two sensors and it works for any boundary conditions, since the spectrum analyzed involved more than 60 case studies. The studies performed on the methodology reveals that the error induced by the symmetry hypothesis is not bigger than the one measured for the estimation with three sensors.

RIASSUNTO

Titolo della tesi:"Procedure dinamiche per la determinazione della forza assiale in catene metalliche storiche"

Le catene metalliche sono state per molto tempo uno dei metodi più usati per contrastare la spinta di archi e volte in muratura, contribuendo anche all'equilibrio della struttura. Riveste un ruolo di primaria importanza la identificazione della forza di assiale agente nelle catene. Tale conoscenza è fondamentale per un adeguato intervento di restauro, la definizione di un piano di monitoraggio o per la realizzazione di rinforzi strutturali di edifici storici.

La tesi riporta i risultati delle ricerche condotte fino ad ora presso l'Università degli Studi di Padova nell'ambito della conservazione di catene metalliche storiche e riassume i diversi metodi dinamici sviluppati negli ultimi anni. Il principale obbiettivo della tesi è di definire la forza assiale nelle catene metalliche con un metodo affidabile e veloce. Al fine di raggiungere tale risultato, numerosi test dinamici sono stati effettuati sui dati raccolti in un precedente Databese, determinando modelli analitici che corrispondessero ai requisiti imposti.

Per convalidare il modello analitico, in termini di accuratezza e risposta, diversi test di laboratorio sono stati condotti seguendo entrambi gli approcci: statico e dinamico. Il singolo test si compone di quattro step di carico e sei diverse condizioni al contorno. I risultati emersi da ambo gli approcci sono stati impiegati per calibrare un modello agli elementi finiti. Il modello così definito ha verificato l'accuratezza del metodo di Tullini & Loudiero del 2008. La prova sperimentale statica ha portato alla calibrazione di un modello agli elementi finiti con riferimento alle condizioni di vincolo, dal momento che comporta la identificazione della rigidezza dei vincoli estremi.

Il secondo obbiettivo della tesi si concentra sullo studio di una metodologia sfruttabile per test in-situ, che può sia affidabile e semplice, riducendo il materiale di lavoro necessario e il tempo impiegato per il set up del test. Partendo dagli studi precedentemente condotti nelle campagne di laboratorio, si propone una applicazione basata sulla metodologia proposta da Tullini & Laudiero ma considerando ipotesi di simmetria della catena e delle condizioni di vincolo. La metodologia richiede l'applicazione di solo due sensori ed è applicabile a qualsiasi condizione di vincolo, dal momento che lo spettro analizzato è costituito da più di 60 casi studio. Gli studi relativi a tale metodo applicativo hanno rivelato che l'errore indotto dalle ipotesi di simmetria non è più alto di quello misurato con una stima a tre sensori.

RESUMEN

Titulo de la Tesis: "Procedimientos dinámicos para la estimación de la carga axial de tirantes históricos"

Los tirantes has sido por largo tiempo la técnica de conservación más utilizada para contrarrestar las líneas de presión desequilibras debido a la presencia de arcos y bóvedas de fabrica, de igual manera han contribuido a la estabilidad estructural conjunta del edificio. En el campo de la conservación cuando debe ser realizado un plan de restauración, monitoreo o refuerzo de dichos tirante o del edificio en el cual se encuentran, es de vital importancia la identificación precisa de la fuerza axial que está solicitando a los tirantes.

El presente trabajo expone los resultados de la investigación realizada en el campo de la conservación de tirantes históricos en la Universidad de Padova. Y además resume las diferentes técnicas dinámicas, desarrolladas en los últimos años, para dar respuesta a la necesidad de conocer el estado tensional de los tirantes. El objetivo principal de la presente tesis es la mejora de los test no destructivos utilizados en el campo de trabajo para estimar, con métodos dinámicos, la fuerza axial actuante en el tirante de manera confiable y expeditiva. El primer paso para alcanzar dicho objetivo fue la comprobación de los distintos métodos dinámicos haciendo uso de una base de datos de tirantes, que permitió la selección de los métodos que cumplían con los requerimientos de precisión y simplicidad.

Para validar el modelo analítico, en términos de confiablidad y performance, se llevaron a cabo una serie de pruebas de laboratorio Dichas pruebas, tanto estáticas como dinámicas, involucraron la evaluación de distintos estados de carga y condiciones de vínculos. Los resultados del laboratorio fueron utilizados para calibrar el modelo de Elementos Finitos, y determinaron la validez y utilidad del método propuesto por Tullini & Laudiero, 2008. Al mismo tiempo, el desarrollo de pruebas estáticas durante el laboratorio permitió la calibración de la rigidez de las condiciones de vinculo.

El trabajo presenta, además, un segundo objetivo, un poco más ambicioso, que involucra el estudio de una metodología para pruebas de campo que se caracterice por ser simple, confiable y expeditivo reduciendo el tiempo y esfuerzo necesario para llevar a cabo la recolección de datos. Contando con los casos de estudios previamente investigados en el marco de la investigación y los casos de estudios obtenidos en la campaña experimental de la presente tesis, se propone una metodología basada en la técnica de Tullini & Laudiero pero añadiendo como prima la hipótesis de simetría, no solo del tirante sino que también de los vínculos. Debido a la simetría, la metodología solo requiere del uso de dos sensores y puede ser aplicado para cualquier tipo de condición de vínculo ya que más de 60 casos reales fueron abarcados en el estudio, con resultados positivos. Finalmente la propuesta revela que el error cometido por la hipótesis de simetría seria solo un poco mayor que el error que se obtiene con tres sensores.

TABLE OF CONTENTS

LIST OF FIGURES

LIST OF TABLES

1. INTRODUCTION

Ties are presented in many building of different times and typologies. Many factors have a negative impact on them, and the damage, due to the pass of time and exposition to a variety of climate conditions that are likely to corrode the tie, lead to a loss of the tension to which the ties were design to absorb at the beginning. The loss of tension is worsened by the fact that the strength of the ancient ties does not present high values due to the ancient metallurgy techniques.

In order to carry out a proper restoration as well as a monitoring and structural strengthening of ancient buildings it is of high importance the accurate estimation of the tensile forces acting on these tie-rods.

On site testing should be carried out to obtained that estimation, and there are many variable that has to be define, and most of the time this variables turn out to be unknowns. Among these unknowns the most important and relevant to define are the boundary conditions, which depend mainly on how the tie is attached to the walls, pillars or columns, and the hypothesis of the boundary condition would define the stiffness of the end supports. Secondly there are the mechanical and geometrical unknowns involving mainly the real length of the tie, which again is related to the boundary condition of the tie, and the cross sections that normally are far from being regular. Nevertheless these characteristics can be easily assessed. In third place it has to be defined the type of test that should be performed, meaning if it should be a static or dynamic test.

The dynamic methods present the advantage of being simpler from the point of view of the equipment setting and the onsite performance. For this reason, several dynamic methods were developed in the last few years, trying to deal with the main unknown that is the boundary conditions. However simpler the dynamic method may seems to be, when the location of the tie does not allow an easy access, mainly due to its height, a method that involves not only a few equipment but present a simpler set up is required.

Until few year ago, the estimation of the axial force was solved by the vibration cords theory, making use of the first natural frequency measured on the tie. However, the simplicity of the method present a main drawback that is the neglect of the stiffness of the tie, which at the end leads to the hypothesis of two extremes boundary conditions, hinged or fixed. The values obtained for such two extremes gives as results very different values of axial force, more than 100% as established by *Facchini, 2003*[1].

Therefore, in the framework of an ongoing research on ties and its response, it is of great interest the development of a method that allow an economic, reliable and expeditious onsite dynamic testing involving only a few sensors, which would allow the estimation of the axial tie with a low error.

The present thesis would continue the work, carried out by the University of Padova, which started with the construction of a tie database and the first testing of the dynamic models

1.1 Goals and methodology

The present work aims to improve the methodology of the non-destructive test, and corresponding analytical tools for their calculation, performed onsite to determine the axial value at which the historical ties are subjected to. Moreover, the end goal is to propose a methodology that allows a simpler, but reliable, and expeditious estimation of the axial force.

Based on the information collected from the former work done at UNIPD on the topic, plus the research carried out on the literature available on dynamic and static techniques proposed in the last few years, the analytical methods that would present a satisfying performance on the cases gathered in the tie database.

The numerical models would be analyzed for different scenarios of tie geometry, load and boundary conditions, and their results of each method would be discuss in accordance to their reliability, accuracy and its expeditious performance.

The analytical model would be validated with experimental data acquire from the laboratory test, which would involved the testing of the tie by dynamic and static methods. Moreover the experimental data would allow the calibration of a FEM model based on the set up of the test, so to simulate more cases without the experimentation phase.

1.2 Organization of the thesis

The thesis is organized in seven chapters:
***Chapter 1*:** Introduction to the thesis topic, and definition of the main objectives and the methodology followed to carry out the work.

***Chapter 2*:** Collects the research carried out until now on the field of conservation of historical ties by the University of Padova, Database construction, and it summarizes the different dynamic methodologies developed in the last years to estimate the axial force on historical ties. Contains also the qualitative evaluation of each methodology studied.

Chapter 3: Introduces the onsite tests carried out to clearly define the main issues faced when performing the test and establish the improvements needed and what is expected from a simplified methodology. Also contains the evaluation of the analytical model of Tullini, Rebecchi and Luong.

Chapter 4: Presents the experimental tests carried out in the laboratory for a tie rod specimen for different load steps and boundary conditions. The experimental results are compared with the analytical and numerical results.

Chapter 5: Analysis of the results obtained from the static and dynamic tests performed. A schematic representation of the outline of this particular chapter is illustrated as following:

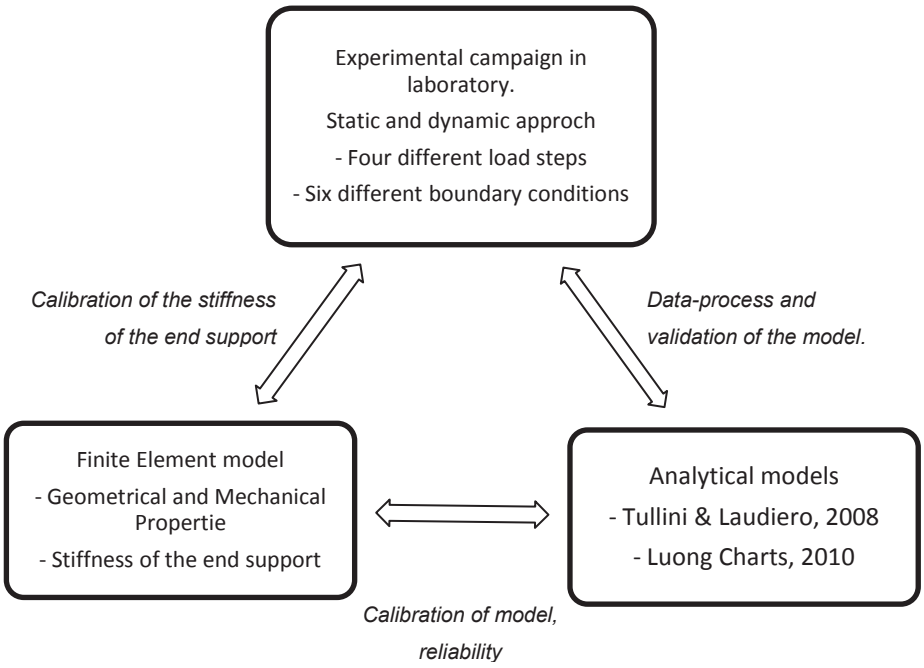

Chapter 6: Presents the proposal for a simplified methodology to estimate the axial force with only two sensors.

Chapter 7: Conclusions and recommendations of the thesis.

2. THE STATE OF ART

2.1 Function of the tie

The use of metal tie-rods represents a simple, old and widespread intervention technique, mostly used to control and counteract the horizontal thrust as a result of permanents loads, due to the presence of arches, vaults and roof, environmental loads, such as earthquakes or wind action. They are particularly suitable in the cases of not effective connection between walls or between walls and floors. The tie-rod is one of the most used methods for consolidation of structures due to its minimum intervention in the structure, its low cost and easy execution.

The methodology consists on the setting of a structural slender element in relation to its cross section, subjected to traction forces, and is at both ends anchors to the wall. It can be said that the stability of the whole system, and therefore its efficiency, is link in the first place to the stability of the supports.

The action of the tie-rods, it is substantially entrusted only to two basic elements, constituting the system as a whole, these elements are represented, firstly, by the bar and secondly by the two anchors on the extremes of the tie rod, the anchorage of the ties to the walls or pillars is guaranteed by metal or concrete end plate that allows the pre-stressing of the bars. The anchorage has the role of containing or restraining the movements, potential or actual, that the walls would have as a consequence of the instability. The stability and, therefore, the balance of the system, will depend, in their mutual cooperation to cancel the active forces exerted by the walls and of those of reaction arisen on the tie-rods. The shape and complexity of the components of the tie rods and anchors, materials used, and the application systems, will depend on the conditions of the registered tensional state of the structures, the characteristics of the instability and the demands of restorative order. In relation to the different factors and different situations, it can be taken different types of tie-rods and anchors.

2.1.1 Counteract the thrust

The ties are most frequently use in the case of horizontal thrust generated due to the presence of a vault or an arch, very well known by past manufacturers that in more than one occasion experienced the benefits, first as provisional elements, subsequently as means of consolidation in the absorption of thrust and, finally, as a real structural part as a contribution of static order. To resolve this problem of stability, since ancient times, it is implemented interventions such as the extension of the wall section of the upright, the construction of localized buttresses or the insertion of tie rods, of wood or metal.

It is recalled that the deformations which are subject vaults or arches and, similarly, although in a more complex way the domes, are substantially attributable to two factors, on one hand to the possible instability of the supports or of the piers, and on the other hand the instability of the arch itself. It is not uncommon, in particular conditions; both conditions contribute to the overall deformation of the structural system.

In the first case, depending on the motion of the piers, the structure will suffer a stretching or shrinkage meaning that the arch would get depressed or raising, involving, in this variation all or some of the parts of the arch, from the haunches to the key. If it is followed the curve of the pressures described along the width of the arc, it would be seen a variation with respect to the original configuration. If the variation, remains within the central core of inertia it could be said that the deformation of the supports will have only led to a change of configuration, somehow compensated by the intrinsic ability of the arc to redistribute the tension. If this does not happen, it will be necessary to intervene before the balance, become unstable and precarious.

In the second case, again, despite the stability of the supports, the constitution does not allow original arc to face the causes that bring into question the structure. The thickness of the arch in relation to the operating loads or the crushing of the mortars which connect the segments, are some of the causes that can configure a deformation of the arch and the vault. Even in this case, as seen above, the arch will be subject to the variation of the curve of the pressures to which its resistant section decreases offering narrower spaces to the correct transit of the tension.

Worth a consideration of the two opposite situations and emblematic: the first examines a classic configuration where the arc suffers a deformation of the key stone, a depression, and an elevation of the haunches; the second, in the same way, is the case in which the haunches suffer from an horizontal turn which results in its depression and the corresponding raising of the key stone, as shown in Fig. 1

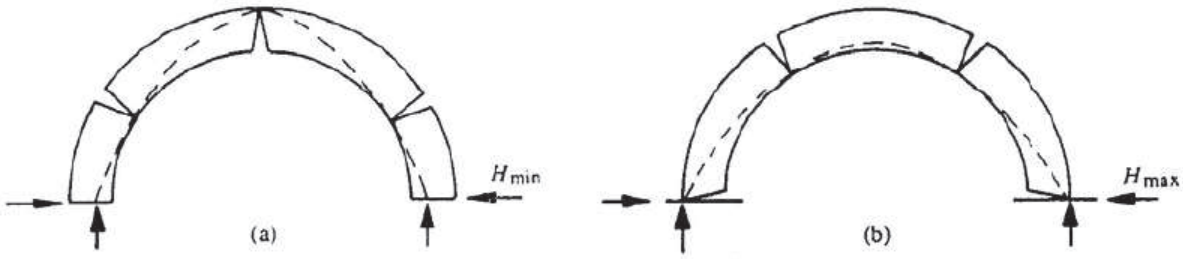

Fig. 1 – Semicircular arch under selfweight - (a) Minimum thrust, depression of the key stone (b) Maximum thrust, rising of the key stone. - Heyman, 1995[2]

The development of the arc deformation could be stopped, as a result of the rebalancing of the curve of pressure induced by the application of tie-rods. By this means the arch transmit only the vertical load to the supports (pier, columns or walls).

The tie-rods should be located in the closest plane to the action of thrust, which is at one third of the haunches, however, in some particular cases, due to aesthetical issues or uses, are placed on the infill of the arches, as shown in Fig. 2 and Fig. 3. It is important to highlight that this disposition is not efficient as the previous one. In fact, the pressure is compensated H horizontally from a force that is

working in a higher level in the masonry pier and then induces a significant bending moment at least in the area between the two units. As a way to improve the effectiveness of the latter condition, the tie can be connected with a turnbuckle to the tie descending towards the working plane and secured to the absorption and transmission of the thrust as seen in Fig. 4

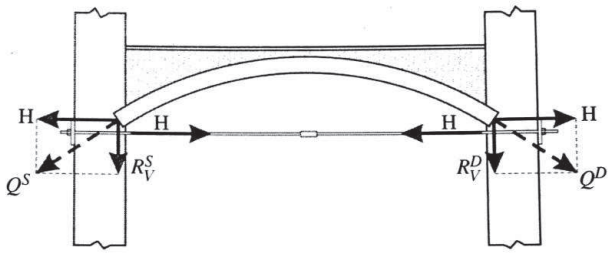

Fig. 2 – Example of the tie located in the spam of the arch – Pisani, 2008 [3]

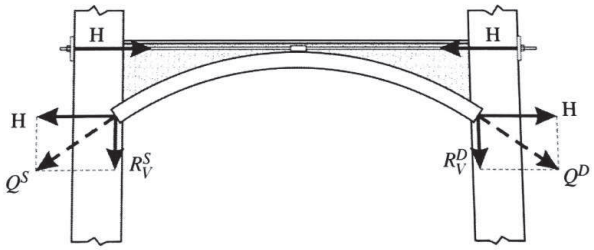

Fig. 3 – Example of the tie hidden in the filling of the arch – Pisani, 2008 [3]

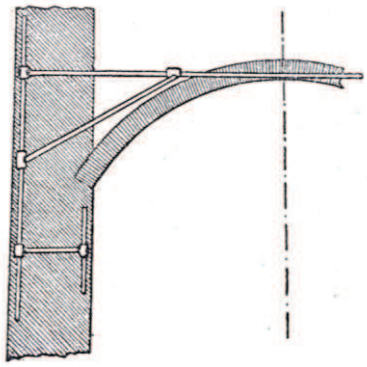

Fig. 4 – Improvement for the solution of the hidden tie.[4]

2.1.2 Box Behaviour

The other main function of the setting of tie-rods is to give the building a box-behaviour, acting as a link between the various parts of the structure. Through the application of ties, it is possible to obtain an effective connection between the load-bearing structure members in correspondence to the slabs, thereby ensuring a function of a monolithic building complex, as shown in Fig. 5. In addition, allows to avoid all the out of plane mechanisms of masonry walls. In particular, one of the main advantages of

the use of tie-rods is its contribution towards the resistance of the structure under seismic action, ensuring an effectively entrusted to shear walls.

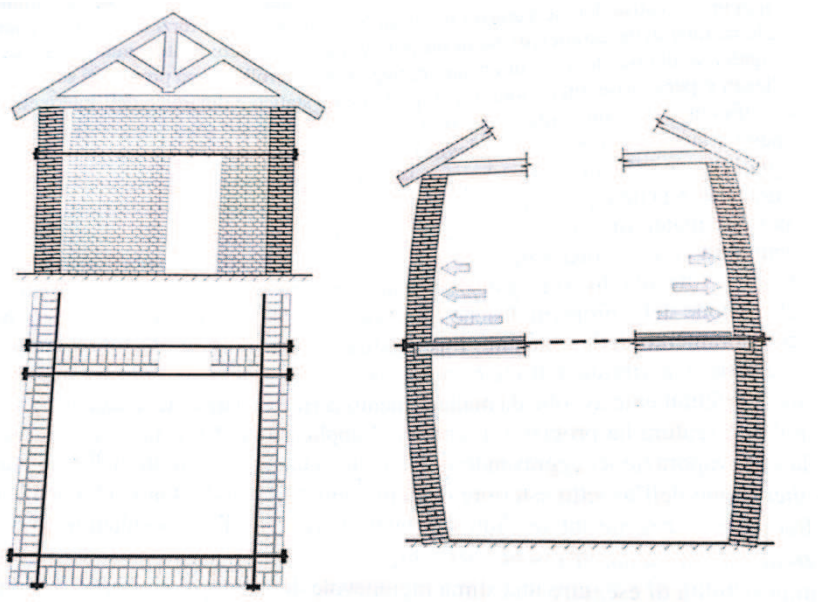

Fig. 5 – Example of box-behaviour connection achieved by the use of tie – Pisani, 2008 [3]

The tie rods can be located inside or outside of the walls. In the first case, the tie rods are made of steel cover with protective sheaths within holes drilled in the thickness of the walls. In the second case the tie rods consist of bars plates or steel profiles, connected to the walls or placed in grooves on their surface. The anchoring devices of the ties connected to the walls are constituted by metal anchoring, such as a plate, which must have characteristics of stiffness and strength such to bring the stresses transmitted to the masonry within allowable values, so as to prevent crushing or localized damages.

As the consequence of the most common use in historical construction of the tie as an action to counteract the horizontal thrust produce as a result of a change in the configuration of the structure, the current thesis focus its attention in the different procedures to estimate the axial force in historical ties located mainly in arches and vaults.

2.2 Proposed methodologies.

There are two methodologies that enable the estimation of the axial force, the static method and the dynamic method.

The *static method* uses the relation between the theoretical deflection of the beam, in the absence of tensile stress and subjected to a generic transversal load *P* applied in any section of its length, and the experimentally measured beam deflection corresponding to the presence at the same time of an unknown tensile stress *H*, and a given applied load *P*.

The method requires defining the restraint conditions, which for historic buildings is a highly complex problem whose evaluation is quite uncertain. The restraint conditions are clearly decisive for both, the expression of the theoretical deflection and the determination of the corresponding critical load.
In addition the static approach requires of the setting of a number of sensors, involving at least three LVDT transducer and three strain gauges, which in terms of onsite testing means high time consumption to carry out the set up of the test.

The *dynamic Method* is based on the vibrating cords *(Belluzzi, 1941)*, and allows the calculation of the axial force H of a beam through the evaluation of the frequencies of vibration. Dynamical tests consist on the temporary fixing of one or two sensors (accelerometers) and on the acquisition of the signal following an impulse which the tie rod is given through a simple impact. The tests are non-destructive and very rapid. Moreover, as it is well known frequencies and modes of vibration are the best suited parameters to identify the structure's response since they are determined by stiffness, masses and boundary conditions. In addition it has to be considered that tie-rods are easily excitable free structures, for which modal frequencies can be easily identified through spectral analysis (*Lagomarsino, 2005)*.
The method has a simple formulation for ties with high slenderness, on which the flexural stiffness can be neglected, and axial force can be calculated for two extreme boundary conditions, pinned and fixed, but they yield approximate results since they neglect the stiffness contribution provided respectively by bending stiffness and constrains, leading to an overrating of the axial tensile force. Therefore due to the complexity of historical construction boundary conditions of historic ties cannot be defined in both ideal extremes. Therefore the hypothesis of no flexural stiffness is not always applicable when it comes to the analysis of historical ties.
To date, the lack of a satisfying method that allows the accurate estimation of the axial force, has led to the development and proposal of several techniques based on the dynamic identification of the tie.

2.3 Static Method.

2.3.1 Briccoli, 2001

The procedure[5] allows determining the pull in a chain directly through static tests alone, without the need for any hypotheses regarding the small size of the increase in pull ΔH, or prior knowledge of the kind of restraints present. The possibility of proceeding in this fashion appears clear if one considers that the change in stress and strain state undergone by the tie-beam consequent to the application of a concentrated load P orthogonal to the axis can be unequivocally determined if we know the values of the consequent sinking, the bending moment in correspondence to any three sections whatever, and the increase in pull ΔH. Such parameters, related by equilibrium equations written in the configuration consequent to the application of the load, give rise to a linear system of three equations with three unknowns.

It is considered a rod subject to its own weight and an unknown tensile force H, and Ω_0 is taken as the equilibrium configuration of the system under such loading conditions. If a further concentrated load P is applied to the configuration in any section of the tie-rod, the stress state will vary, and the beam will therefore take on a new equilibrium configuration Ω', as shown in Fig. 6.

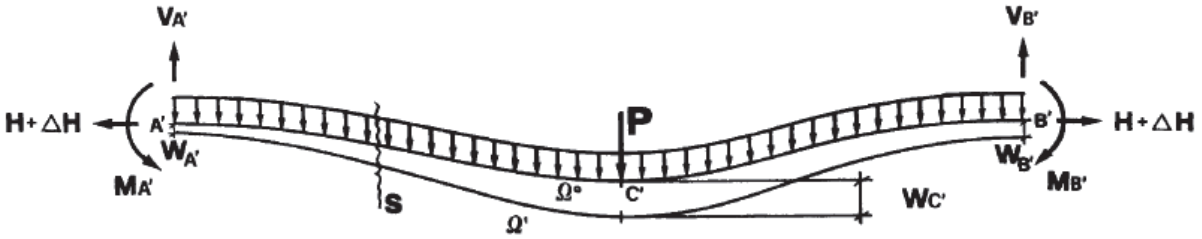

Fig. 6 – Briccoli, S - Tonietti, U (2001) – Equilibrium Configuration – Experimental Method for estimating in situ tensile force in tie rods.

The variation of the bending stress in any given section S will be, neglecting the increase in pull,

$$M_s = M_{ts} - Hw_s \tag{2.1}$$

The change in the bending moment M_S in any given section *S* resulting from the application of load *P* can be revealed through application of a pair of strain gauges placed on the upper and lower margins of the tie-rod; the rise *w* can be measured by displacement transducers so that the terms M_{tS} and *H* will appear as unknowns in equation (2.1). With reference to Fig. 6, the variation in M_S revealed by the strain gauges is made up of a portion that is a sole function of the applied load and the restraint conditions, and one portion that is a function of the unknown pull *H* and its increase ΔH consequent to the application of *P*, and does not depend on the tie-rod's own weight.

It should be stressed that the readings furnished by the strain gauges, from which the value of the bending stress can be derived, are never representative of a pure bending state, but bending accompanied by axial load. However, the amount of strain due to the increase in tension can easily be deduced from the values measured by the strain gauges. If, in fact, ε_1 and ε_2 are the strain values measured respectively at the extrados and intrados of the tie-rod, the maximum strain ε_{mf} due to bending and the portion $\varepsilon_{\Delta H}$, due to the increase ΔH, will be

$$\varepsilon_{mf} = \frac{\varepsilon_1 - \varepsilon_2}{2}, \quad \varepsilon_{\Delta H} = \frac{\varepsilon_1 + \varepsilon_2}{2} \tag{2.2}$$

Therefore, from the strains recorded by the strain gauges, the increase ΔH owing to application of *P* can be determined unequivocally.

Measuring the variation in bending moment and displacement in any section of the tie, it leads to a system of three algebraic equations with four unknowns. Being those sections the one shown in Fig. 6 as *A', B', C'* the system equation will be,

$$_{A'} = M_{tA'} - (H + \Delta H)w_{A'} \tag{2.3}$$

$$M_{B'} = M_{tB'} - (H + \Delta H)w_{B'} \tag{2.4}$$

$$M_{C'} = M_{tC'} - (H + \Delta H)w_{C'} \tag{2.5}$$

Where $M_{A'}$, $M_{B'}$ and $M_{C'}$ are the values of the bending moment revealed by the strain gauges readings, ΔH is the increase of the normal force due to the application of P and $w_{A'}$, $w_{B'}$, $w_{C'}$ are the vertical displacement revealed through the transducers.

If the bending moment in section C is expressed as a function of P, M_A and M_B, and it is replace in equations (2.3) to (2.5), the value of the unknown pull H can be obtained as follow:

$$H = \frac{a'(M_{C'} - M_{B'}) + b(M_{C'} - M_{A'}) - Pa'b'}{a'(w_{B'} - w_{C'}) + b'(w_{A'} - w_{C'})} - \Delta H \tag{2.6}$$

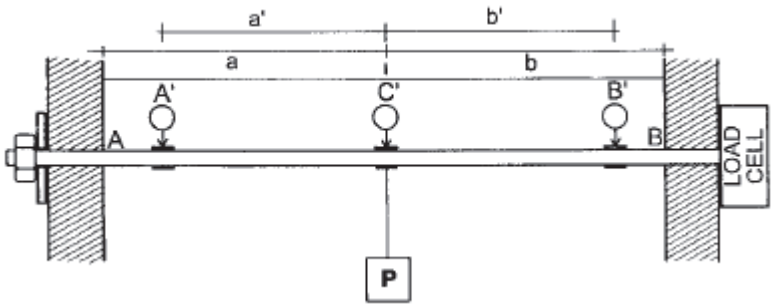

Fig. 7 – Briccoli, S - Tonietti, U (2001) – Schematic representation of experimental equipment – Experimental Method for estimating in situ tensile force in tie rods.

2.4 Dynamic Methods.

2.4.1 Theory of the wire-rod (Teoria dei fili tesi)

Until a few years ago, the problem of the unknown tensile force was solved by considering the tie-rods as a vibrating wire and measuring its first modal frequency. The first natural frequency of vibration was calculated with the following equation:

$$\omega_n = \frac{n\pi}{l}\sqrt{\frac{T}{\mu}} \tag{2.7}$$

Knowing that $\omega = 2\pi f$, it can be considered two limit cases, taking into consideration the boundary conditions. The first case is the fixed-fixed situation, in which it is considered that the effective length for deflection is half of the current length, for this case the Axial force can be obtained with the following equation:

$$T = f^2 l^2 \mu \tag{2.8}$$

Where:

T : Axial force of the ties in [N]

f : first natural frequency of vibration [Hz]

l : length of the tie [m]

μ: linear density, ρ·A [kg/m^3]

A: cross section of the tie [m^2]

The second case is the pinned-pinned condition, in which the effective length of deflection is *l*, the equation use to estimate the axial force is the following:

$$T = 4f^2 l^2 \mu \tag{2.9}$$

The approach is certainly acceptable if the slenderness of the tie-rod is high. However in many circumstances both the chain sections and the devices anchoring them in the surrounding masonry are such that the bending stiffness cannot be neglected. This is particularly the case or age-old constructions due to the transverse dimension of the tie-rods used. (Briccoli, 2001).

2.4.2 Dardano, Miranda, Persichetti &Valvo (2005)

The procedure [6] modelled the tie as a beam “tenso-inflessa” with a length L and a constant cross section. The system has three unknowns: the axial force *T*, the rotational stiffness of the springs *ka* and *kb*. (See Fig. 8)

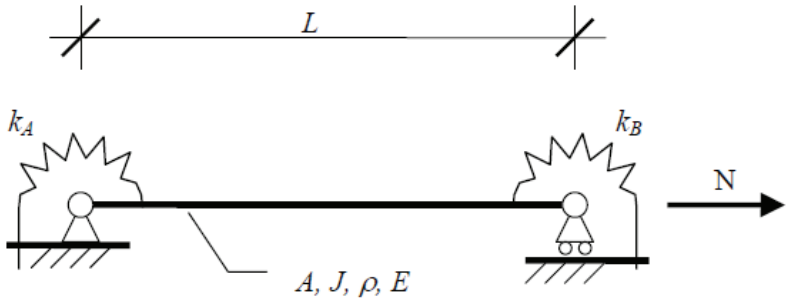

Fig. 8 – Dardano, D.- Miranda, J.C.- Persichetti, B.- Valvo, P. (2005) – Static scheme of the tie model – Un metodo per la determinazione del tiro nelle catene mediante identificazione dinamica.

The equation of motion can be written as following:

$$EJ\frac{\partial^4 w(x,t)}{\partial x^4} - N\frac{\partial^2 w(x,t)}{\partial x^2} + \rho A\frac{\partial^2 w(x,t)}{\partial t^2} = 0 \tag{2.10}$$

Where A and J are the area and the moment of inertia respectively, ρ and E are the density and the young modulus of the material that compound the tie and w(x,t) is the displacement in the transversal direction on the x axis as a function of t.

Boundary conditions, no displacement in the supports, then:

$$w(x,t)|_{x=0} = 0 \ , w(x,t)|_{x=L} = 0 \ , \ \forall t \geq 0 \tag{2.11}$$

$$-EJ \frac{\partial w^2(x,t)}{\partial x^2}\Big|_{x=0} = -k_A \frac{\partial w(x,t)}{\partial x}\Big|_{x=0} , -EJ \frac{\partial w^2(x,t)}{\partial x^2}\Big|_{x=L} = -k_B \frac{\partial w(x,t)}{\partial x}\Big|_{x=L} , \forall t \geq 0 \tag{2.12}$$

The moment in the fixed support is proportional to the rotation of the same section:

k_A and k_B are the stiffness of the rotational springs in the extremes of the beam x= 0 and x= L.

The division of the variable is made by a solution of the type as follow:

$$w(x,t) = X(x) \cdot T(t) \tag{2.13}$$

Where X(x) and T(t) are function of only one variable. The solution for this equation is then given by:

$$X(x) = A \cos \alpha x + B \sin \alpha x + Ce^{\beta x} + De^{-\beta x} \tag{2.14}$$

$$T(t) = E \cos \omega t + F \sin \omega t \tag{2.15}$$

$$\alpha = \sqrt{\frac{\sqrt{1 + 4(\frac{\lambda \omega}{c})^2} - 1}{2\lambda^2}} \tag{2.16}$$

$$\beta = \sqrt{\frac{\sqrt{1 + 4(\frac{\lambda \omega}{c})^2} + 1}{2\lambda^2}} \tag{2.17}$$

$$\lambda^2 = \frac{EJ}{N} , c^2 = \frac{N}{\rho A} \tag{2.18}$$

Substituting the expressions (2.14) and (2.15) in (2.13), and taking into consideration the boundary conditions and initial conditions, it is possible to obtained a non trivial solution. In order to reach this solution the determinant of the matrix, which contains the coefficients that determine the system of equations, must be equal to zero.

$$DET = 2\left(\frac{EJ}{L}\right)^2 (d_1 \sinh \beta L + d_2 \cosh \beta L - 2\mu_A \mu_B \alpha\beta) = 0 \quad (2.19)$$

Where

$$d_1 = (\mu_A + \mu_B)\alpha(\alpha^2 + \beta^2)L \cos \alpha L + [\mu_A \mu_B(\alpha^2 - \beta^2) - (\alpha^2 + \beta^2)^2 L^2] \sin \alpha L \quad (2.20)$$

$$d_2 = 2\mu_A \mu_B \alpha\beta \cos \alpha L - (\mu_A + \mu_B)\beta(\alpha^2 + \beta^2)L \sin \alpha L \quad (2.21)$$

Where the adimensional stiffness of the rotational spring is determined as follow:

$$\mu_A = \frac{k_A L}{EJ} \; ; \mu_B = \frac{k_B L}{EJ} \quad (2.22)$$

To keep the simplicity of the formulation, the analysis is developed on the base that the support on the extremes of the tie are equal, meaning that $k_A = k_B = k$, $\mu_A = \mu_B = \mu$.
Also it is define the variable G, Degree of constrain (“Grado di Incastro), which establishes the relation between the moment on the fixed support for a beam with elastic joints and for a beam with perfect fixed joints, both subjected to the same load.

$$G = \frac{\mu\,(\mu + 6)}{\mu^2 + 8\mu + 12} \quad (2.23)$$

The values of equation (2.23) vary from 0 to 1 depending if the supports are pinned or fixed respectively.
From the acquisition of the first two frequencies through the equation (2.19) can be obtained the axial forces N_1 and N_2 as a function of G. By means of the equation (2.22) it can be obtained the stiffness of the springs k_A, k_B.

2.4.3 Lagomarsino &Calderini (2005)

Frequencies and modes shapes or vibration are the best suited parameters to identify the structure’s response, since they are determined by stiffness, masses and boundary conditions. In addition tie-rods are easily excitable free structures, for which modal frequencies can be easily identified through spectral analysis.
The structural model employed [7] is illustrated in Fig. 9, the tie-rod is assumed to be a beam, with uniform section subjected to a constant axial tensile force, it is assumed to be spring-hinged at both ends, since the clamp is not perfect. Its free vibration is governed by the equation (2.10), and with the boundary conditions established in equations (2.11) and (2.12). In this formulation the unknown variables are, besides T, the bending stiffness of the section EJ and the stiffness of the rotational

springs *k.* The evaluation of EJ is particularly difficult, since tie-rods are hand wrought and present an irregular section that is difficult to assess with precision. Moreover, the mechanical characteristics are difficult to determine through non-destructive test. Finally corrosion may have altered the geometrical and mechanical properties of the section. However, the geometrical characteristics are considered to be a data of the problem measured with enough accuracy.

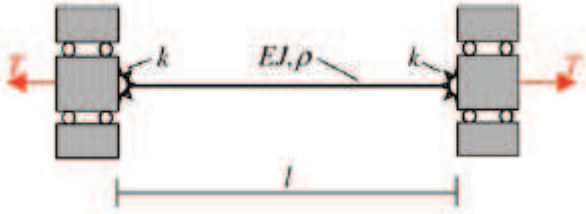

Fig. 9 – Lagomarsino, S.- Calderini, C. (2005) – Scheme of the model employed – The dynamical identification of the tensile force in ancient tie-rods

The definition of the model turns to be not perfectly realistic for two reasons: non-homogeneity of the bending stiffness along the tie-rod and the possibility of a different amount of rotational stiffness at its opposite extremes. Using a separation of variables as equation (2.13), and with the solution stated in the equations (2.14) to (2.17), the author proposes a numerical solution.

It is considered two cases, one in which the bending stiffness *EJ* is negligible provided that ($EJ/T \cdot l^2 \approx 0$) , this case is the “wire” and it analytical solution is:

$$f_n = \frac{n}{2l}\sqrt{\frac{T}{\rho}}\,, T = \frac{4\rho f_n^2 l^2}{n^2} \tag{2.24}$$

The other case is the one in which the spring stiffness *k* can be considered negligible ($k \cdot l/EJ \approx 0$), this case is the “pre-stressed pinned beam” and the general solution is:

$$f_n = \frac{n}{2}\sqrt{\frac{n^2\,\pi^2 EJ}{\rho l^4} + \frac{T}{\rho l^2}} \tag{2.25}$$

In this case, we have only two unknown variables, (T, EJ), so it is necessary to know at least two natural frequencies, and the solution is found by solving the inverse problem.

$$T = \frac{4\mu L^2 f_n^2}{n^2} - \frac{n^2\pi^2 EJ}{L^2}$$

Numerical solution procedure

As reference the value of the first modal frequency of the *pinned-pinned beam*:

$$\varpi = \pi^2\sqrt{\frac{EJ_S}{pl^4}} \tag{2.26}$$

Where EJ_S represents an empirical reference value for bending stiffness, and introducing the following parameters:

$$\varphi = 2\pi^2 \frac{EJ_s}{Tl^2}, \qquad \gamma = \frac{kl}{EJ_s}, \qquad \delta = \frac{EJ}{EJ_s} \tag{2.27}$$

The solution can be written as a non-dimensional form as follow:

$$\begin{aligned} g\left(\varphi, \gamma, \delta, \frac{\omega_n}{\varpi}\right) = \sin\alpha \sinh\beta \left[(\alpha^2+\beta^2)^2 - \frac{\gamma^2}{\delta^2}(\alpha^2-\beta^2)\right] \\ + 2\frac{\gamma}{\delta}(\alpha^2+\beta^2)(\beta \sin\alpha \cosh\beta - \alpha\cos\alpha \sinh\beta) - 2\frac{\gamma^2}{\delta^2}\alpha\beta(\cos\alpha\cosh\beta \\ - 1) \end{aligned} \tag{2.28}$$

$$\alpha = \pi \sqrt{\frac{1}{\delta\varphi}\left(\sqrt{1+\delta\varphi^2\left(\frac{\omega_n}{\varpi}\right)^2} - 1\right)} \tag{2.29}$$

$$\beta = \pi \sqrt{\frac{1}{\delta\varphi}\left(\sqrt{1+\delta\varphi^2\left(\frac{\omega_n}{\varpi}\right)^2} + 1\right)} \tag{2.30}$$

In general the inverse problem solution would require the knowledge of at least three natural frequencies, and the solution of three non-linear equations system:

$$\begin{cases} g_1 = g\left(\varphi, \gamma, \delta, \frac{\omega_1}{\varpi}\right) = 0 \\ g_2 = g\left(\varphi, \gamma, \delta, \frac{\omega_2}{\varpi}\right) = 0 \\ g_3 = g\left(\varphi, \gamma, \delta, \frac{\omega_3}{\varpi}\right) = 0 \end{cases} \tag{2.31}$$

The authors propose to solve the system minimizing the function G:

$$G(\varphi, \gamma, \delta) = g_1^2 + g_2^2 + g_3^2 \tag{2.32}$$

The minimization was performed through an IMSL routine.

2.4.4 Park et al. (2006)

The proposed sensitivity method[8] is first validated using numerical data from a beam structure. Then, the impact of model uncertainty to the performance of the parameter identification is investigated. Finally, experimental verification is performed using laboratory test data from a bar.

It is considered a bar member subjected to an axial load *P*. Supposed that the member has *r* elements with *q* discrete masses. Let λ_i *(i=1,...,n)* represent the identifiable eigenvalues of a structure; let m_n *(n=1,...,q)* represent the n^{th} discrete mass of the member and let k_j *j=1,...,r)* represent the stiffness of the j^{th} structural element. If assume that the mass of the bar remains constant then:

$$\lambda_i = \lambda_i(k_1, \dots, k_r; m_1, \dots, m_q; P) \tag{2.33}$$

$$\delta\lambda_i = \sum_{j=1}^{r} \frac{\partial \lambda_i}{\partial k_j}\delta k_j + \frac{\partial \lambda_i}{\partial P}\delta P \tag{2.34}$$

Where $\delta\lambda_i$ is the variation in the i^{th} eigenvalue, δk_j is the variation in the stiffness of the j^{th} element, and δP is the variation in the axial load P.

Dividing both sides of the equation (2.34) by λ_i and setting $Z_i = \delta\lambda_i/\lambda_i$

$$Z_i = \frac{\delta\lambda_i}{\lambda_i} = \sum_{j=1}^{r} \frac{k_j}{\lambda_i}\frac{\partial \lambda_i}{\partial k_j}\frac{\delta k_j}{k_j} + \frac{P}{\lambda_i}\frac{\partial \lambda_i}{\partial P}\frac{\delta P}{P} \tag{2.35}$$

If K_i and M_i are, respectively, the i^{th} modal stiffness and the i^{th} modal mass, substituting $\lambda_i=K_i/M_i$ into equation (2.35) and simplifying yields:

$$Z_i = \frac{\delta\lambda_i}{\lambda_i} = \sum_{j=1}^{r} F_{ij}\alpha_j + H_i\psi \tag{2.36}$$

$$F_{ij} = \frac{k_j}{K_i}\frac{\partial K_i}{\partial k_j};\ H_i = \frac{P}{K_i}\frac{\partial K_i}{\partial P};\ \alpha_j = \frac{\delta k_j}{k_j};\ \psi = \frac{\delta P}{P} \tag{2.37}$$

$$Z = A\gamma \tag{2.38}$$

F is an *n x r* stiffness sensitivity matrix determined from a theoretical model of the bar, *H* is an *n x 1* axial force sensitivity matrix determined from a theoretical model of the bar, *Z* is an *n x 1* matrix containing the fractional changes in eigenvalues between the two systems, *α* is a *r x 1* matrix containing unknown stiffness adjustments, and *ψ* is a scalar containing unknown axial force adjustments. Then stiffness and axial force adjustments can be determined from the equation:

$$\gamma = A^{-1}Z \tag{2.39}$$

A^{-1} is the generalized inverse

To generate the elements of the sensitivity matrix A with the limited number of frequencies, the following procedure is used:

(1) Assume an initial model of the structure to be identified and compute λ_i *(i = 1,. . . ,n)* for that structure;

(2) Set a single $\gamma_k = \gamma$ and set all other $\gamma_j = 0$ (i.e., j ≠ k);

(3) Compute λ^*_i *(i = 1, . . . ,n)* of the structure to be identified;

(4) Compute eigenvalue sensitivities $Zi = \delta\lambda_i/\lambda_i$ *(i = 1,. . . ,n)* where $\delta\lambda_i = \lambda^*_i - \lambda_i$

(5) Compute the *ik*th element of the A matrix using the result $Aik = Zi/\gamma$; and

(6) Repeat for k = 1,. . ., r.

Once the matrix A was assembled, the general identification procedure can be accomplished using the following steps:

(1) Develop an initial FE model for the target member;

(2) Compute the sensitivity matrix A from the FE model;

(3) Compute the fractional changes in eigenvalues, Z, between the FE model and the target member;

(4) Solve Equation (2.39) for γ using generalized inverse technique;

(5) Update the spring stiffness and axial force of the FE model using the relationships $k_j^* = k_j(1+\alpha_j)$ and $P^* = P(1 + \psi)$; and

(6) Repeat Steps (2)–(5) until convergence (i.e., $\alpha_j \approx 0$ and $\psi \approx 0$).

2.4.5 Tullini &Laudiero (2008)

The identification method proposed [9] by the authors is bases on the Euler - Bernoulli beam model and assumes geometric and elastic properties as known parameters. Making use of any natural frequency and of three displacement components of the corresponding mode shape, it is shown that both axial loads and stiffness of end flexural springs of a beam subjected to tensile or compression force can be obtained.

Governing equations

The model is constituted by a simply supported prismatic beam of length L, constrained by two elastic-springs with k_o and k_1 flexural stiffness, subjected to an axial resultant N (positive sign). Young's Modulus E, mass per unit length μ ans cross-section area and moment J are assumed to be constant and know as well.

Making use of a nondimensional coordinate x=X/L and neglecting both rotational inertia and shear deformation, circular frequencies ω and vibration modes v(x) are ruled by the following eigenvalue problem:

$$v''''(x) - nv''(x) + \lambda^4 v(x) = 0, \qquad 0 < x < 1 \tag{2.40}$$

$$v(0) = 0, \qquad v''(0) - \beta_0 v'(0) = 0, \qquad for\ x = 0 \tag{2.41}$$

$$v(1) = 0, \qquad v''(1) - \beta_0 v'(1) = 0, \qquad for\ x = 1 \tag{2.42}$$

$$n = \frac{NL^2}{EJ}, \qquad \lambda^4 = \omega^2 \frac{\mu L^4}{EJ}, \qquad \beta_0 = \frac{k_0 L}{EJ}, \qquad \beta_1 = \frac{k_1 L}{EJ} \tag{2.43}$$

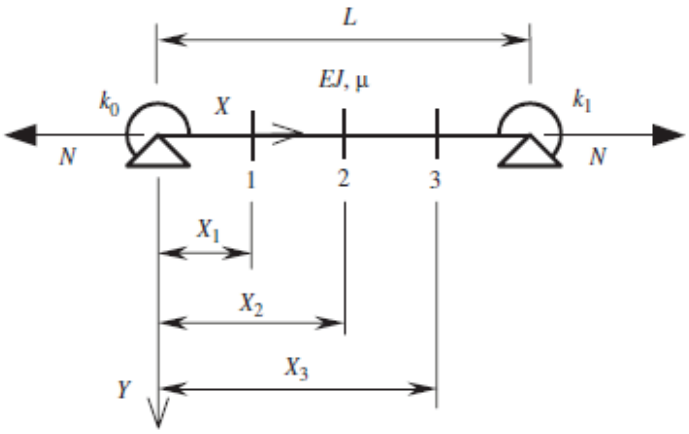

Fig. 10 – Tullini, N.- Laudiero,F. (2008) – Beam with end flexural constraints and location of the instrumented sections – Dynamic identification of beam axial loads using one flexural mode shape

The solution for the equation (2.40) takes the form

$$v(x) = C_1 \cos q_1 x + C_2 \sin q_{1x} x + C_3 \cosh q_2 x + C_4 \sinh q_2 x \tag{2.44}$$

$$q_1^2 = \frac{1}{2}\left(\sqrt{n^2 + 4\lambda^4} - n\right) q_2^2 = \frac{1}{2}\left(\sqrt{n^2 + 4\lambda^4} + n\right) = q_1^2 + n \tag{2.45}$$

From equation (2.45) yields $\lambda^2 = q_1 q_2$. Making use of equations (2.43) and (2.45), circular frequency ω can be written in the form:

$$\omega = 2\pi f = \lambda^2 \sqrt{\frac{EJ}{\mu L^4}} = q_1 \sqrt{\frac{N}{\mu L^2}} \sqrt{1 + \frac{q_1^2}{n}} \tag{2.46}$$

In order to identify the axial load *N* and the stiffness k_o and k_1 of the end flexural constraints, is required one vibration frequency and the corresponding mode shape at three locations.

If the control points are assumed at sections having nondimensional coordinates x_1*=1/4,* x_2*=1/2,* x_3*= 3/4,* and if $v_2 \neq 0$, meaning no node is formed in that coordinate, then:

$$\frac{v_1 + v_3}{v_2} = \frac{1 + 2\cos\left(\frac{q_1}{4}\right)\cosh\left(\frac{q_2}{4}\right)}{\cos\left(\frac{q_1}{4}\right) + \cosh\left(\frac{q_2}{4}\right)} \tag{2.47}$$

$$\beta_0 = (q_1^2 + q_2^2)\frac{a\left(\frac{v_1}{v_2}\right) - b}{c\left(\frac{v_1}{v_2}\right) - d}, \qquad \beta_1 = (q_1^2 + q_2^2)\frac{a\left(\frac{v_3}{v_2}\right) - b}{c\left(\frac{v_3}{v_2}\right) - d} \tag{2.48}$$

Where *a,b,c,d* are given by the following relations:

$$a = \sin q_1 \sinh\frac{q_2}{2} - \sin\frac{q_1}{2}\sinh q_2\,;\quad b = \sin q_1 \sinh\frac{q_2}{4} - \sin\frac{q_1}{4}\sinh q_2 \tag{2.49}$$

$$c = 2\left(\cos\frac{q_1}{2} - \cosh\frac{q_2}{2}\right)\left(q_1 \cos\frac{q_1}{2}\sinh\frac{q_2}{2} - q_2 \sin\frac{q_1}{2}\cosh\frac{q_2}{2}\right) \tag{2.50}$$

$$\begin{aligned} d = {} & q_1\left(\cos q_1 \sinh\frac{q_2}{4} + \sinh\frac{3q_2}{4} - \cos\frac{q_1}{4}\sinh q_2\right) \\ & + q_2\left(\cosh q_2 \sin\frac{q_1}{4} + \sin\frac{3q_1}{4} - \cosh\frac{q_2}{4}\sin q_1\right) \end{aligned} \tag{2.51}$$

2.4.6 Amabili et Al. (2010)

As part of the method [10], the tie-rod is modelled as a simply supported Timoshenko beam, the supports are assumed at the beam edges inside the masonry wall and the portion of the beam inside the wall is subjected to an elastic Winkler foundation simulating the interaction between the beam and the wall, as show in Fig. 11. The beam is considered isotropic of a length L and with a non-uniform prismatic section A. It is assumed that the centroidal axis is coincident with the elastic axis so that bending-torsion coupling is negligible.

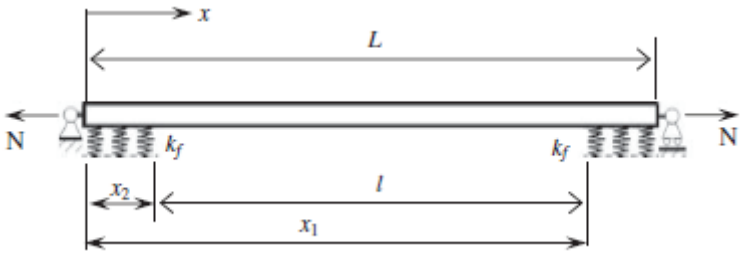

Fig. 11– Amabili, A et al. (2010) – Model of the tie-rod – Estimation of tensile force in tie-rods using a frequency-based identification method.

Identification Method

In order to identify the axial force F and the stiffness k_f of the elastic foundation, the weighted difference between the calculated and identified natural frequencies is introduced:

$$err_{RMS}(F, k_f) = \sqrt{\frac{1}{M}\sum_{i=1}^{M}\delta_1^2} \tag{2.52}$$

Where *M* is the number of the natural modes included in the identification process and δ_1 is the difference between the *i*-th computed and experimentally measured natural frequency.

2.4.7 Luong (2010)

The method [11] is based on a standard charts for three boundary conditions: pinned-pinned, fixed-pinned, and fixed-fixed. The charts were obtained throughout a parametric study of the theoretical equation for obtaining the frequency for a tie-rod with a pinned-pinned condition. (See Equation (2.25)) The charts show the relationship between the frequency and the tensile stress of the tie-rod. These charts were done to cover a wide range of different tie-rods. To achieve this, from the study of the combination of different factors outline during the parametric study, are obtained correction factors, which will relate the ties with different characteristics to those which are already know.

The charts were done taking into consideration the following characteristics:

- Length (L_1 [m])
- Cross-section with a height or diameter of h_1 [m]
- Measured frequency of the n^{th} mode f_1
- Material properties assumed: *E=210Gpa* and ρ_s*=7850 kg/m*^{3}

Moreover, the charts are made in a range of *h/L= 0,0004 to 0,04* and *n=1 L=1* and *σ=0-200Mpa.*

The correction factors needed to identify the axial force in the charts are the following:

Rectangular Cross-section	Circular Cross-section
$\begin{cases} \left(\frac{h}{L}\right)_{corrected} = n_1\left(\frac{h_1}{L_1}\right) \\ f_{n_{corrected}} = \left[\left(\frac{1}{n_1}\right)L_1\right] f_1 \end{cases}$	$\begin{cases} \left(\frac{h}{L}\right)_{corrected} = 0.8660 \cdot n_1\left(\frac{h_1}{L_1}\right) \\ f_{n_{corrected}} = \left[0.9098 \cdot \left(\frac{1}{n_1}\right)L_1\right] f_1 \end{cases}$

Where H1, L1 and n1 are the parameters of the tie-rod whose tensile stress is to be determined and $(h/L)_{corrected}$ and $f_{n\_corrected}$ are the values to be used on the charts.

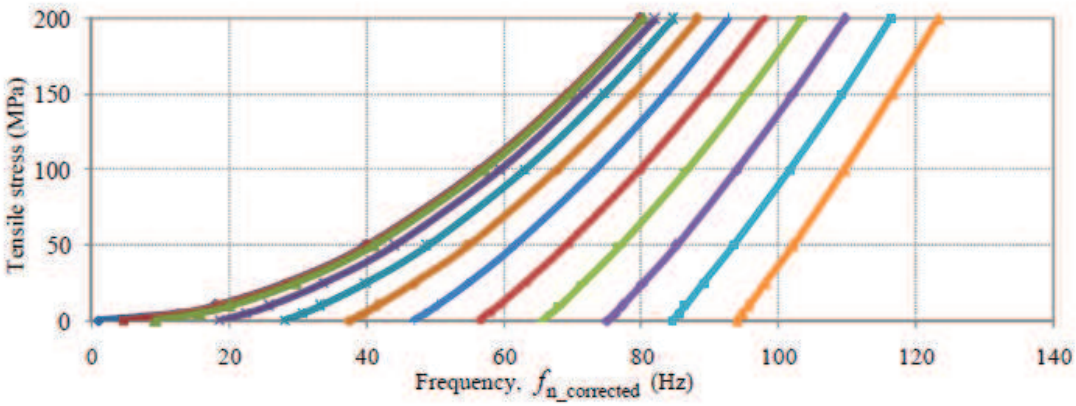

Fig. 12– Luong. (2010) – Standard Chart I_a (pinned-pinned condition) – Identification of the tensile force in tie-rods using modal analysis test.

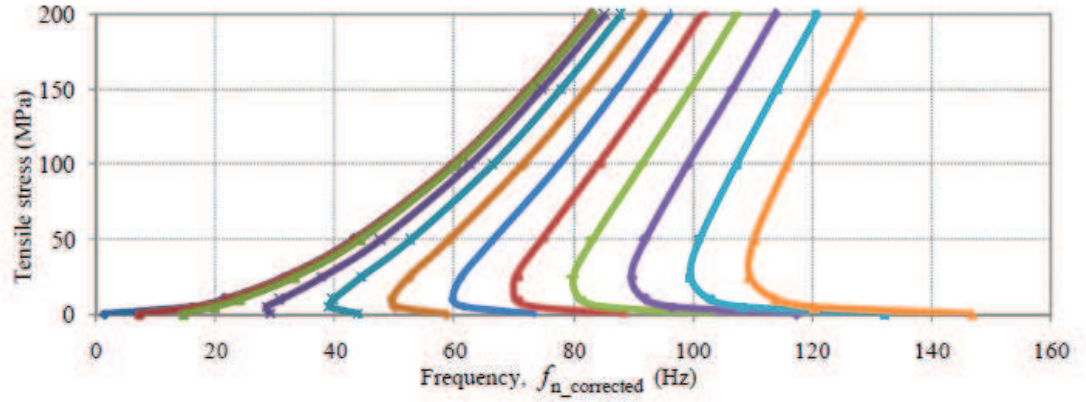

Fig. 13 – Luong. (2010) – Standard Chart I_b (fixed-pinned condition) – Identification of the tensile force in tie-rods using modal analysis test.

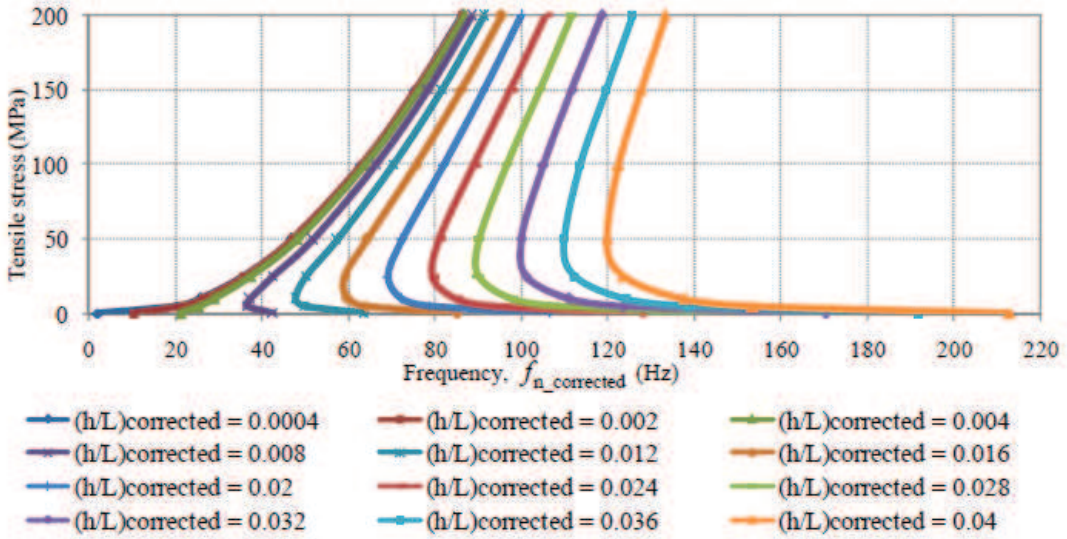

Fig. 14 – Luong. (2010) – Standard Chart I_c (fixed-fixed condition) – Identification of the tensile force in tie-rods using modal analysis test.

2.4.8 Rebecchi, Tullini &Laudiero (2013)

The identification method proposed by the authors[12] generalizes the axial force identification algorithm described by Tullini, 2008, to study the more general problem of a prismatic slender beam with unknown boundary conditions. Making use of any frequency and of five amplitudes of the corresponding mode shape, the proposed algorithm is able to estimate the axial force of an Euler-Bernoulli beam with known geometric and elastic properties.

In Fig. 15 is shown the model use for this method. Tie-rods extremities are embedded in masonry walls making doubtful the beam length and the location of the end constraints. To overcome this

problem, the length is adopted. The model shown is constituted by a prismatic beam, of length L, constrained by two sets of elastic end springs whose frequency-dependent parameters are collected by the 2 x 2 stiffness matrices K_0 and K_1. The beam is subjected to an axial force resultant N, Young's modulus E, mass per unit length m and cross-section second area moment J are assumed to be known constants.

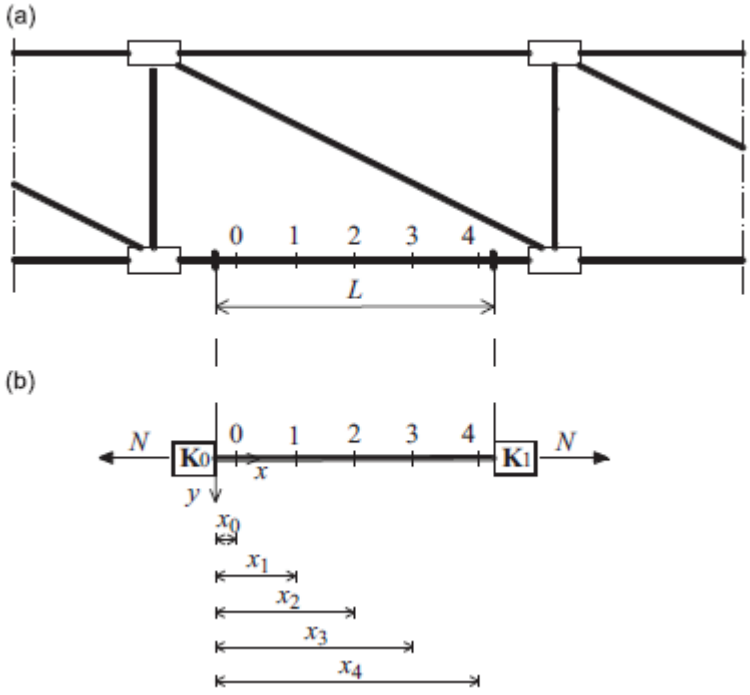

Fig. 15 – Rebecchi (2013) – Beam belonging to a truss girder (a) and reference model with location of the instrumented sections (b) – Estimate of the axial force in slender beams with unknown boundary conditions using one flexural mode shape.

Using the Equations (2.43) to (2.46) and the system equations obtained by evaluating the five instrumented sections, it can be obtained the following equation,

$$C_1(\lambda,n)\cos q_1 z_4 + C_2(\lambda,n)\sin q_1 z_4 + C_3(\lambda,n)\cosh q_2 z_4 + C_4(\lambda,n)\sinh q_2 z_4 - v_4 = 0 \tag{2.53}$$

The equation (2.53) can be simplify if the control points are assumed to be in the sections having nondimensional coordinates z_0=0, z_1=1/4, z_2=1/2, z_3=3/4 and z_4=1.The equation then yields,

$$\frac{v_1 + v_3}{v_2} = \frac{\left(\frac{v_0 + v_4}{2v_2}\right) + 1 + 2\cos\frac{q_1}{4}\cdot\cosh\frac{q_2}{4}}{\cos\frac{q_1}{4} + \cosh\frac{q_2}{4}} \tag{2.54}$$

The axial force can be estimated according to the following steps:

- Estimate one fundamental frequency *f* and the corresponding mode shape amplitudes v_0, v_1, v_2, v_3, v_4 by means of experimental modal analysis.

- Compute λ using Equation (2.43)
- Solve the equation (2.54) for the unknown constant *n* by using the ratios$(v_1 + v_3)/v_2$, $(v_0 + v_4)/2v_2$, and the definitions for q1 and q2 in Equation (2.45) where the value of λ is required
- Use Equation (2.43) to find the analytical axial force $N_a = nEJ/L^2$

2.5 Analysis of the methods

The method studied in the previous section, were analyzed to evaluate its numerical applicability, accuracy and quantify its performance. The examples done by the authors in the scientific publication were carried out in order to verify the methodology proposed for each case and obtain an evaluation of each method.
The observation for each method are the following, showing the main advantages and main issues faced during their applications.

2.5.1 Static Method

- The static method proposed by Briccoli [5], has shown it efficiency to estimate the axial force with great accuracy, but it presents two main drawbacks. Firstly from the point of view of the practicality of the method, it requires some more equipment than other methods, LVDT Transducers, Strain Gauges, two load cells, and a data collector. This is the reason why the method is not easy to perform on field, where, for example, the tie is located at great height. The second drawback is it sensitivity regarding the measurements gathered during the testing.

2.5.2 Dynamic Methods

- The wire-rod theory [13] has as a main problem the neglect of the bending stiffness and the real boundary conditions, reason why cannot always be applied in the field of historical ties where the boundaries are hardly known. The boundary hypothesis has to be of great accuracy; otherwise the result may lead to a value higher than the real one, or under that value. As the axial force of the tie increases, the method presents a larger gap between the two boundary conditions.

- The method proposed by *Dardano* [6], showed during the testing of the example that works properly for short and stiff beams that can be considered as fixed in both extremes, meaning that the value of G is near one. The characterization of the tie studied is shown in Table 1.
From the Fig. 16 obtained it can be observed that the method convergences to estimate the axial force. However, for cases where the boundary condition cannot be taken as pinned-pinned, the value of G obtained surpasses the value of 1. Hence the convergence is not reach due to several causes, firstly the values of G are above 1, and secondly the variation of the values of G with the load present no large difference, making both lines to be almost overlap.

GEOMETRICAL CHARACTERIZATION		
Length	L [m]	5
Diameter	d [mm]	40
Area	A [mm2]	1256.64
Inertia	J [mm4]	125663.71
Young Modulus	E [N/mm2]	206000
Density	ρ [kg/m3]	7830
Normal Stress	σ [Mpa]	4

Table 1 – Characterization of tie analyzed

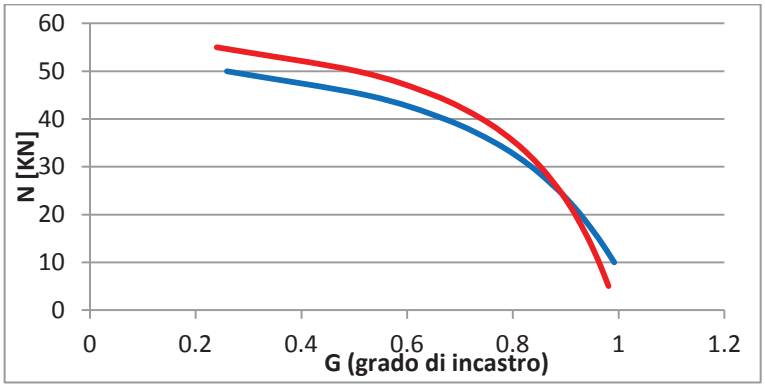

Fig. 16 – Graph obtained by the method.

- The method proposed by *Lagomarsino* [7], presents the main drawback that is the minimization of the function G, is not possible to achieve.

- The method proposed by *Park*[8], depends on the construction of the sensibility matrix A, which is built through and algorithm where a parameter γ_K has to be defined. The main drawback of the method is associated with the definition of such parameter and its relation with the acquisition of the eigenvalue of the problem. The matrix cannot be easily built with the algorithm presented by the authors.

- The method proposed by *Tullini*[9], works properly and is numerically applicable. The method presents no further complication to reach the value of the axial force. The example presented by the Author in the scientific paper had the following features, Table 2.

In Table 3 can be seen the results obtained applying the Method, and the results obtained by the Author, showing the expediency of the method, and its mathematical simplicity to estimate the axial force. Regarding the onsite testing, the method requires only a few equipments, only three accelerometers and a central data collector. The simplicity not only from the numerical point of view but also from the on field application, make the method a good option to measure the tension in historical ties.

GEOMETRICAL CHARACTERIZATION		
Length	L[m]	3.625
Diameter	h [m]	0.02
Area	A[m2]	0.00031416
Inertia	J[m4]	7.85E-09
Density	ρ [kg/m3]	7850
Density per unit length	μ [kg/m]	2.466
Young Modulus	E [N/m2]	1.96E+11

Table 2 – Properties of the tie, Tullini 2008

	f_1	v1+v3/v2	v1/v2	v3/v2	ω_1	λ^4	n	N [N]	β_o	β_1
Example	6.66	1.235	0.624	0.611	41.85	484.41	13.93	**1632**	13.50	15.78
Author	6.66	1.235	0.624	0.611	41.85	483.83	15.09	**1640**	13.4	12.9

Table 3 – Comparison of the result obtained through the method proposed by Tullini.

- The charts proposed by *Luong* [11], worked for the examples done, and presents a reduction of the range of axial forces than the one calculated with the wire-rod theory. The charts have some drawback related mainly to the fact that is based on the theory of the wire-rod which is now known to have some shortcomings and should not be applied on historical ties. In addition to the latter, the charts presents some inconvenient for low frequencies of circular cross section, where due to the slenderness of the tie, and the low frequencies gathered, is not possible to fit the particular case inside the spectrum of frequencies considered by the method.

One example of this problem is presented in the case of “Museo Archeologico di Ascoli”[14], for the ties identified as CAT4 and CAT5 inside the database, for which the method cannot be applied due to its slenderness and low first frequencies.

ID	Section	Base (mm)	High (mm)	Area (mm2)	J (mm4)	Length (m)	Freq. [Hz]	h_1/L_1	f_{corr} [Hz]	h/L
CAT5	Rect.	20	45	900	30000	2.8	6.20	0.0071	17	0.008
CAT4	Rect.	20	45	900	30000	2.8	7.55	0.0071	21	0.008

Table 4 – Database (Mosca, 2015), Case study Museo Archeologico di Ascoli.

InTable 4 are shown the features of the ties, and the variable used to perform the method. For the first case, the frequency is too low to be found inside the Chart I (PP condition, see Fig. 12) and in the second case the some happens for the Chart III (FF condition see Fig. 14).

However, the method can be applied not only to the first frequency of vibration, but with some correction to another natural frequency, what means that if gathered more information including higher modes of vibrations, the axial force can be estimated.

- The method proposed by *Rebecchi* [12], is a new version of the method proposed by Tullini, works properly but the results tend to be higher than the values obtained with the Tullini Method. In addition, for some cases where the ratio v1+v3/v2 present high values, the method showed problems of convergence.

2.6 Database

In order to carry out a significant analysis, on the quantification of the performance of the dynamic method, with a large number of case studies, it was used a tie database (Mosca, 2015 [14]), created as tool to determine which are the parameters that can influence the structural and dynamic behaviour of the tie.

This database contains 350 case studies of 22 different buildings; some of them previously analyzed and others obtained by the database author [14]. The database is compound of four sections: the first one with the general data regarding the location of the tie, the dating and its ID. The second section has the specification of the typology of the vault where the tie is located, and the characterization of that vault for each tie. The third section includes the geometrical features of the tie such as the type of cross section (rectangular or circular) and its dimensions, the specification of the material; including density, Young Modulus, and the length. The final section display the dynamic identification of the tie with the first frequency gathered.

The gathering of such database had the aim of determining the most common features of the ties which would allow the development of the model of a historical tie typology that could be tested numerically and in the laboratory. For which the information gathered, was analyzed from different point of view, including geometrical characterization and dynamic features.

From these previous studies can be highlighted the following observations. The geometric characterization that cares the most is the cross section and its length. A first division of the ties was done regarding its cross-section, where a 14% of the ties studied are circular, while the other 86% are rectangular. A second subdivision was due to length, which led to the following distinction:

- Short tie if the length is inferior to 5 meters
  - → Average length: 3,7 m
  - → A= 500 – 1000 mm^2
- Long tie if the length is superior to 5 meters.
  - → Average length: 6,9 m
  - → A= 1500 - 2500 mm^2

The other study was done on the relationship between the frequency of vibration and the shape and dimension of the cross-section of the tie, from which it was obtained that when the shape of the cross-section is the same, the frequency is similar. This observation is also supported by the parametric study carried out by Luong, 2010 [11].

After the study of the main features on the database, a generic tie was modelled with FEM software in order to analyse the performance of the dynamic methods.

For the FEM analysis the tie was modelled as a BEAM with a uniform section subjected to an axial constant load. The constrains were assumed to be elastic, and the stiffness reaches both extremes: pinned-pinned (stiffness=0) and fixed-fixed (stiffness=∞). The material properties, are the ones given by the Eurocode 3, 2003 $\rho = 7850\ Kg/m^3$, E= 210 GPa, v= 0,3.

The model was tested in order to determine the influence of the variables that influence the most the response of the tie, and are presented as uncertainty when the onsite measurement has to be carried out. The variables are the flexural stiffness, the real length and the boundary conditions.

From the results obtained after the FEM analysis, which include a sensitivity analysis of the number of elements included in the model, and the comparison of several cases in which was studied for a range of tension between 0 to 200Mpa, three different boundary conditions:

- *K=0 (pinned-pinned)* → $0 - 10^3$ *Nmm/rad*
- $0<K<\infty$ *(intermediate situation)* → $10^3 - 10^8$
- $K=\infty$ *(fixed-fixed)* → $10^9 - \infty$

And three cases of flexural stiffness:

- *Case A: cross section 40 x 40 mm,* $EJ=7{,}55 \times 10^{10}$ *Nmm/rad*
- *Case B: cross section 40 x 10 mm,* $EJ=2{,}37 \times 10^9$ *Nmm/rad*
- *Case C: cross section d=20 mm,* $EJ=3{,}30 \times 10^9$ *Nmm/rad.*

The analysis led to the following observations:

- As the normal tension increases, the frequency for each mode increases, and how it does it is related to the boundary condition and the length of the tie.
- Regarding the boundary conditions, the frequency for the clamped conditions presents higher values, and depends again on the length, the cross-section and the tension. The Fig. 17 shows the distribution of frequency according to length, where it can be noticed that for the long ties of the database (L> 5,00 meters), there is a major concentration of values of the first frequency under 15Hz and of the short ties the first frequency are under 35 Hz (Mosca,2010)

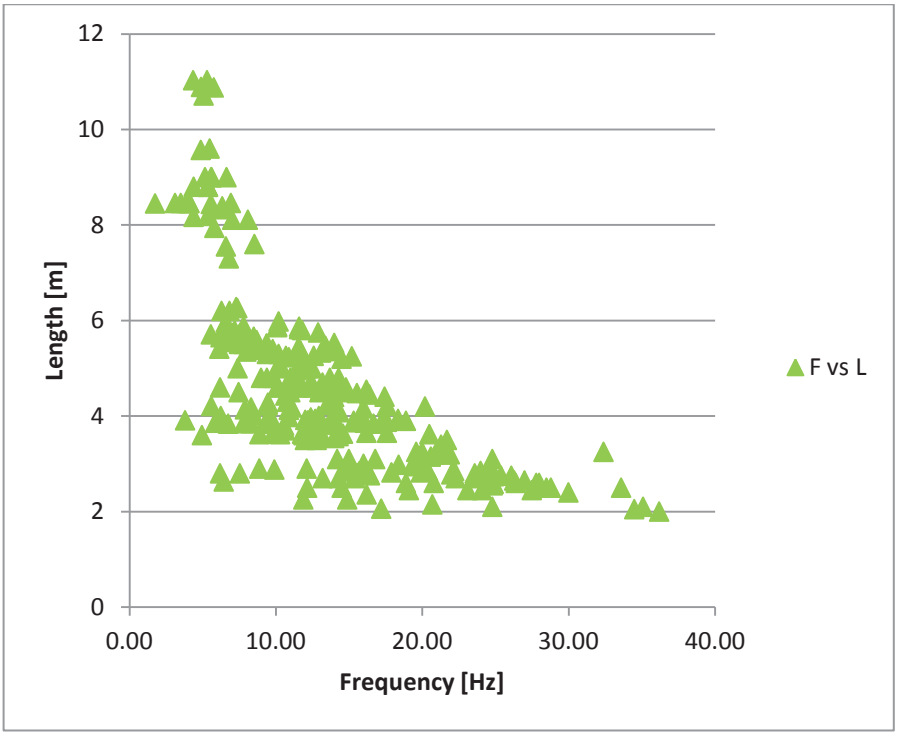

Fig. 17 – Database, Frequency – length relation for rectangular ties.

- When analyzed the stiffness of the constrains, it has to be considered that the relation between boundary conditions and the stiffness of the constraints is linked to the flexural stiffness of the chain and to its length. So the grade of constrain is compared with the following variable:
- Index **L** (Facchini et Al., 2003) [1]

$$L = \frac{EJ}{lk} \tag{2.55}$$

The Author specifies that for L< 0,015 the constrains is fixed-fixed, and for L> 1,0 the constrains is pinned-pinned.

Finally the combination of the studies carried out on the database, and the FEM model, it can be drawn some conclusions:
- The highest the axial force to which the tie is subjected the higher the frequency of vibration.
- For the same axial force, the frequency increases when the boundary condition changes from pinned-pinned to fixed-fixed.
- The longest the tie, the lower the first frequency gets.

2.6.1 Current Analysis on the Database

Based on the observations and studies carried out on the database, and considering the different dynamic techniques studied in the section before, the database was used to prove some of the

methods that were tested and turn out to have a satisfactory response, being those the method of Luong [11] and the method of Tullini [9].

If are considered the variables determined on the method propose by Tullini which are *n (adimensional axial force)* and *λ*, variable that depends only on the geometric characteristics of the tie and its circular frequency, and both are graphed against each other, it can be obtained the Fig. 18.

It must be noted that the adimensional axial force was calculated using the Axial force obtained by the theory of the wire-rod for both extremes cases, pinned and clamped.

The resulting graph shows the relation between the two variables for the two extremes boundary conditions PP and FF for all the rectangular tie from the database. The tendency lines show the potential function, grade four, of these two boundaries. Meaning that all the intermediate cases of boundary conditions should find it curve inside these limits.

One observation should be done on the graph and is that it is based on the wire-rod theory which neglects the stiffness of the support ends, reason why the graph depicts an incongruence with the current methods. In the Fig. 18 it can be seen that for higher values of axial force, there is a significant difference between the two boundary conditions when in fact as the value of the axial force gets higher the estimation is no longer dependent on the boundary conditions as it is shown in Fig. 19. The latter was developed to determine the admissible data allowed by the method (*Tullini, 2008)*, and is showing how the lower dotted line, that represents the clamped situation, gets closer to the upper one that represents the pinned condition, yielding the conclusion that as tighten the tie gets the less influence the boundary condition has in its response.

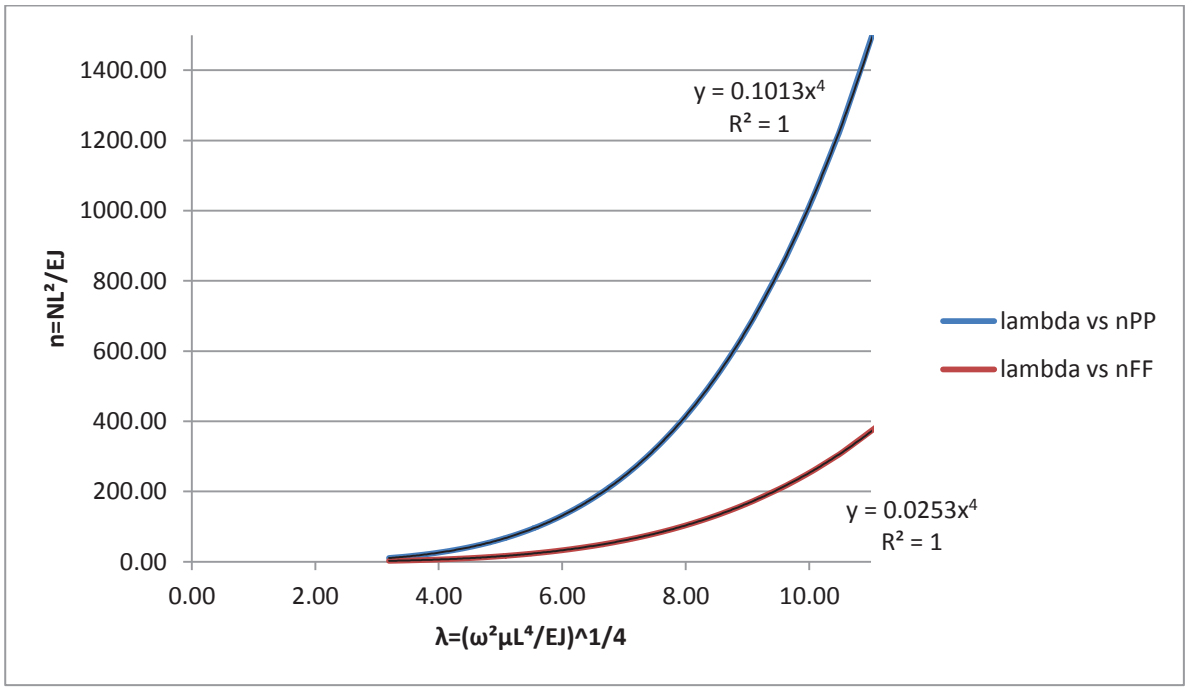

Fig. 18 – Tullini Method – λ vs n

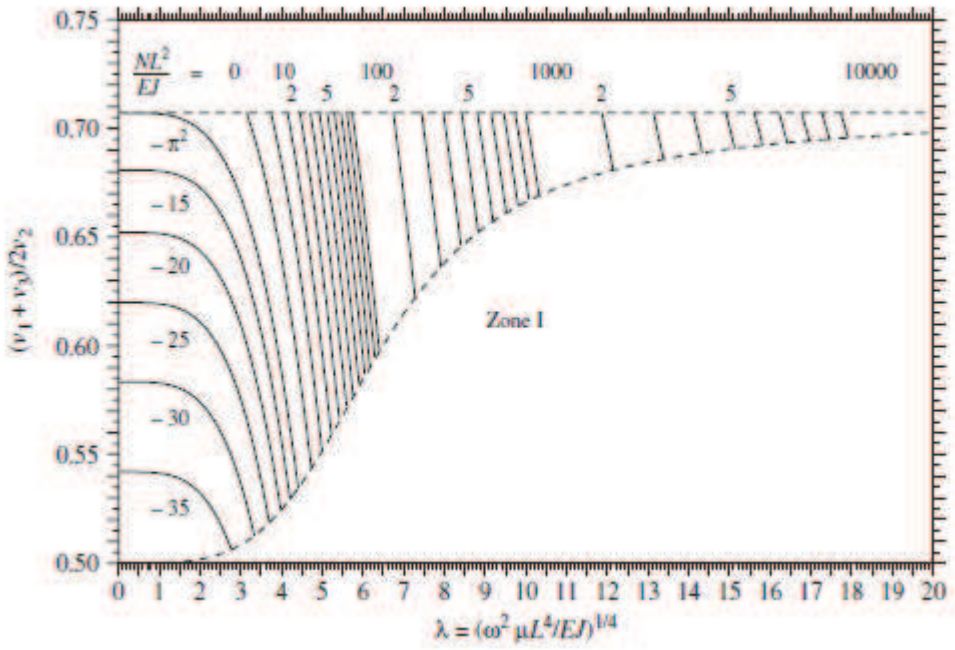

Fig. 19 – Tullini, 2008 – Ratio $(v_1+v_2)/2v_2$ versus λ for the first vibration frequency, for some given values of *n* – Dynamic identification of beam axial loads using one flexural mode shape.

Analysing all the ties of the database with the Charts built by Luong [11], and following the some procedure describe before to build the curves considering the variable of Tullini method, it was obtained Fig. 20.

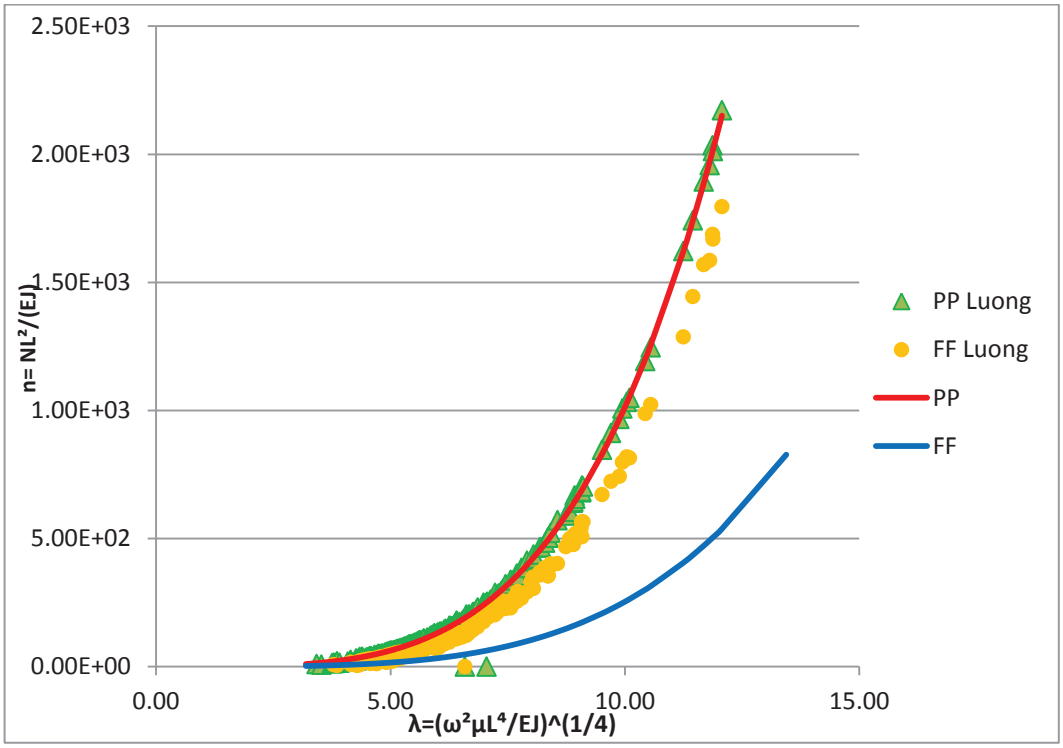

Fig. 20 – λ vs n - Comparison between the wire-rod theory and Luong's method.

The values of both are based on the axial force obtained by applying the theory of the wire, what means the tie is considered as a chain. However as it observed that the values obtained by applying the Charts I and III reveals values much more accurate with the stream of thought of the current dynamic methods, the values for the both extremes conditions are no longer apart as the adimensional axial force grows. Which allow concluding that even though the method of Luong is based on a theory that is not matching the real behaviour of the ties, the calibration done, by means of experimental testing and FEM parameterization, led to a better and accurate estimation of the axial force.

After being analyzed the different methodologies, the analytical method that showed the best performance was the one developed by Tullini. Method that in addition to its good response it can be considered as one of the simplest set up.

3. CASE STUDY: CASTEL SAN PIETRO.

To evaluate the performance of the dynamic methodologies to estimate the axial force, it was carried out an onsite test. The aim of the test was to define and clearly establish the difficulties that can be faced when the analytical method are translated to on sites tests and to which extend it can be influence the estimation.

3.1 Description of case study

Castel San Pietro is located in the city of Verona; the design of the building is in neo-Romanesque style. The Castle was built over the ruins of a Church, with a Military purpose, known as Habsburg Barracks. In Fig. 21 are shown the plans of the Barracks from 1853.

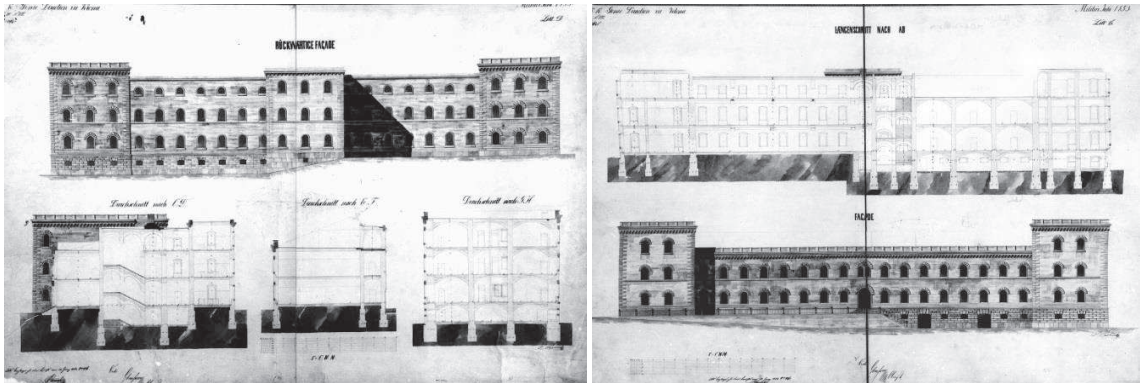

Fig. 21 – Plans of the barracks from 1853 – SAHC Integrated Project 14/15 [15]

The Habsburg Barracks, is composed of three parts in a line. The middle part is a three, partially four story building. The number of floors adjusts to the slope of the land. On the two sides two towers are standing with one additional floor on both sides.
The tests that hereafter are described were performed in the middle room of the second floor of the North-west Tower.

3.2 Description of the tie-rods

The dynamic identification test was performed on two ties, located in the room. One of the ties was an ancient one (T1), from the XIXth Century, embedded inside the vault of the room, uncovered during the setting for the vaults studies. The other one was a new tie (T2), set on the site as a tool to absorb the thrust of the vaults during the test carried out on them.
Tie T1 presents a cross section of 13 x 43 mm, and a length of 5,60 meters. Due to its position inside the vault can be detected an extensive damage on the surface of the tie making its cross section irregular and with presence of corrosion, as shown in Fig. 22. The ends are embedded in masonry walls of 80 cm thick but its boundary conditions are stated as unknown.

Fig. 22 – Damage observed in the ancient tie tested in Castel San Pietro, Verona.

Tie T2, a threaded rod M20, presents a circular cross section, with a diameter of 19.75 mm and a net area of 245 mm^2. The tension in the tie is regulated by a system of two hexagonal couplings, located at one meter from the ends, which are the union between the three rods that compound the tie.

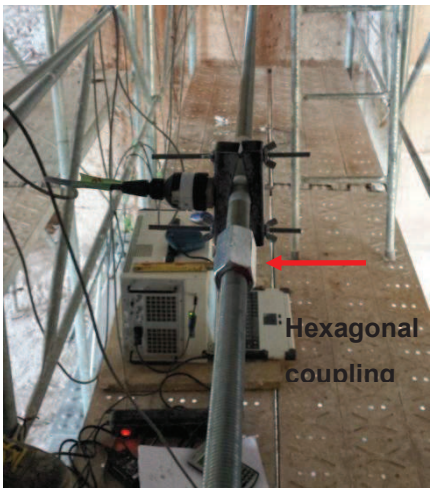

Fig. 23 – Nut

For both tie-rods, T1 and T2, it was assumed a density ρ=7850 kg/m^3 and the Young Modulus was assumed E= 210 Gpa.

3.3 Test set up

The set up of the test is composed by the central data collector (portable platform to 16 channels with a processor, hard disk, monitor and keyboard National Instruments mod NI PMA 1115 - capture cards Digital National Instruments mod. NI PXI 4472) and five acceleration sensors (PCB Piezotronics 393 B12) connected to the data collector by coaxial cables PCB 012R10 low impedance (length 3.0 m),

the management acquisition and gathering of the information is done by software developed in LabVIEW environment.

Fig. 24 – Acceleration sensor – PCB Piezotronics

Fig. 25 – Data collector NI PMA 1115

The methods that wanted to be tested were the ones developed by Tullini [9] and the improvement of the method developed by Rebecchi [12]. For the performance of the two methods, five accelerometers were used in the ties T1 and T2 in order to gather information that would allowed the analysis of both methods.

For the first method, Tullini, only three accelerometers were needed. One located in the middle and the other two in the quarters. For the Rebecchi method, two more other accelerometers needed to be added in the ends of the tie. Both set up are shown in Fig. 26.

The accelerometers were fasten to the tie by means of metallic wrappers (Fig. 24) and wired to a data acquisitions computer where it was recorded the ambient excitation and the impact excitation. The impact was generated manually by touching the tie-rods.

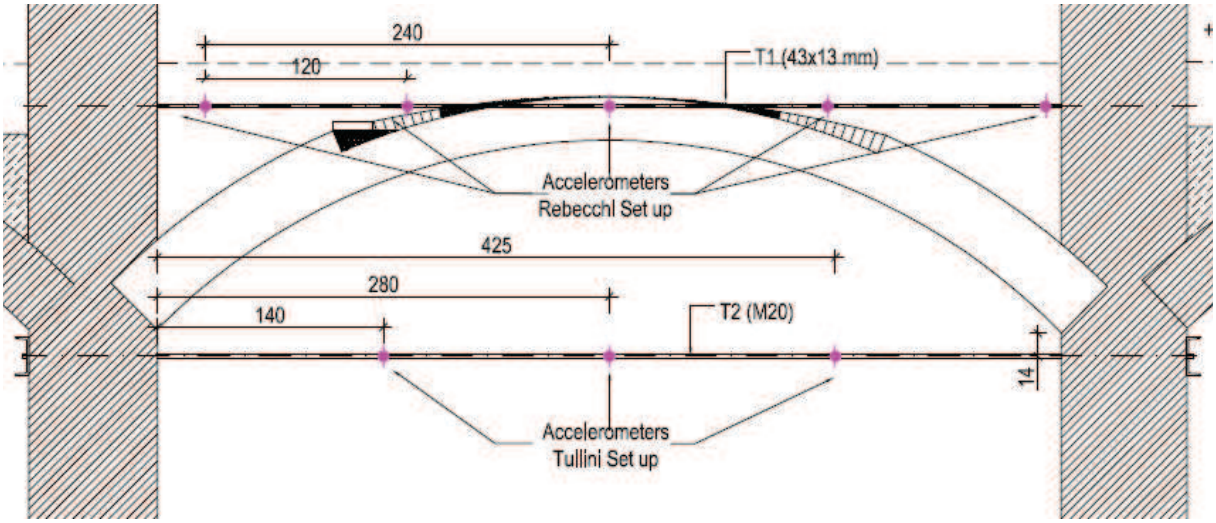

Fig. 26 – Set up of the accelerometer for both methods, Tullini and Rebecchi.

The type of analysis was based only on the response of the system considering an unknown input, in this case the manual excitation. The data acquisition was done with a resolution of 200 Hz, during 80 seconds. This resolution allowed an accurate identification of the three first natural frequencies of the ties. For each sampling case, ambient and force excitation, three acquisitions were gathered. This procedure was carried out for both dispositions, Tullini and Rebecchi.

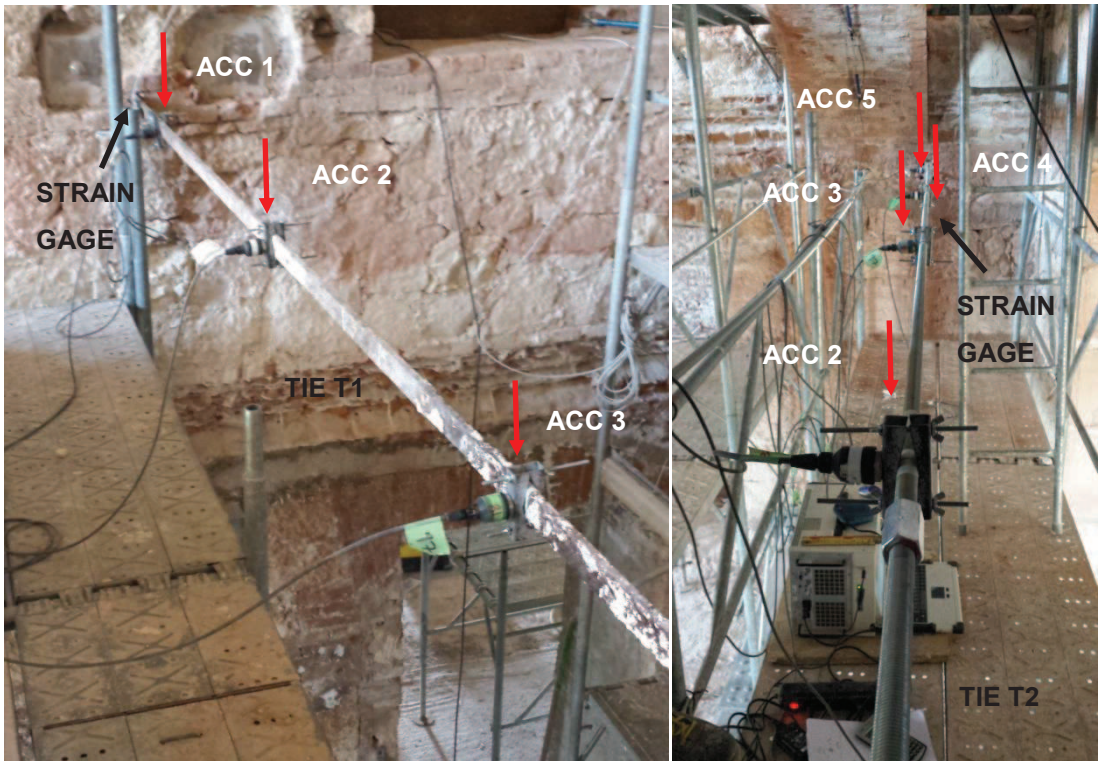

Fig. 27 – Instrumental display in T1 (left) and T2 (right)

In order to have an unbiased verification of the real axial force of the tie, a static verification was made through the measurements obtained through strain gauges, located on one of the extremities as shown Fig. 27.

For tie T1, the strain observed during the test was constant, however the real axial force cannot be assess using the strain because in order to obtain the variation of strain the tie should be released.

In the case of tie T2, since it is regulated from the two couplings, the strain can be measured and recorded for different situation. For this reason, three different conditions were analyzed, to identify the tension at which the tie was working in each case. These conditions were, completely loose, manually tighten using a wrench and finally an intermediate case achieved by releasing the tension of the tie.

3.4 Strain gauge for tie T2

The *strain* is defined as the deformation per unit length or fractional change in length and its equation form is $\varepsilon = \Delta L/L$, it can be observed that the strain is a ratio and, therefore, dimensionless. To maintain the physical significance of strain, it is often written in units of mm/mm. In practice, the magnitude of measured strain is very small. Therefore, strain is often expressed as microstrain, which is $\varepsilon \times 10^{-6}$.

While there are several methods of measuring strain, the most common is with a strain gage, a device whose electrical resistance varies in proportion to the amount of strain in the device. The most widely used gage is the bonded metallic strain gage.

The metallic strain gage consists of a very fine wire or, more commonly, metallic foil arranged in a grid pattern. The grid pattern maximizes the amount of metallic wire or foil subject to strain in the parallel direction (Fig. 28). The cross-sectional area of the grid is minimized to reduce the effect of shear strain and Poisson Strain. The grid is bonded to a thin backing, called the carrier, which is attached directly to the test specimen. Therefore, the strain experienced by the test specimen is transferred directly to the strain gage, which responds with a linear change in electrical resistance.

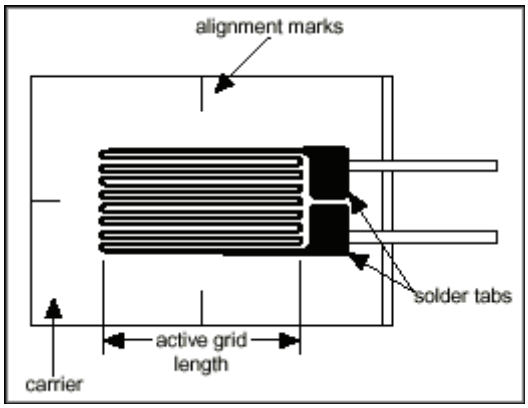

Fig. 28 – Bonded Metallic Strain gauge

The stress, at which the tie is subjected to, is obtained through the *stress-strain relationship.* $\sigma = E \cdot \varepsilon$. According to the stress obtained, it can be calculated the axial force of the tie $N = \sigma \cdot A$.

3.4.1 Strain controlling value

For the case study, there were used two strain gauges, one per each tie, to determine the internal stress on the tie during the dynamic identification test, and then verify the accuracy and veracity of the axial value obtained through the method aforementioned.

In the case of T1, the strain gathered was constant, or with a small variation, during the test. However, since the T2 has the regulation device, to have a certain level of control of the tension at which the tie was being subjected a procedure for controlling the tensile forces applied to the tie-rod was carried out.

• Before applying any tensile force, the stain of the loosen tie was collected from the strain gauge set on the tie and the tensile stress σ_0 was calculated.

• Since the fasten of the ties was performed manually with a wrench, after it, the strain was again collected and the $\Delta\sigma$ was calculated by means of $\Delta\varepsilon$;

• For the intermediate case, the regulation device was release, while the strain was monitor until it reached an average value. The average value was selected to be in between the last two measurements made. Again with the value obtained $\Delta\sigma$ was calculated.

The values obtained allowed the verification of the accuracy of the method use to estimate the axial force on the tie T2.

In order to get to know the properties of the joint, where the strain was being measured, it was performed a pulling test on the coupling. The test consisted in the joint of two bars with the coupling of the experimental testing, and it was subjected to an axial force, allowing the construction of the curve tension-deformation. From the curve was possible to define the young's modulus E=215.85 Gpa. Also it was possible to define the net area of the element as 465.3 mm^2. These parameters were used to calculate the real tension on the tie at the moment of testing, which are displayed in Table 5 .

Axial Force obtained with strain gauge T2								
ID	Young Modulus	Area	Strain			Axial Stress	Axial Force	Axial Force
	E [N/m2]	A[m2]	$\varepsilon_{initial}$	ε_{final}	$\Delta\varepsilon$	σ [N/m2]	N [N]	N [KN]
CSP_T2_L	2.16E+11	0.000465	-	1100	-	-	-	-
CSP_T2_I	2.16E+11	0.000465	1100	1175	0.000075	16188750	7533	7.53
CSP_T2_T	2.16E+11	0.000465	1100	1265	0.000165	35615250	16572	16.57

Table 5 – Static analysis of T2

3.5 Signal Processing

The information recorded during the dynamic identification, was processed in ARTeMIS Extactor 4.0 software [16]. The software is a tool for effective modal identification for the cases where the output is known, meaning acquisitions in environmental conditions or forced conditions. The frequency

response functions (FRF), are obtained by means of Fast Fourier Transformation (FFT), which convert the results from the time domain to the frequency domain.

To identify the characteristics of the tie in the frequency domain, meaning the natural frequencies of vibrations, is used the Frequency Domain Decomposition (FDD) technique, as seen in Fig. 29 and Fig. 30. The technique performs an approximate decomposition of the system response into a set of independent single degree of freedom systems one for each mode. The decomposition is performed by decomposing each of the estimated spectral density matrices, and the singular vectors are estimated of the mode shapes. The modes are obtained purely by signal processing.

Each forced acquisition, for each tie, was processed with this software, and in the case of the acquisition gathered with the Tullini layout, three natural frequency and corresponding mode shapes were obtained. For the signal acquire with the Rebecchi layout, five natural frequencies and modes shapes were extracted.

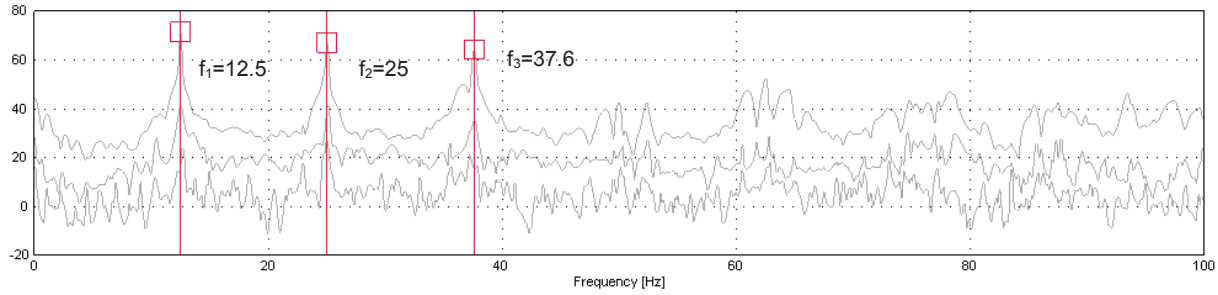

Fig. 29 – Peak-picking of the first three frequencies for T1 for Tullini Method

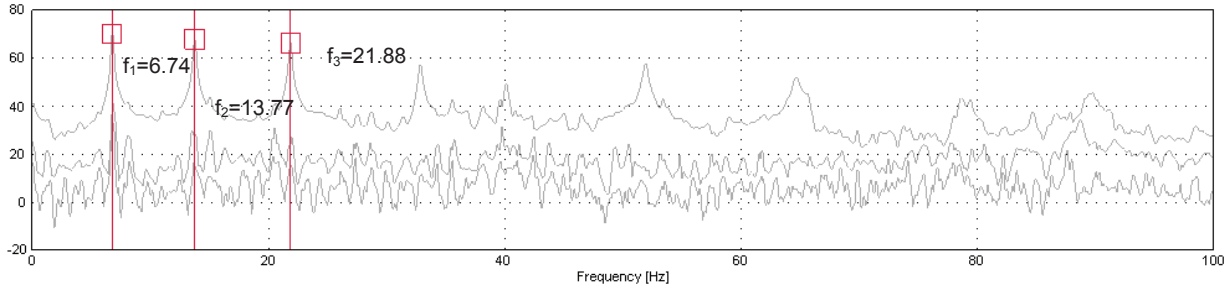

Fig. 30 – Peak-picking of the first three frequencies for T2 for Tullini Method

3.6 Finite Elements Model

In addition to the static verification carried out as aforementioned, a FEM model was developed using FX+ for DIANA software [17]. The tie was modelled as a beam with uniform cross-section (rectangular 43 x 13 mm) of 5.6 meter length, with a pinned-pinned condition and subjected to a constant axial load. The model has 28 elements and 29 nodes. The density assumed for the model was 7850 kg/m3, the Poisson ratio 0.3 and the Young's Modulus E= 210.0 Gpa.

To verify the validity of the methods, Tullini and Rebecchi, the axial force calculated is the one assumed for the model.

A non linear analysis was performed on the model, and at the same time the eigenvalue analysis was carried out to obtain the natural frequencies and mode shapes of the structure. These mode shapes obtained for the FEM model are then compared with the experimental ones, measure of site with accelerometers. The degree of correlation between the values is obtained through a Modal Assurance Criterion (MAC).

	LOOSE CONDITION		***INTERMEDIATE CONDITION***		***TIGHTEN CONDITION***	
	$f_{ON\ SITE}$ [Hz]	f_{FEM}[Hz]	$f_{ON\ SITE}$ [Hz]	f_{FEM}[Hz]	$f_{ON\ SITE}$ [Hz]	f_{FEM}[Hz]
MS 1	1.76	1.55	5.57	6.21	6.84	7.12
MS 2	4.59	4.78	11.33	12.95	13.77	14.71
MS 3	9.38	10.06	18.36	20.66	21.88	24.62

Table 6 – Comparison of the frequencies obtained onsite and obtained with FEM models for T2.

	T1	
	$f_{ON\ SITE}$ [Hz]	f_{FEM}[Hz]
MS 1	12.50	11.81
MS 2	25.00	23.85
MS 3	37.60	36.37

Table 7 – Comparison of the frequencies obtained onsite and obtained with FEM models for T1.

3.7 Modal Assurance Criterion (MAC)

The modal assurance criterion is defined as a scalar constant relating the degree of consistency between one modal and another reference modal vector as follows:

$$MAC(\varphi_{iA}, \varphi_{iB}) = \frac{\left|\{\varphi_A\}_i^T \{\varphi_B\}_j\right|^2}{\{\varphi_A\}_i^T \{\varphi_A\}_j \{\varphi_B\}_j^T \{\varphi_B\}_j} \quad (3.1)$$

The MAC takes on values from zero, representing no consistent correspondence, to one, representing a consistent correspondence. In this manner, if the modal vector under consideration truly exhibits a consistent, linear relationship, the modal assurance criterion should approach unity and the value of the modal scale factor can be considered reasonable.

The modal assurance criterion can be used to verify and correlate an experimental modal vector with respect to a theoretical modal vector (eigenvector).[18]

For this study, the MAC correlation would be carry out to determine the accuracy of the Method to estimate the axial force by using the output data of the onsite test, and comparing it with the results of the FEM model, where the ties is subjected to the estimated Axial force calculated with the Method.

3.8 Analysis of the Results

As it was explained in Section 2.4.5 and 2.4.8, the methods procedures were followed to obtain the estimation of the axial force of the tie T1. In Table 8 are shown the geometric characteristics of the ties that were tested, and the data gathered and processed, for each tie. In the case of tie T2, there are three cases, where CSP_T2_L stands for the loosen condition, CSP_T2_I stands for the intermediate case of stress, and finally CSP_T2_T refers to the tighten situation of the tie.

ID	*Type*	*L[m]*	*h [m]*	*b [m]*	*A[m2]*	f_1	f_2	f_3	v_o	v_1	v_2	v_3	v_4
CSP_T1	Rect.	5.6	0.043	0.013	0.000559	12.5	25	37.6	-	0.491	0.724	0.485	-
CSP_T2_L	Circular	5.6	0.01975	-	0.000245	1.76	4.62	9.38	-	0.513	0.729	0.454	-
CSP_T2_I	Circular	5.6	0.01975	-	0.000245	5.57	11.4	18.4	-	0.538	0.680	0.498	-
CSP_T2_T	Circular	5.6	0.01975	-	0.000245	6.84	13.8	21.9	-	0.533	0.686	0.496	-

Table 8 – Geometric characterization of the tie-rods tested and the data gathered

ID	Type	L[m]	h/D [m]	b/d [m]	f_1[Hz]	N_{PP} [KN]	N_{FF}[KN]	N_{tull}[KN]	N_{Reb}[KN]
CSP_ T1	Rectangular	5.6	0.043	0.013	12.5	86.01	21.50	76.26	96.02
CSP_T2_L	Circular	5.6	0.01975	-	1.76	0.75	0.19	0.02	-
CSP_T2_I	Circular	5.6	0.01975	-	5.57	7.48	1.87	9.03	15.08
CSP_T2_T	Circular	5.6	0.01975	-	6.84	11.17	2.79	11.81	-

Table 9 – Axial Force estimation with the wire-rod Theory, Tullini Method and Rebecchi Method.

The axial force was estimated with three different methods, Tullini, Rebecchi and the Chain theory. It can be observed that for T2, as the tension on the tie gets higher, the difference between the estimation of the Axial force with the method of Tullini and the theoretical value calculated for pinned-pinned condition, gets smaller. At the same time the values obtained for T1 are close to the value of the theoretical calculation for pinned condition.

The comparison demonstrates the inaccuracy obtained with the chain method if the boundary conditions are not properly assess.

3.8.1 MAC correlation T1

The mode shapes obtained after processed the information gathered, were compare with the mode shapes obtained through the FEM model for the pinned pinned condition, an using as input the load estimated with the analytical method. The results are shown in the following table and graphs.

	MAC		
	1	2	3
1st MS	0.999	0.000	0.001
2nd MS	0.000	0.997	0.003
3rd MS	0.005	0.005	0.990

Table 10 – MAC for Tullini Method, tie T1

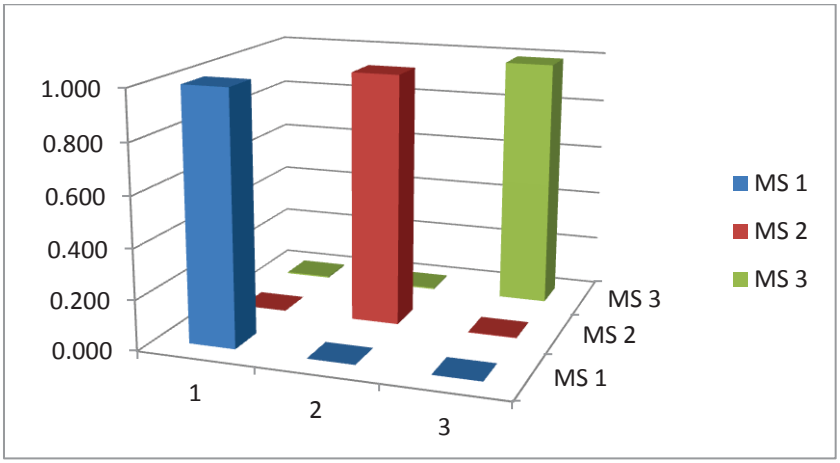

Fig. 31 – MAC Correlation between Tullini Method and FEM – Tie T1

	MAC				
	1	2	3	4	5
1st MS	0.99	0.00	0.01	0.13	0.04
2nd MS	0.00	0.99	0.02	0.13	0.11
3rd MS	0.03	0.08	0.98	0.11	0.02
4th MS	0.13	0.18	0.05	0.99	0.02
5th MS	0.00	0.00	0.07	0.10	0.89

Table 11 – MAC for Rebecchi Method, tie T1

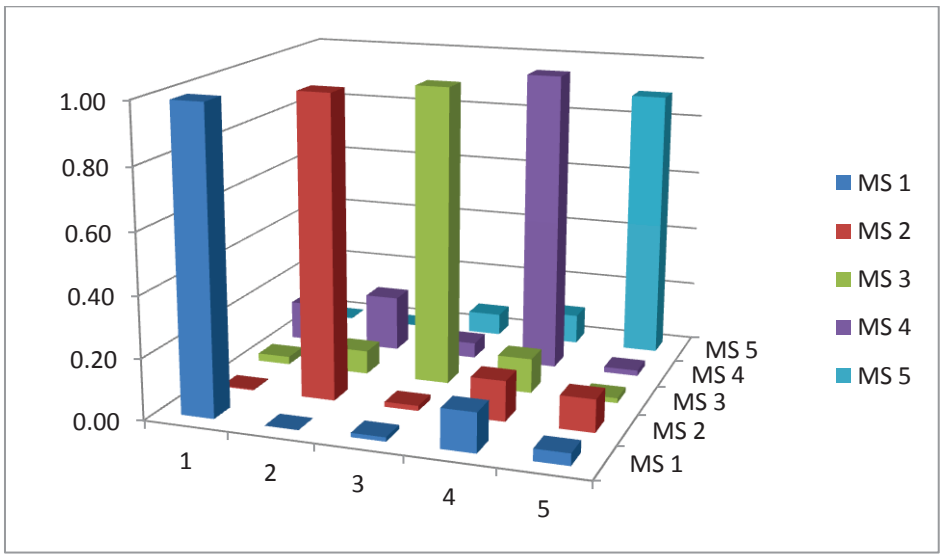

Fig. 32 – MAC Correlation between Rebecchi Method and FEM – Tie T1

From the correlation obtained through the MAC it can shed some light regarding the performance of the method analyzed, Tullini Method shows much more accuracy in its correlation with the FEM model than the Rebecchi Method where it can be appreciated some non zero values on non diagonal places.

Which can be explained in the resolution use for the acquisition during the tests, which were enough for defining accurately the first three modes but not higher, as required by that method.

Complementing the values obtained with the analytical model, which compared with the theoretical model for the pinned conditions were of similar value, plus the great correlation seen with the MAC, it can be conclude that the boundary condition of T1 although unknown it was closer to a pinned condition.

From here it can be said that the definition of the boundary condition of real cases can change drastically the results obtained. The hypothesis of the rotational stiffness of the boundary condition cannot be taken as a light matter.

3.8.2 MAC correlation T2

The same correlation was done for T2 between the experimental data and the numerical model done in FEM.

	MAC		
	1	2	3
1st MS	0.996	0.004	0.000
2nd MS	0.004	0.996	0.000
3rd MS	0.000	0.009	0.991

Table 12 – MAC for Tullini Method, T2 Loose condition

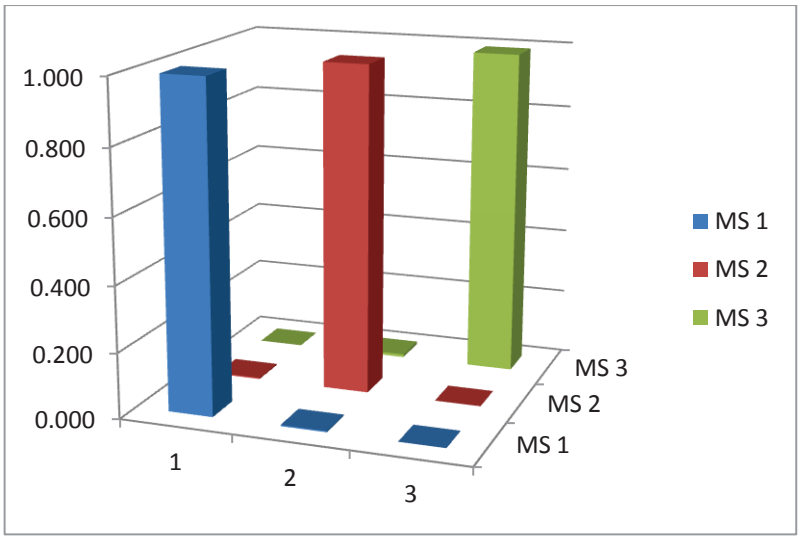

Fig. 33 – MAC for Tullini Method, T2 Loose condition

	MAC		
	1	2	3
1st MS	0.998	0.001	0.001
2nd MS	0.003	0.997	0.000
3rd MS	0.016	0.000	0.984

Table 13 – MAC for Tullini Method, T2 Intermediate condition

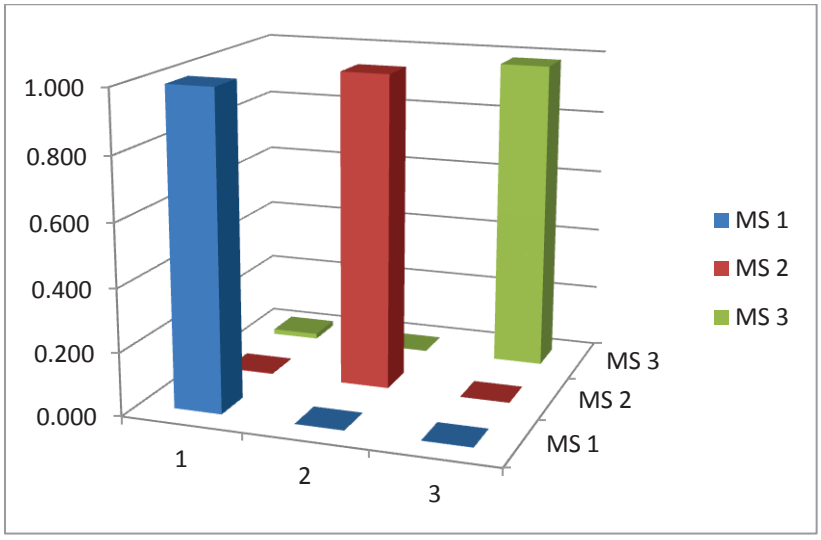

Fig. 34 – MAC for Tullini Method, T2 Intermediate condition

	MAC		
	1	2	3
1st MS	0.999	0.000	0.000
2nd MS	0.000	0.996	0.004
3rd MS	0.020	0.000	0.980

Table 14 – MAC for Tullini Method, T2 Tight Condition

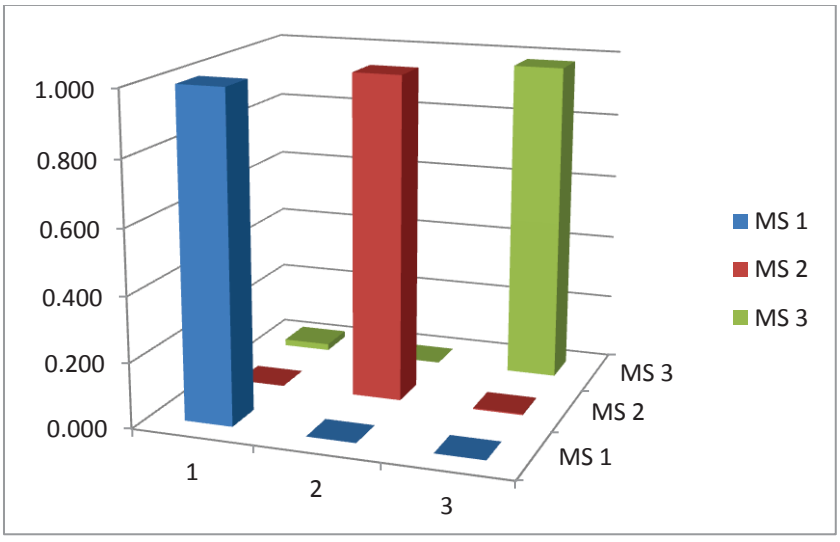

Fig. 35 – MAC for Tullini Method, T2 Tight Condition

The FEM model built for the analysis of the ties shows a good accuracy since the values obtained are similar for frequencies, and it has been obtained a good correlation in the MAC matrices between the modes shapes measured experimentally and the ones obtained with the FEM model.

Again as it was explained for T1, the election of a FEM model with a boundary pinned condition, was based on the similarities of results obtained for theoretical and analytical values. However the non

zero values in the non-diagonal places in the matrix, help to determine that even though the values are similar the boundary condition is not exactly pinned but nearly.

3.8.3 Comparison between different methods

After being obtained the estimated axial force through the method described, an extra method was performed to verify the others aforementioned. The method of Loung was carried out, making use of the Charts I (pinned-pinned condition) and the chart III (fixed-fixed) to estimate the axial force. The results for the tie T2 in the intermediate condition and the tighten condition, are compared in the following table.

	WIRE THEORY		***STATIC***	***TULLINI***	***REBECCI***	***LUONG METHOD***	
ID	N_{PP} [KN]	N_{FF}[KN]	N [KN]	N_{tull}[KN]	N_{Reb}[KN]	N_{PP} [KN]	N_{FF}[KN]
CSP_T2_I	7.48	1.87	***7.53***	***9.03***	15.08	6.81	3.31
CSP_T2_T	11.17	2.79	***16.57***	***11.81***	-	10.62	6.41

Table 15 – Comparison of the results obtained through different methods for T2.

In Table 15 are compared the values obtained by the theoretical equation of the wire-rod theory, the values obtained through the static method, and the three dynamic method,Tullini, Rebecchi and Luong, analyzed in Section 2.4,

The results shed some light on a number of issues:

- The higher the tension in the tie the more accurate the values between the estimation of the studied methods. This can be seen in the values obtained from all the methodologies are similar for the T2 T, which is the most tight condition studied.
- Even though Luong Method is obtained from the wire-rod theory the range of values is narrower than the range from the wire-rod similar. However the estimation with this method reveals lower values that the other two methods. The possible cause for this is the lack of curve corresponding with the ratio between the geometrical parameters of the tie.
- Even though the performance of the dynamic tests showed consistency in the results, the difference between the estimations and the axial force obtained through the static analysis of the tension is an issue that has to be considered in further investigations.

3.9 Conclusion

The onsite testing allowed the definition of the current problems faced when a historical tie has to be assessed. The main issues before starting were the definition of the length, as to know the right location of the sensor. It must be remained that the authors [9] recommend the positioning of the sensor in the quarters and middle, for which is important to establish the real length of the tie. This definition led to the main issue that was the definition of the boundary condition.

Finally the procedures performed on field allowed the verification of their simplicity, when talking about the setting of the equipment needed to gather the information, and also the procedures showed to be expeditious as to process the information and obtained the estimation of the axial force.

In addition, the method showed coherence between the results of the estimation, even though that there is a difference with the static method that should be taken into account when assessing the axial force.

The application on field proves, beside the possible error on the estimation, an economic and expeditious way to estimate the axial force, since it does not required neither the need of sophisticated equipment nor is numerically complex.

4. EXPERIMENTAL TEST IN LABORATORY

Taking into consideration the experience of the onsite testing of a historical tie in the Castel of San Pietro, Verona (see Section 3), a series of experimental test in the laboratory were planned in order to determine how the different variable, such us boundary conditions, stiffness and length, influences the estimation of the axial force.

4.1 Test set up

A series of experimental laboratory test were carried out to verify and validate the analytical models studied and used in the campaign.

The test was performed on a tie with a rectangular cross-section of 40.43x15.38 mm, obtained as an average from the measurement taken from the tie in three different sections, and a length of 4.82 meters. It was adopted a Young Modulus of E=210 Gpa and a density of ρ = 7850 kg/m^3.

The tests consisted in the pulling of a tie, with different boundary conditions, with a hydraulic jack to subject the tie to a certain axial force and perform a dynamic identification by an impact excitation. Set up of the test is illustrated in

Fig. 36.

To assure the capability of the test to experience different conditions of supports, at one end of the tie it was set a hinge system guaranteed by a bidirectional joint of a beam HEB140, which was anchored to the concrete wall of the laboratory as seen in Fig. 37. The axial load was induced to the beam by a hydraulic jack, which at the same time was controlled by the load cell (CL1000 mV/V 2.0000) that was also located in the same end, as show in Fig. 38. The details of the connection of the beam HEB 140 to the wall, and the detail of the devices of regulation of the stiffness of the supports used to perform the tests for different boundary conditions can be seen in Fig. 39.

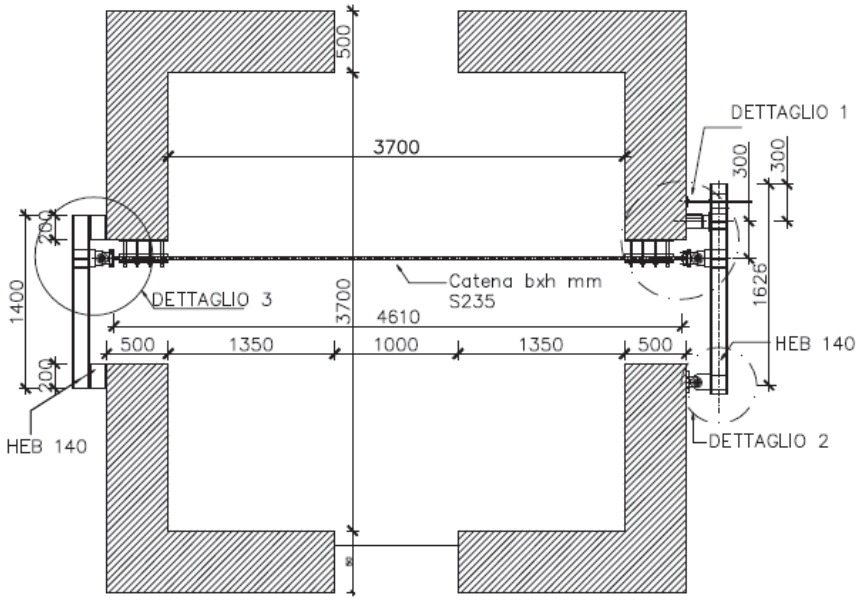

Fig. 36 – Layout of the Laboratory test.

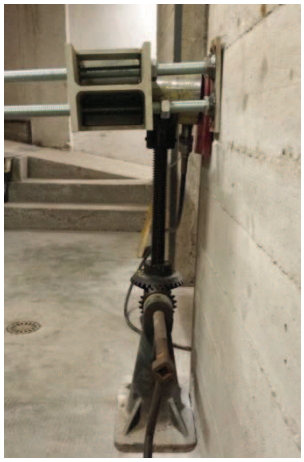

Fig. 37 – Profile HEB140 attached to the concrete wall and hydraulic jack.

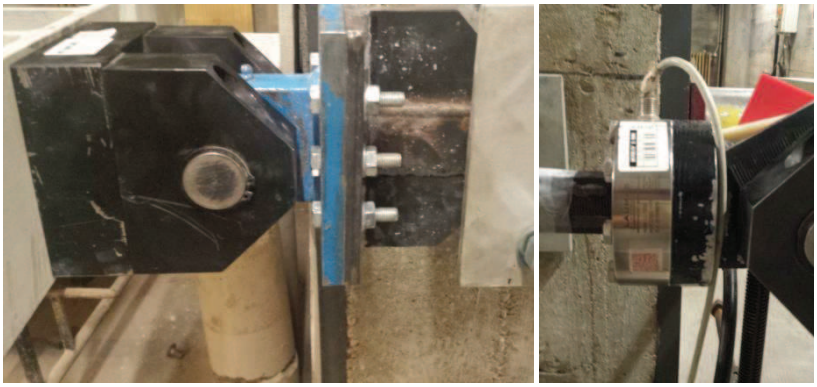

Fig. 38 – (Left) Hinge system – (Right) Load Cell

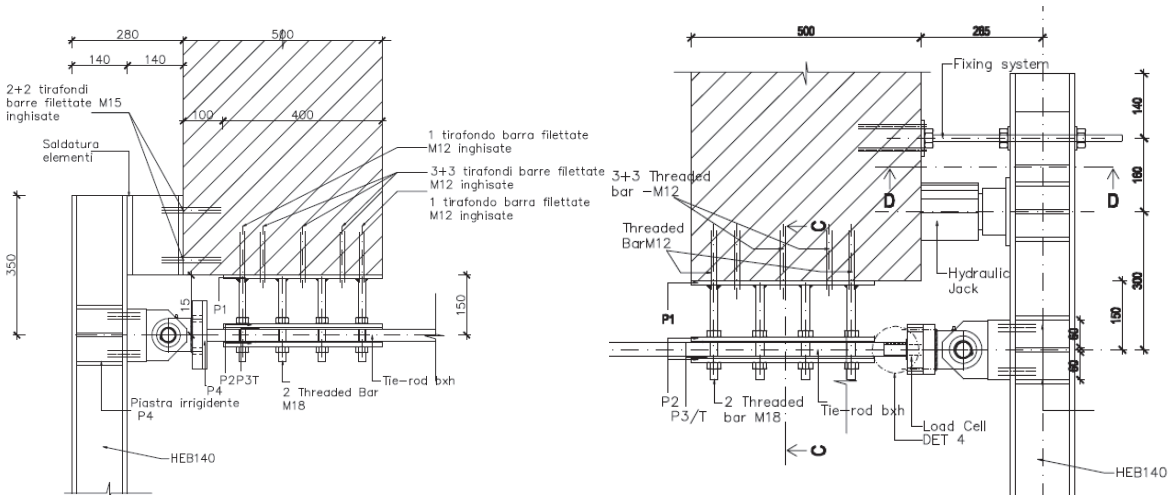

Fig. 39 – Details of the connection and regulating device to determine the boundary condition of the tie for each test.

4.2 Procedure

The analysis was based on the study of the response of the system considering an unknown load. The set up of the test is composed by the central data collector (National Instruments mod NI 4472) and the fixing of acceleration sensors (PCB Piezotronics 393 B12) connected to the data collector by coaxial cables PCB 012R10 low impedance (length 3.0 m), the management acquisition and gathering of the information is done by software developed in LabVIEW environment, *Vibration analysis*.

The test involved five accelerometers to gather the response of the tie, which were fastened to the tie by means of metallic wrappers.

Since the method that was trying to be tested was the one proposed by Tullini, the position of the accelerometers were fixed on the quarters and the middle of the tie, as show in Fig. 40. The position of the accelerometers depends on the free length of the tie, therefore there are two situations to be considered, the first situation is the pinned condition, in which the length is considered from the eyelet of the hinge from one side to the one on the other, 4.82 meters length. The second disposition of sensors is shown in Fig. 41 which considers the length of the tie when the extremes are clamped, so the length is reduced. For the latter the position of the sensor is in the quarters and middle of the reduced length.

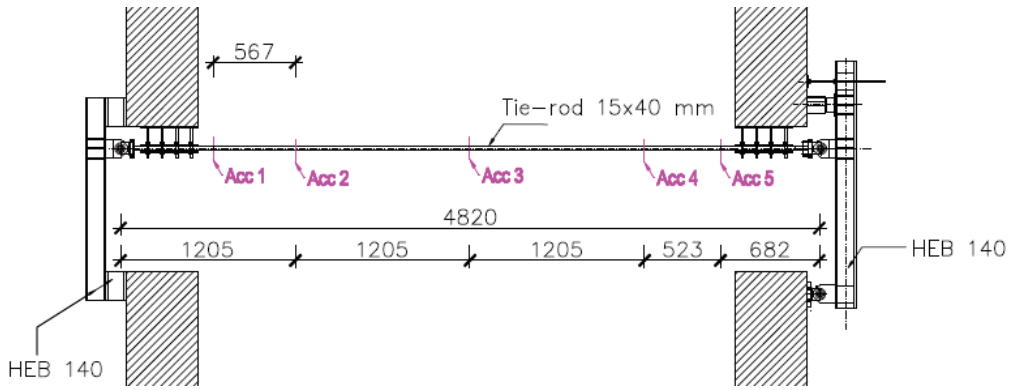

Fig. 40 – Position of the accelerometers to carry out the test with the method of Tullini and for a pinned-pinned boundary condition

In addition, the Rebecchi method was also tested in some of the cases as a comparison due to the similarly with the method being tested. For this case the accelerometers of the extremes were located at ten centimetres from the steel plates, one in the middle and the remaining two were set at equal distance from the previous ones.

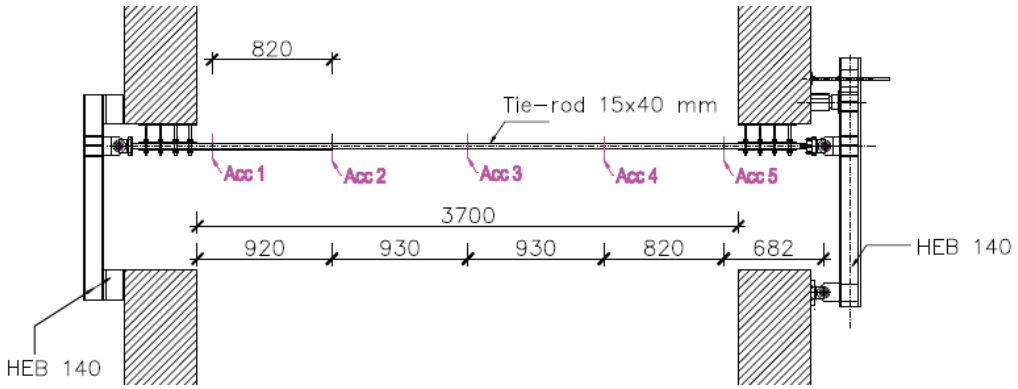

Fig. 41 – Position of the accelerometers to carry out the test with the method of Tullini and for a fixed-fixed boundary condition

The test also involves the setting of 3 LVDT to measure the displacements of the tie. The transducers were placed in the middle point and at twenty centimetres from the steel plate, as show in Fig. 42. The devices enable the performance of the static method applying the method of Briccoli [5]. The transducers were recording the displacement of the tie when a perpendicular force was applied with a load cell (WAGEZELLE Typ U2A 1KN = 2 mV/V) as show in Fig. 43.

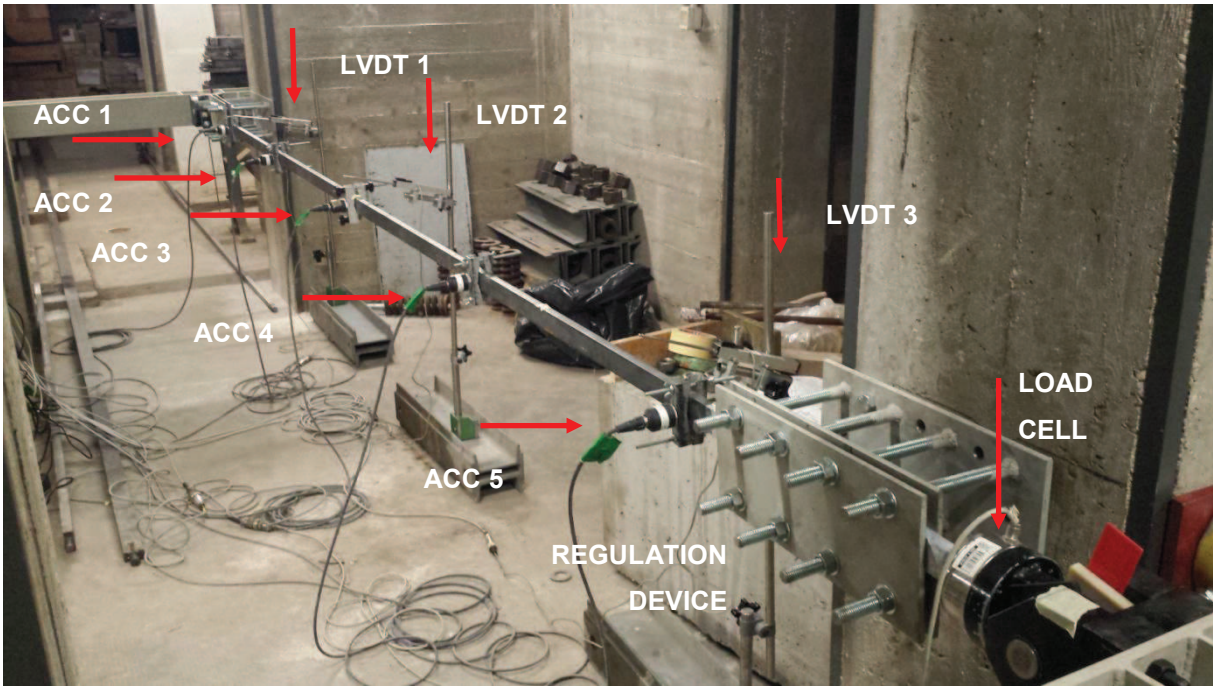

Fig. 42 – Position of the instruments used during the testing

The dynamic test was performed by gathering the response of the ambient vibration and a forced excitation. The latter was obtained by hitting manually. Each type of acquisition was gathered twice, to perform an average of the response. The data acquisition was done with a resolution of 1000 Hz, during 180 seconds. The information was processed in ARTeMIS Extactor 4.0 software and the

frequency response functions (FRF), were obtained by means of Fast Fourier Transformation (FFT), which convert the results from the time domain to the frequency domain, extracting the first three natural frequencies of vibration an its corresponding mode shapes.

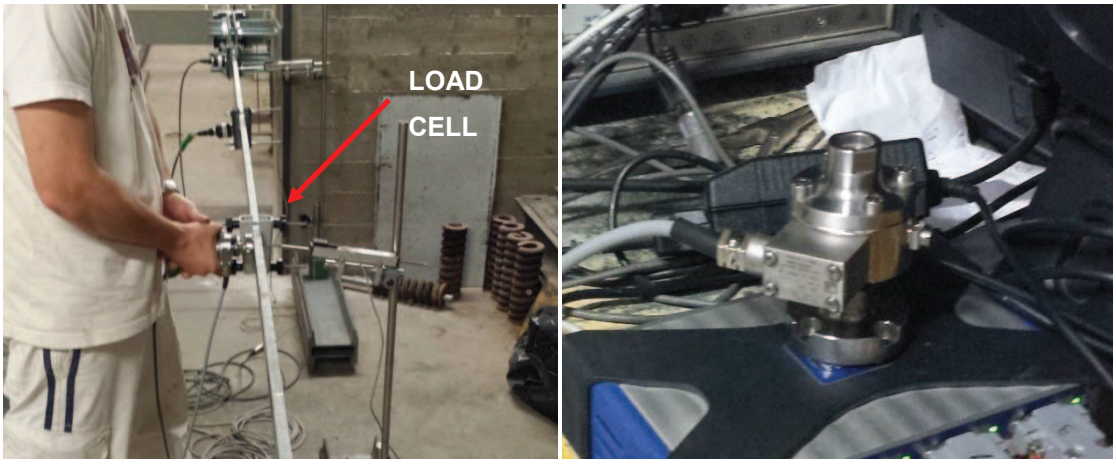

Fig. 43 – Load cell used for the static method

4.3 Boundary conditions and length

The tests were done in two stages. Firstly as it was planned, the tests were performed for four different boundary conditions which were pinned, fixed, and two more intermediate conditions, with unknown end stiffness.

The regulation of the boundary condition was achieved through a mechanism compound by two steel plates and a system of eight adjustable threaded bars, as shown in Fig. 44, with the interposition of sheets of Teflon, to avoid friction.

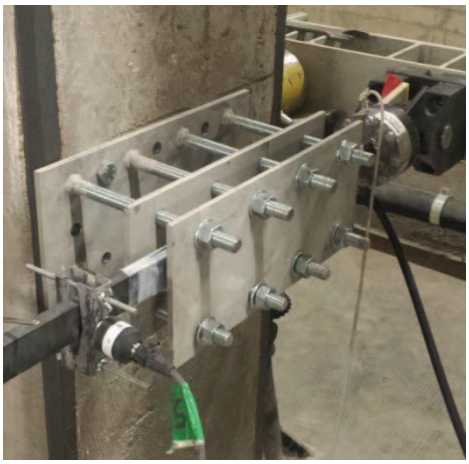

Fig. 44 – Regulation device of the boundary conditions

For the case of pinned condition (PP), the steel plate were left loose, without confining the tie, as shown in Fig. 45 (left). For the fixed condition (FF), the steel plates were screw together manually,

using a wrench to fasten as much as possible the screws (see Fig. 46), simulating a clamped support, as show in Fig. 45 (right).

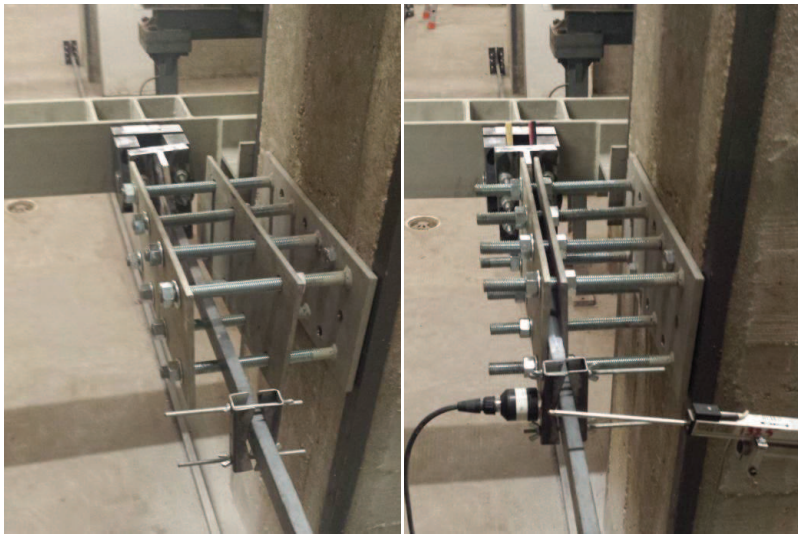

Fig. 45 – Boundary conditions (left) Pinned-Pinned (right) Fixed-Fixed

For some of the load steps, were analyzed two intermediate conditions, these conditions were achieved by releasing some of the nuts from the steel plate, allowing the movement of the tie inside the plate.

Fig. 46 – Fasten of the screw with a wrench

The second stage consisted in the division of the steel plates in four equal smaller plates, obtained by cutting the first plate into four pieces of 10 centimetres length as show in Fig. 47, tag as *B1, B2, B3* and *B4*.

This new set up allowed the variation of the end stiffness by fastening one plate at the time, what led to a four new intermediate boundary conditions. Each at a time the individual plates were fastened, while the remaining three were left loose. The four boundary conditions are shown in Fig. 48.

Fig. 47 – New regulating device for boundary conditions

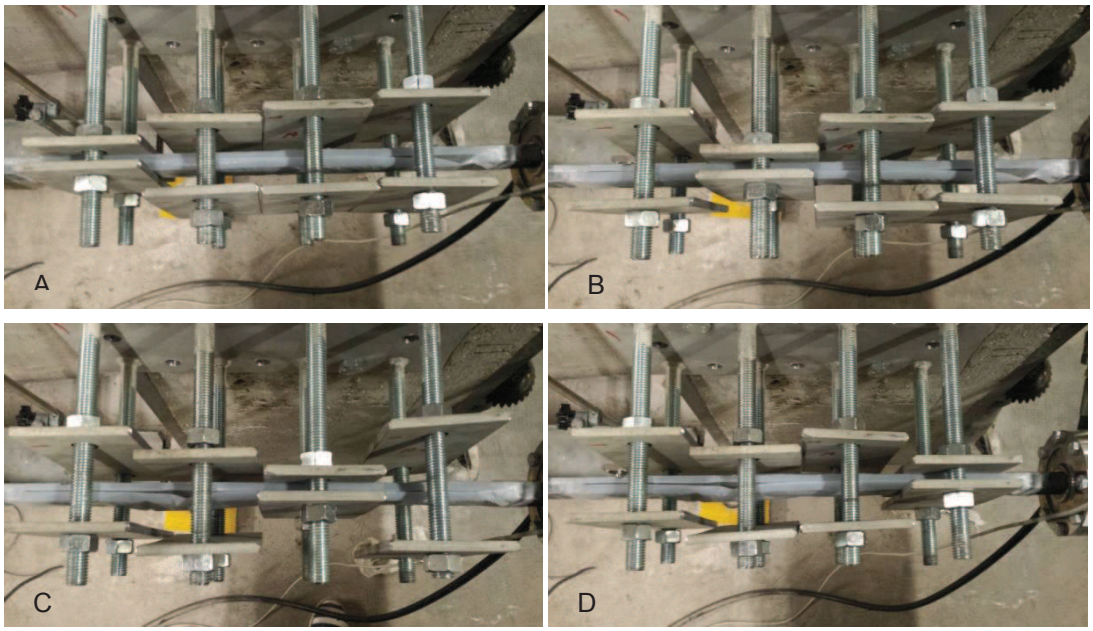

Fig. 48 – (A) B1 fastened, (B) B2 fastened, (C) B3 fastened, (D) B4 fastened.

The first case in which the plate B1 is tightened, the resulting case should be equal to the fixed condition, and the case in which the plate B4 is tightened the results should be similar to the pinned condition. This is because the translation of the fastened plate from B1 to B4 generates the decreasing of the stiffness of the support from fixed to nearly pinned.

As it was stated before, is important to highlight the fact that the length is an important variable for the accuracy of the result, reason why for each boundary condition different length were used to located the accelerometers to measure the dynamic response. In the case of PP the total length was used 4.82 meters and the three accelerometers were positioned in the middle and in the quarters. For the case of FF, considering that the confinement of the tie inside the plates is achieved, the length considered is the inner length between plates, meaning 3.68 meters. For the intermediate condition of

the complete plate, initially was assumed the some length as the FF condition, however, the release of the screw gave the tie some movement, making the real length higher than the one considered. For the intermediate condition of the separate plates, the length used was much more precise, since it was possible to use the complete length of the tie from the plates that were fastened. The procedure of tighten each at a time required the new positioning of the sensors with each new boundary condition. The lengths used were 3,68 meters for B1, 3.89 for B2, 4.09 for B3 and 4.24 for B4.

4.4 Load steps

The modal analysis test was performed with a desired value of the change in the axial force. The load steps performed were 0 KN – 20 KN – 40 KN – 60 KN – 80KN, and for each of them different boundary conditions were tested.

In the Table 16 are shown the different tests that were carried out, the identification name of each test announced the Method that was being tested, Tullini (Tull) or Rebecchi (Reb), the load step, and the boundary condition, pinned-pinned (PP), fixed-fixed (FF), intermediate condition 1 (IC1) intermediate condition 2 (IC2) involve the complete steel plate and partial intermediate condition 1 (PIC1), intermediate condition 2 (PIC2), intermediate condition 3 (PIC3), and intermediate condition 4 (PIC4), which are regarding the smaller steel plates B1 to B4, note that the P stands for partial.

In addition, it was performed a sensibility test considering different length of the ties, reason why for the cases of pinned condition for the load steps 40-60-80 KN there are tests tag as *New.* This tag stands for the case of the test in the pinned condition taking into consideration the real length on the tie, while the test for the same load step and boundary condition without the tag of new is associated with the test in which the length is the one between plates.

				Position of the accelerometer					
Nº	Nominal Load	Identification	Length Used	ACC11	ACC12	ACC13	ACC14	ACC15	Real Load
1	0	Tull_0KN_PP	4.8	-	1.2	2.4	3.6	-	0.000
2	20	Tull_20KN_PP	4.8	-	1.2	2.4	3.6	-	20.100
3	20	Tull_20KN_FF	3.68	-	0.92	1.84	2.76	-	20.800
4	20	Tull_20KN_IC1	3.68	-	0.92	1.84	2.76	-	21.060
5	20	Tull_20KN_IC2	3.68	-	0.92	1.84	2.76	-	20.006
6	20	Reb_20KN_FF	3.68	0.1	0.97	1.84	2.71	3.48	20.800
7	20	Reb_20KN_IC1	3.68	0.1	0.97	1.84	2.71	3.48	21.060
8	20	Reb_20KN_IC2	3.68	0.1	0.97	1.84	2.71	3.48	20.000
9	40	Tull_40KN_PP	4.8	-	1.2	2.4	3.6	-	40.009
10	40	Tull_40KN_FF	3.68	-	0.92	1.84	2.76	-	40.060
11	40	Tull_40KN_IC1	3.68	-	0.92	1.84	2.76	-	40.030
12	40	Tull_40KN_IC2	3.68	-	0.92	1.84	2.76	-	40.210
13	40	Reb_40KN_PP	4.8	0.66	1.53	2.4	3.27	4.04	40.002
14	40	Reb_40KN_FF	3.68	0.1	0.97	1.84	2.71	3.48	40.090

15	40	Reb_40KN_IC1	3.68	0.1	0.97	1.84	2.71	3.48	40.060
16	40	Reb_40KN_IC2	3.68	0.1	0.97	1.84	2.71	3.48	40.190
17	60	Tull_60KN_PP	4.8	-	1.2	2.4	3.6	-	60.025
18	60	Reb_60KN_PP	4.8	-	1.2	2.4	3.6	-	60.006
20	40	TullNew_40KN_PP	4.82	-	1.205	2.41	3.615	-	40.070
21	60	TullNew_60KN_PP	4.82	-	1.205	2.41	3.615	-	60.030
22	60	TullNew_60KN_FF	3.68	-	0.92	1.84	2.76	-	60.100
23	80	TullNew_80KN_PP	4.82	-	1.205	2.41	3.615	-	80.050
24	80	TullNew_80KN_FF	3.68	-	0.92	1.84	2.76	-	79.200
25	20	Tull_20KN_PIC1	3.68	-	0.92	1.84	2.76	-	20.400
26	20	Tull_20KN_PIC2	3.89	-	0.97	1.945	2.915	-	20.104
27	20	Tull_20KN_PIC3	4.09	-	1.0225	2.045	3.0675	-	20.480
28	20	Tull_20KN_PIC4	4.24	-	1,07	2.14	3.21	-	20.462
29	40	Tull_40KN_PIC1	3.68	-	0.92	1.84	2.76	-	40.423
30	40	Tull_40KN_PIC2	3.89	-	0.97	1.945	2.915	-	40.397
31	40	Tull_40KN_PIC3	4.09	-	1.0225	2.045	3.0675	-	40.250
32	40	Tull_40KN_PIC4	4.24	-	1,07	2.14	3.21	-	40.157

Table 16 – Test performed in the laboratory.

4.5 Uncertainties

During the performance of the test, there were a number of parameters that were assumed or were established as unknown.

The first uncertainty is related to the non-uniform distribution of the applied tensile force on the tie's cross-section. Even though there were set two strain gauges on the intrados an extrados of the middle section of the tie, the lack of stability that they present led to the dismiss of the data. However the tensile force was controlled by means of the load cell which was connected to the data acquisition.

The second uncertainty is related to the positioning of the accelerometers and LVDT. These uncertainties are not only in terms of accuracy of the position but also on the possible deviation suffer during the set up or due to the vibration suffered while the tie was tested.

Finally the uncertainties associated with the material properties of the ties due to the manufacturing process of the tie. For these reason the properties used in the analytical model and the FEM model analysis where stated according to the Eurocode 3, 2003.

All these uncertainties have to different extent an effect on the results. The assumption of the properties of the materials and the rotation of the horizontal plane of the accelerometers, in addition with the continuous changing of the position of them according to the boundary conditions, can be reflected in the numerical model with a variation of the estimated value and the real one, which at the same time considering the first uncertainty mentioned could also suffered from a slight variation.

5. ANALYSIS AND RESULTS

The laboratory test involved four load steps, each one tested for two boundary conditions, 20KN and 40KN load steps also were tested for six intermediate conditions (complete plate and partial plates). That gives a total of 32 tests performed for the two methods, Tullini and Rebecchi., with two different position of accelerometers, and a total of 23 cases analyzed (considering that some load steps and boundary condition were tested for both methods)

For each test were carried out two recording for the ambient excitation and the forced excitation, so to take the average of the measurements.

5.1 Static analysis

The importance of the boundary condition on the estimated results is reflected in the accurate length that is taken too locate the accelerometers. As it was showed, the used of the free length instead of the effective length of the tie induce some error that would be reflected on the results. When there is particular interest in an accurate estimation of the axial force, the boundary conditions should be well defined in order to have not only a correct positioning of the accelerometers but also the possibility to verify the results by comparing the experimental campaign with a FEM model.

In order to be able to follow this approach and obtain the real stiffness of the supports of the tie, it must be known the deformed shape of the tie by performing a static test.

5.1.1 Pinned and fixed conditions

During the testing, the tie was subjected to perpendicular loads applied by a load cell. The test consists in the loading and unloading of the tie, while the three LDVT were measuring and recording the displacement suffered by the tie while being load and unload, as shown in Fig. 49. This information later permits the construction of Force-displacement curves of the tie for each load stage, as shown in Fig. 50. From which can be observed the influence of the stiffness of the ends for the same step of load, and in addition how this difference between the two extremes conditions (PP and FF) find themselves reduce when the axial force, at which the tie is subjected, increases.

The aim of the static test was not only corroborate its validity as a NDT to be performed on site, but also a way to evaluate the stiffness of the end support for the intermediate conditions. In order to do so, the deformed shape was obtained for all the cases evaluated for a perpendicular load of 100 N. Moreover, the FEM model was also tested to see it response when facing a perpendicular load, and compare the deformation values obtained with the real ones. In the Fig. 51, is depicted the deformation of the tie while it was clamped compared with the values obtained with the FEM model. It can be stated the reliability of the FEM model, hence the FEM model built for the dynamic procedures can be calibrated and used for the intermediate conditions.

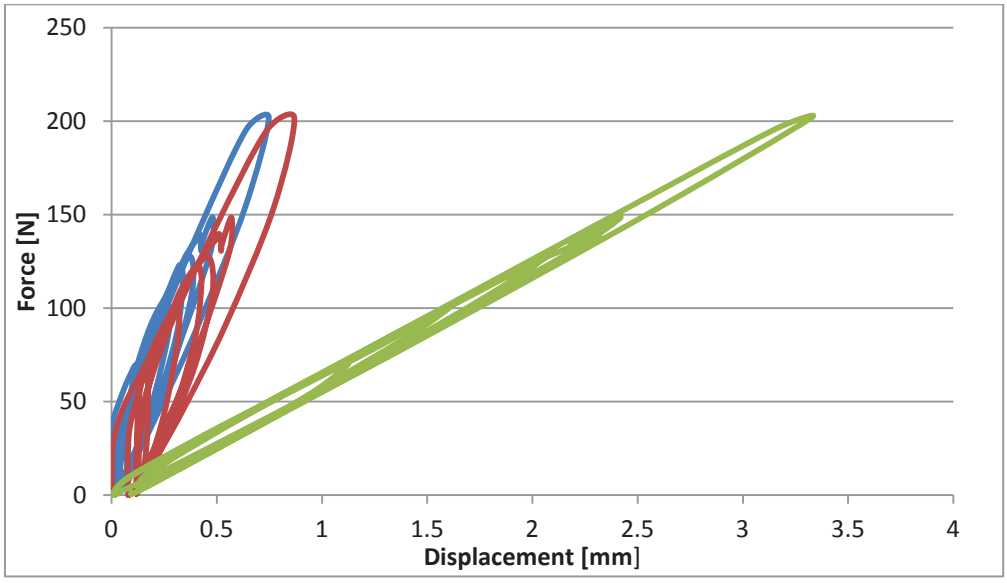

Fig. 49 – Loading and unloading of the tie for the load step 60KN PP condition.

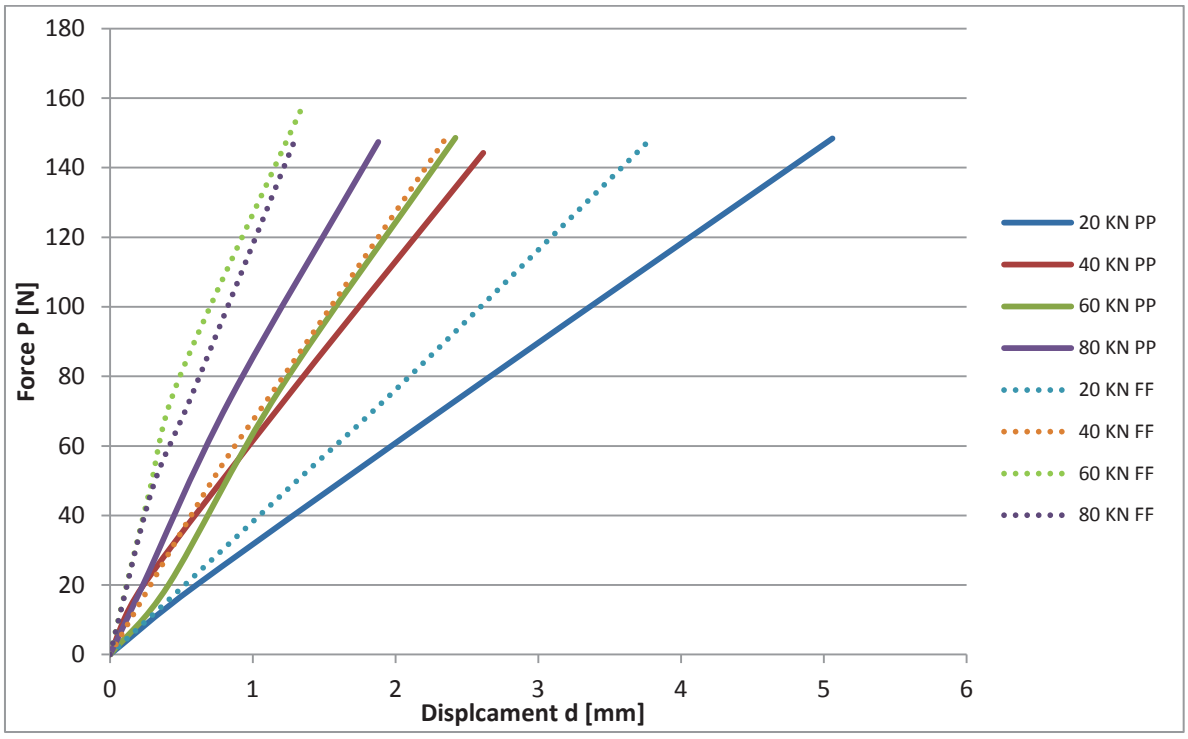

Fig. 50 – Force vs Displacement for each load step and PP condition and FF condition

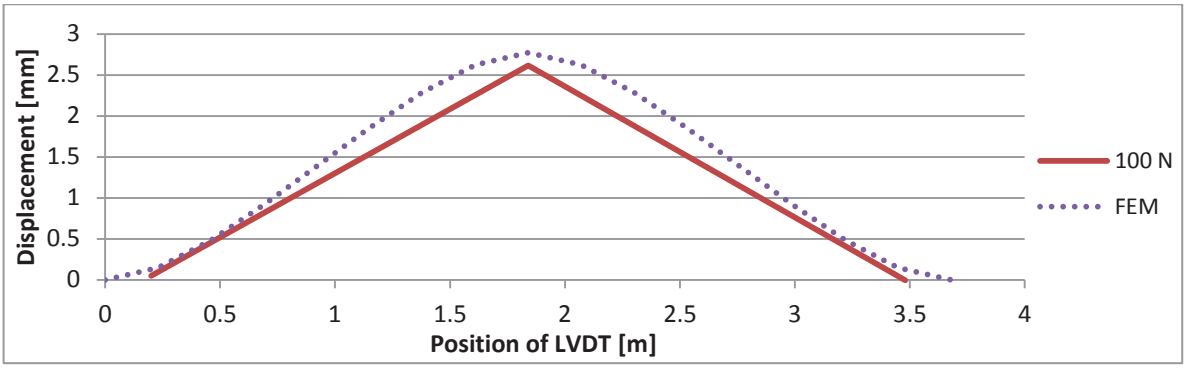

Fig. 51 – Comparison of the deformed shape obtained on campaign and the FEM response.

For the extreme boundary conditions, pinned-pinned and fixed-fixed, the method of Briccoli [5] was applied to estimate the axial force was and the results are shown in Table 17.

Even though the method is reliable and is numerically simple and of great accuracy with the real value measured on laboratory, as it was explained before its set up demands for more equipment than the dynamic one, involving LDVT and strain gauges beside the data collector and loading device, which translates to time consumption and economy of the testing makes it in disadvantage with the dynamic test.

Nominal load	*Real axial load [KN]*	*P [N]*	*Real P [N]*	*H estimated [N]*
20	20.8	50	47.54	20821.94
		100	98.40	20821.43
		150	149.06	20821.29
40	40.06	50	49.85	40035.95
		100	99.05	40035.04
		150	149.75	40034.72
60	60.1	54	53.62	60112.29
		100	99.07	60109.81
		150	135.41	60109.42
80	79.2	50	47.24	80032.69
		100	97.69	79944.49
		150	149.49	80029.38

Table 17 – Axial force estimation with static method proposed by Briccoli, 2001.

5.1.2 Intermediate conditions

For the cases of intermediate condition, IC1, IC2 and PIC1 to PIC4 for loads 20 KN and 40KN, where the stiffness of the constrains were not known, the static method was useful to determine the translational stiffness of the springs represented by the threaded bar in the regulating device, and modelled as translational springs in the FEM model.

During the static test, the perpendicular load was applied in 3 different sections of the tie in correspondence with the position of the LDVTs, as shown in Fig. 52

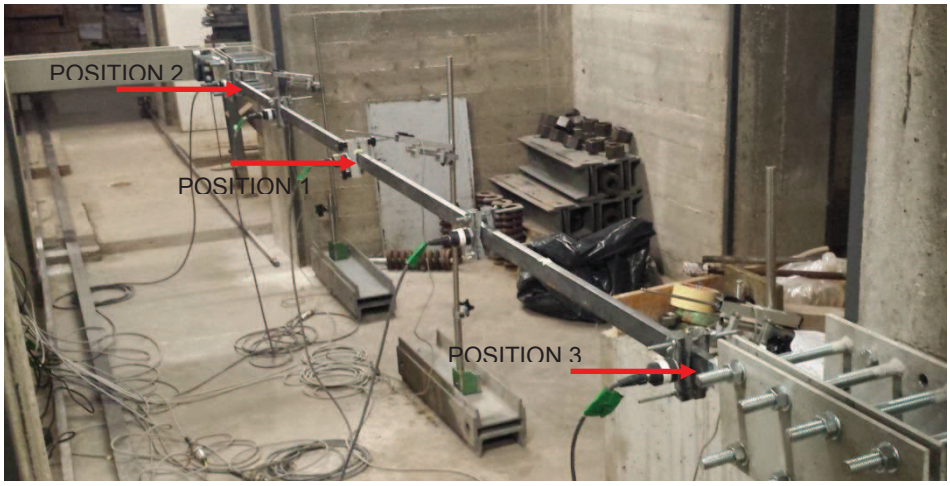

Fig. 52 – Scheme of the position were the perpendicular load was applied

The loading in position number 1 gave the deformed shape of the tie by using the displacement measured by each LDVT. The loading in position number 2 and 3 revealed the deformation suffered by the threaded bar (acting as a spring) by means of extrapolation of the function that determines the deformed shape. If the displacement of the spring is known, the stiffness can be calculated as the ratio between the load applied and the displacement of the spring (deformation).If then is assumed an hypothesis of rigid body, even though is not the case of the tie, the rotational spring of the tie, that is the principal unknown of the onsite testing, can be calculated, approximately, as a function of the translational spring and the length between the support and the vertical spring.
For the intermediate boundary conditions tested in the laboratory and achieve by fastening each partial steel plate at a time, the stiffness was calculated as mentioned and using the FEM model the stiffness was calibrated until the deformation were similar to the experimental ones.

The procedure used to analyze the intermediate condition was:
- With the displacement got from static testing in position 2 it was obtained the deformation Δx suffered by the threaded bar
- The stiffness of the spring Kv was calculated as $Kv = F/\Delta x$
- The FEM model was run with the value of stiffness calculated and the deformed shape obtained was compared with the experimental one. The stiffness was increased or decreased, depending of the requirements of the experimental displacements, until they matched.
- With the calibrated stiffness, the model was analyzed to obtained the eigenvalues of the problem and the numerical model was performed and the axial load estimated
- Finally the mode shapes obtained during the dynamic analysis of FEM were correlated with a MAC with the experimental mode shapes acquire in the laboratory.
- The rotational stiffness is estimated assuming a rigid body motion and calculated as $K_R = K_v l^2 + K_f$

Being l the distance between the spring and the end pinned and- Kf the flexural stiffness of the remaining length of the tie $K_f = \frac{E \cdot J}{L}$.

From the Fig. 53 to Fig. 56 can be observed the deformed shape of each boundary condition and it correspondence calibration with the FEM model deformed shape (dotted line). It must be noted that the difference between experimental and analytical is of a tenth of millimetre, the graph are magnified for a better understanding.

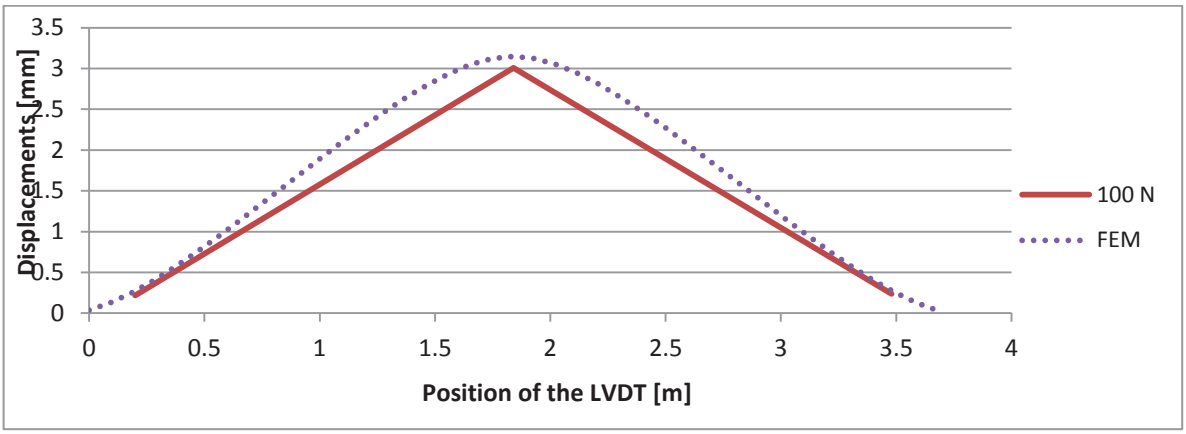

Fig. 53 – Deformed shape of the tie subjected to an axial load of 20KN for an intermediate boundary condition, PIC1

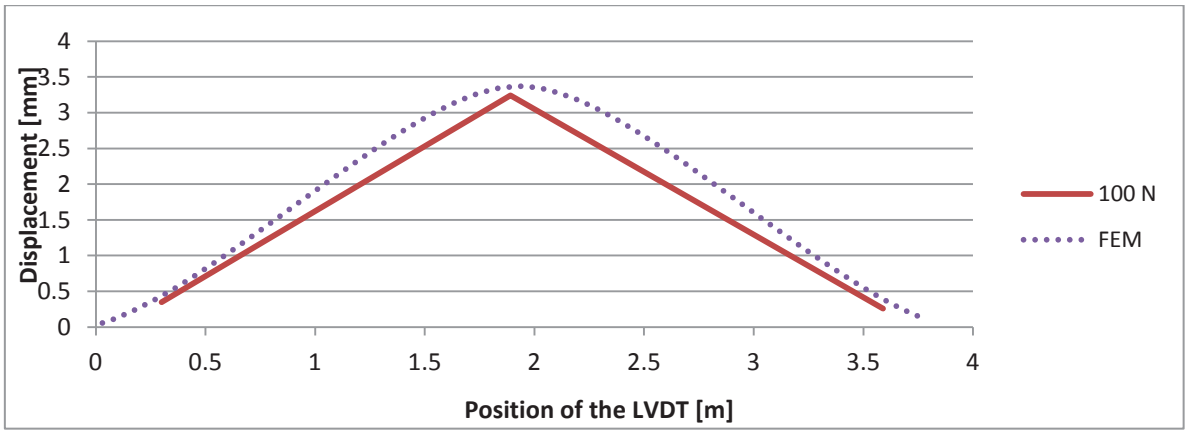

Fig. 54 – Deformed shape of the tie subjected to an axial load of 20KN for an intermediate boundary condition, PIC2

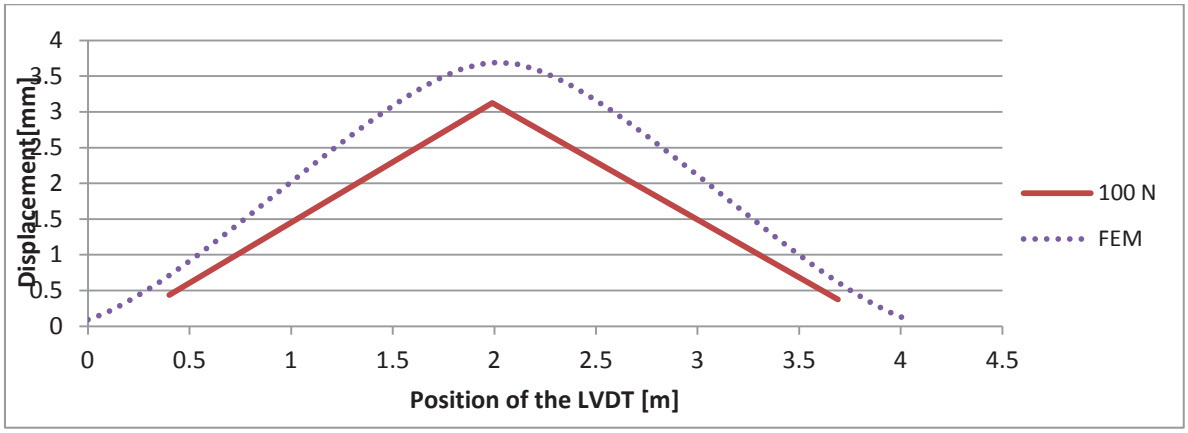

Fig. 55 – Deformed shape of the tie subjected to an axial load of 20KN for an intermediate boundary condition, PIC3

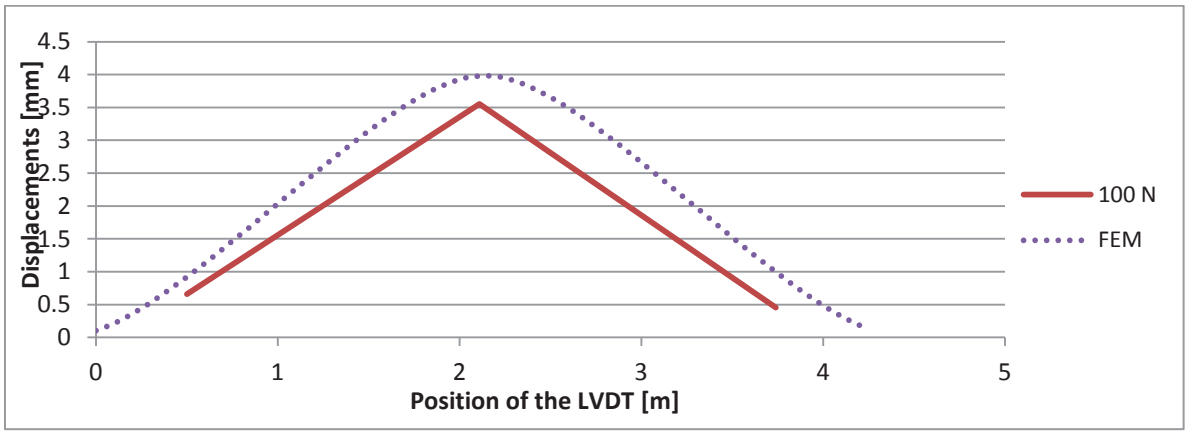

Fig. 56 – Deformed shape of the tie subjected to an axial load of 20KN for an intermediate boundary condition, PIC4

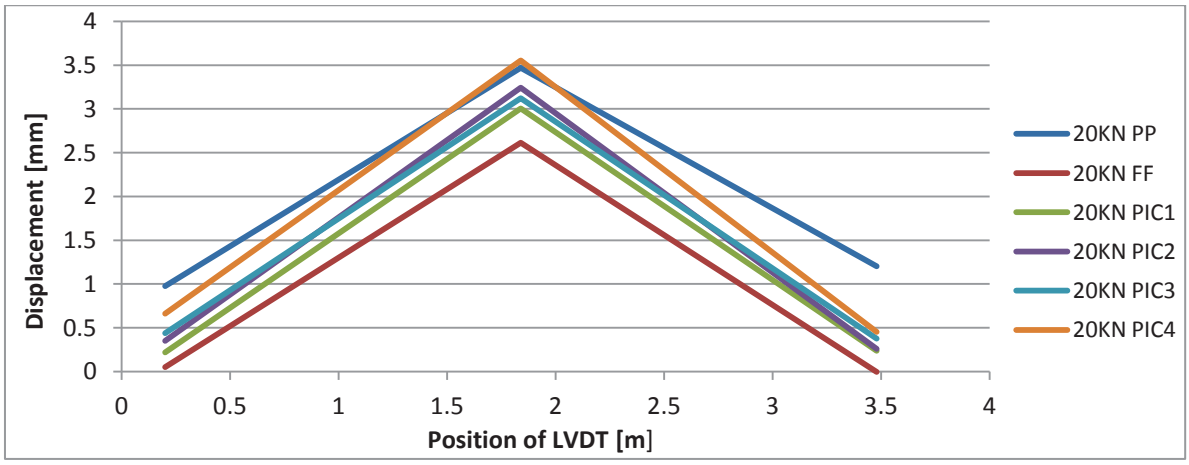

Fig. 57 – Comparison of the deformed shape of the tie for all intermediate condition and extremes conditions for 20 KN, and a transversal load of 100 N

As a result, all the conditions evaluated for 20KN were graphed together to visualize the variation of stiffness and its relation with the deformation. Fig. 57 depicts for each boundary condition the displacement measured when the tie was subjected to a perpendicular load of 100 N.

The extremes conditions define the limits of displacements, while the intermediate conditions move inside this range. As it was assumed, the stiffness of the end supports decreases while moving towards the extremes, hence the displacement increases while the length of the tie is increased.

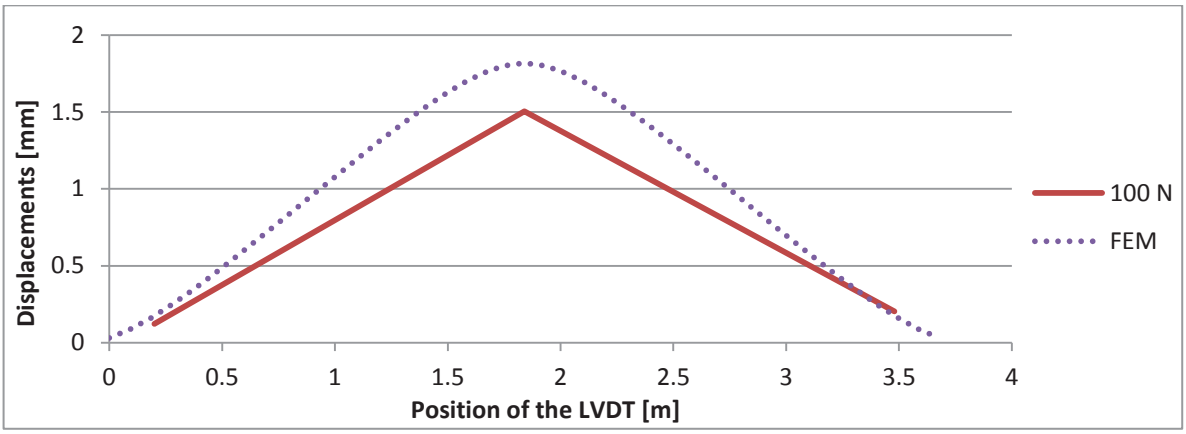

Fig. 58 – Deformed shape of the tie subjected to an axial load of 40KN for an intermediate boundary condition, PIC1

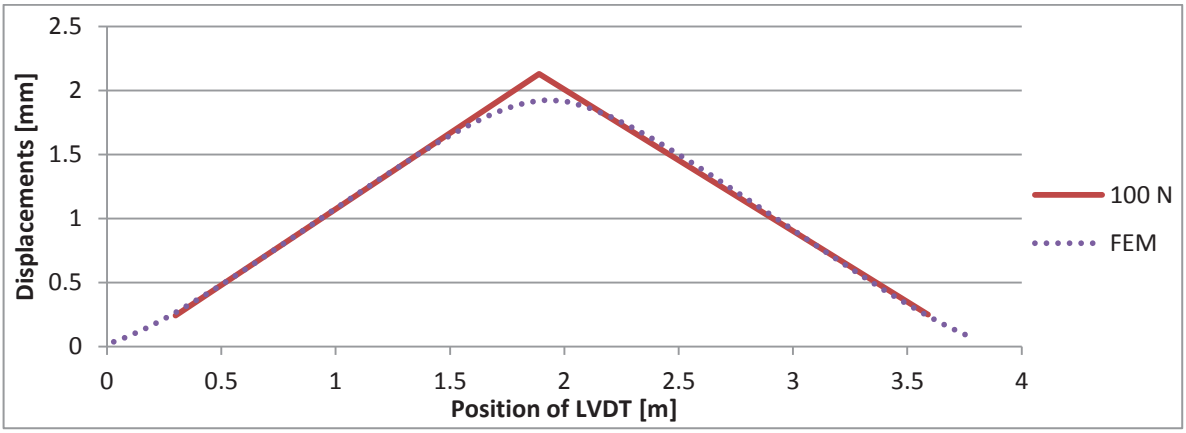

Fig. 59 – Deformed shape of the tie subjected to an axial load of 40KN for an intermediate boundary condition, PIC2

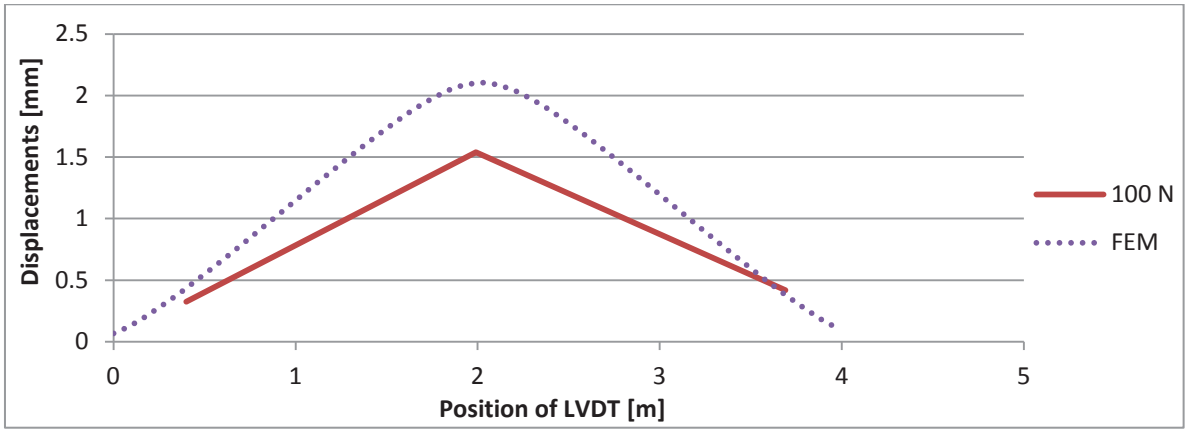

Fig. 60 – Deformed shape of the tie subjected to an axial load of 40KN for an intermediate boundary condition, PIC3

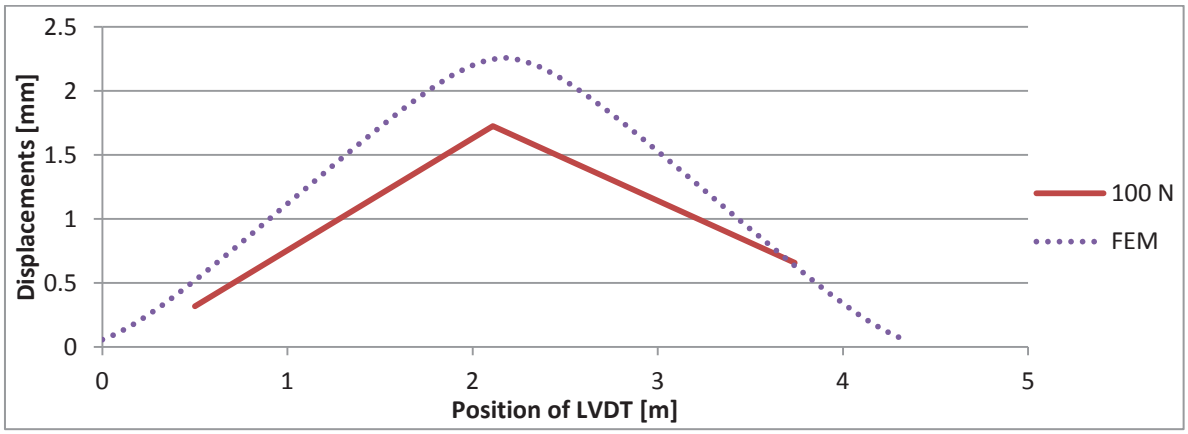

Fig. 61– Deformed shape of the tie subjected to an axial load of 40KN for an intermediate boundary condition, PIC4

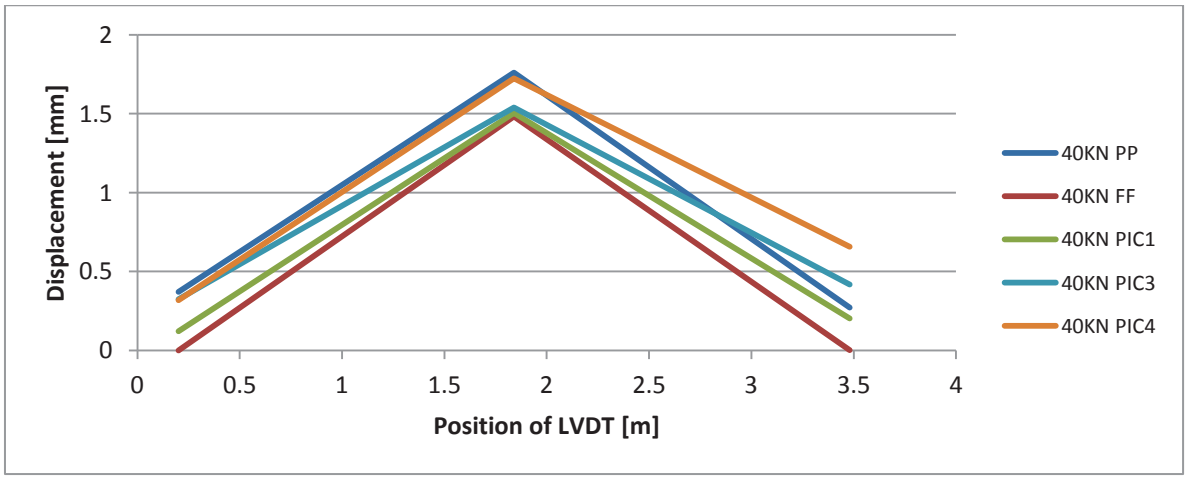

Fig. 62 – Comparison of the deformed shape of the tie for all intermediate condition and extremes conditions for 40 KN, and a transversal load of 100 N

As explained before for the load step of 20KN, in Fig. 61 is depicted the behaviour of the different intermediate conditions for 40KN when the tie is subjected to a perpendicular load of 100 N. Once more the extremes conditions establish the limits where the intermediate condition. It has to be noted that intermediate condition PIC2 has not been graph due to the lack of values in the surrounding of the load 100N.

Finally, for each case was obtained the followings translational and rotational stiffness as shown in Table 18 :

B.C	Length [m]	K_V [N/m]	K_f [Nm]	K_R [Nm]
B1	0.5	2.00E+06	5166	5.1E+05
B2	0.4	1.00E+07	6457.5	1.6E+06
B3	0.3	2.00E+06	8610	1.9E+05
B4	0.2	2.00E+06	12915	9.3E+04

Table 18 – Definition of the translational and rotational stiffness

The results of the estimation of the rotational stiffness confirm the fact that as the boundary condition is moved towards the pinned end, the stiffness decreases, allowing more displacements as it was shown by the experimental graphs.

The test of the static method has showed to be of great use to calibrate the FEM model improving the knowledge of the stiffness of the end support.

It can be conclude that the best approach regarding the estimation of the axial force is the combination of the dynamic methodology with the static method as a corroboration method, mainly when the estimation is of major importance and the boundary conditions are unknown.

5.2 Dynamic test

Each acquisition was processed by the modal identification software ARTeMIS extractor. The processing of the signal involves the removal of noises and the transformation from the time domain to the frequency domain, where the average frequency values from all the accelerometers can be obtained. From the FRF (Frequency response functions) can be picked the natural frequencies and modes shapes, as shown in Fig. 63.

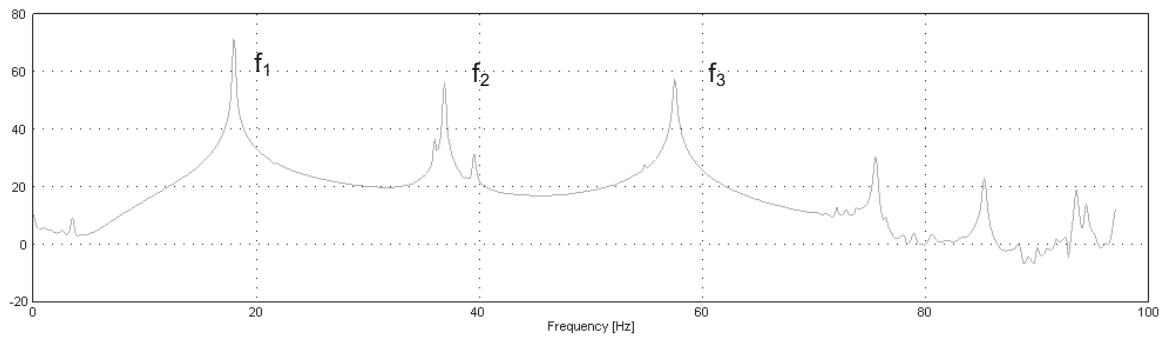

Fig. 63 – Pick Picking, Frequency Domain Decomposition for test 15 – 80KN FF.

Once obtained the first three frequencies and modes shapes the axial forces were estimated using the first natural frequency and its corresponding mode shape. For the numerical model was assumed a density of ρ= 7850 Kg/m^3 and a Young's Modulus of E=210Gpa

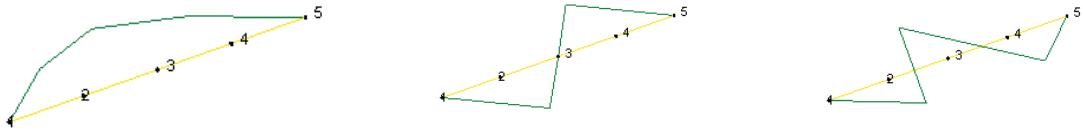

Fig. 64 – First three modes shape given by the data processing in ARTeMIS.

Table 19 summarizes the results for the 23 cases analyzed, which were obtained with the three different methods, Tullini, Rebecchi and Luong, with which the axial force was estimated.

Nº of analysis	Identification	Results [KN]						
		$N_{tullini}$ (1)	N Rebecci	N LuongPP	N LuongFF	Real load Tullini (2)	Real load Rebecchi	Δ(2)-(1) [%]
1	0KN_PP	***1.556***	-	3.46	-	-	-	-
2	20KN_PP	***20.62***	-	28.47	18.30	20.1	-	2.6%
3	20KN_FF	***17.51***	20.48	25.66	15.33	20.8	20.8	-16%
4	20KN_IC1	***18.20***	117.61	23.26	13.35	21.06	21.06	-14%
5	20KN_IC2	***18.29***	20.86	20.87	11.44	20.01	20.00	-9%
6	40KN_PP	***37.69***	-	49.56	36.45	40.01	40.00	-6%
7	40KN_FF	***41.93***	46.75	47.24	34.08	40.06	40.09	5%
8	40KN_IC1	***38.72***	43.53	40.59	27.97	40.03	40.06	-3%
9	40KN_IC2	***37.78***	47.62	40.59	27.97	40.21	40.19	-6%
10	60KN_PP	***60.20***	108.041	68.92	54.26	60.03	60.01	0.3%
11	TullNew_40KN_PP	***42.90***	-	49.95	36.86	40.07		7%
12	TullNew_60KN_PP	***54.96***	-	69.53	54.74	60.03		-8%
13	TullNew_60KN_FF	***56.67***	-	65.00	51.15	60.1		-6%
14	TullNew_80KN_PP	***89.59***	-	86.42	70.37	80.05		12%
15	TullNew_80KN_FF	***61.32***	-	82.19	66.10	79.2		-23%
16	Tull_20KN_PIC1	***18.20***	-	26.59	15.89	20.4	-	-11%
17	Tull_20KN_PIC2	***18.39***	-	26.94	16.26	20.104	-	-9%
18	Tull_20KN_PIC3	***19.02***		26.88	16.20	20.48	-	-7%
19	Tull_20KN_PIC4	***17.88***	-	25.94	15.29	20.462	-	-13%
20	Tull_40KN_PIC1	***43.35***	-	46.38	32.66	40.423	-	7%
21	Tull_40KN_PIC2	***41.45***	-	46.27	32.56	40.397	-	3%
22	Tull_40KN_PIC3	***37.91***	-	48.22	34.56	40.25	-	-6%
23	Tull_40KN_PIC4	***37.81***	-	45.78	32.05	40.157	-	-6%

Table 19 – Results obtained for the laboratory tests performed.

From this results can be conclude that, the coefficient of variation obtained by calculating the axial force through the method of Tullini for the extremes cases of boundary conditions, pinned and fixed, and the different intermediate conditions, is of 8.7% with an average ratio of 0.953.
This variation, suffered by the results, could be related to the uncertainties exposed in the previous section, which in the case of intermediate conditions reveals a significant influence on the result. The lack of knowledge of the real length of the tie, may lead to a wrong positioning of the accelerometers making the estimation results sensitive to the variation on the position of the sensor. Even though if it is looked punctually to the major error committed for the intermediate condition during the testing is less than 20%.
If this situation is translated to the onsite measurement scenario where most of the time the boundary conditions are not easy to assess, the error of taking the free length between supports as the real length would not reflect a larger variation on the estimation, considering the low coefficient of variation in the intermediate condition which is of 6% with an average ratio of 0.94, value that should be considered when assessing the situation of the tie for repair or strengthening.

Regarding the two other method evaluated, on one hand Rebecchi shows great accuracy for some of the cases, but as it was said before, presents a lack of convergence when the ratio $v_1 + v_2/v_3$ turns to be high like in the case of 40KN FF (test nº 6) or the estimation is over the real case value, like in the case of 60KN PP (test nº10). On the other hand, Luong Charts presents a range were the real value is found but for the cases of extremes conditions, the results are not as accurate are they were expected to be, this confirms that the equations proposed by the vibrating cords theory, for pinned and fixed ties, is not correct at all mainly the one for the fixed condition.
In Fig. 65 is showed the correlation between the values estimated and the real axial force measured during the laboratory tests. It can be seen as it was said before, that there is a good correlation between the values. Such correlation makes the method of great interest to be performed on site, considering the small error that undertakes and the expeditious of the testing as it was stated before. As it was mentioned before the coefficient of variation is of 8.7%

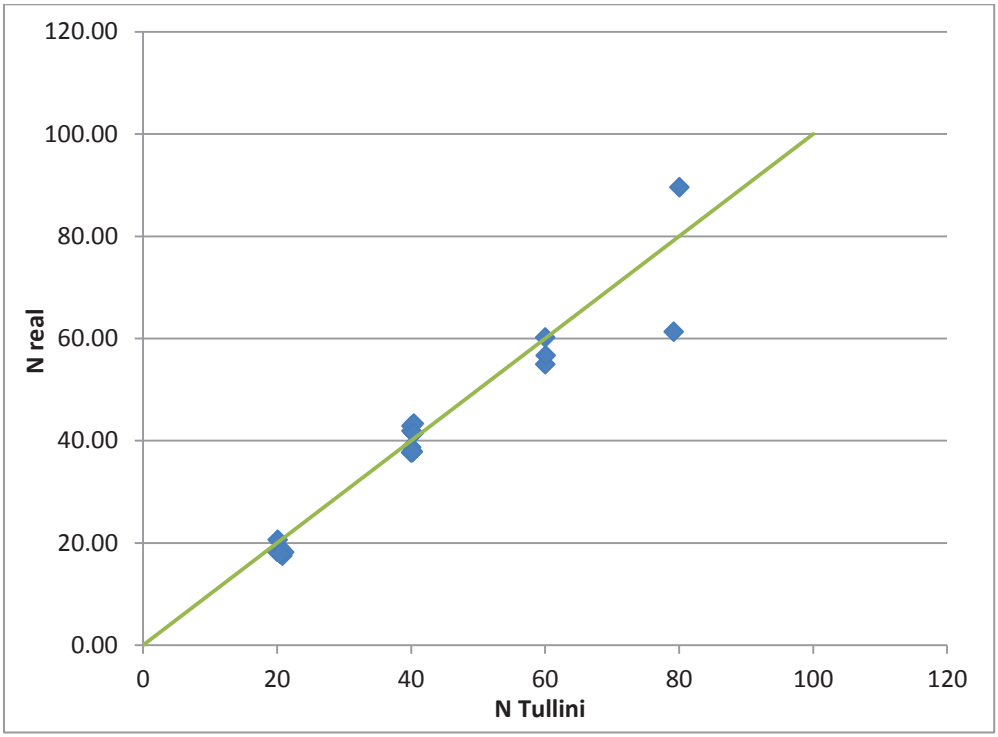

Fig. 65 – Comparison between the estimated axial force and the real one.

As for the intermediate boundary conditions, it should be highlighted that there is an improvement of the results for the intermediate conditions achieved by the partial plates. The reason why the plates were cut it in the first place, was to avoid the contribution of the stiffness of the plates in intermediate conditions were some of the nuts of the device were tighten and the other were not. By cutting the plate the independence of stiffness for each plate was achieved and the results show more accuracy.

5.2.1 FEM models

Extreme boundary conditions

Once the estimation of the axial force for each case was done, the values were compared with a FEM model using FX+ for DIANA software. For the extremes cases of boundary conditions, two different models were built to take into consideration the different length use to performed each test. As it was said before, for the pinned condition the total length was 4.82 meter, while the length for the clamped situation was 3.68 meter.

The ties were modelled as a beam with uniform cross-section with an area of 622 mm^2 (rectangular 40.43 x 15.38 mm) subjected to a constant axial load in correspondence with each load step, from 20 to 80 KN. The models were compound by 20 elements and 21 nodes for the pinned condition model and 16 elements and 17 nodes for the fixed condition model.

The density and Young Modulus assumed for the models were 7850 kg/m^3, E= 210.0 Gpa and the Poisson ratio 0.3.

For each load step, a non linear analysis was performed on the model, and at the same time an eigenvalue analysis was carried out to obtain the natural frequencies and mode shapes of the structure.

These mode shapes obtained for the FEM model, shown in Fig. 66 and Fig. 67 were then compared with the experimental ones, acquired on site with the accelerometers. The degree of correlation between the values was obtained through a Modal Assurance Criterion (MAC), shown from Fig. 68 to Fig. 71.

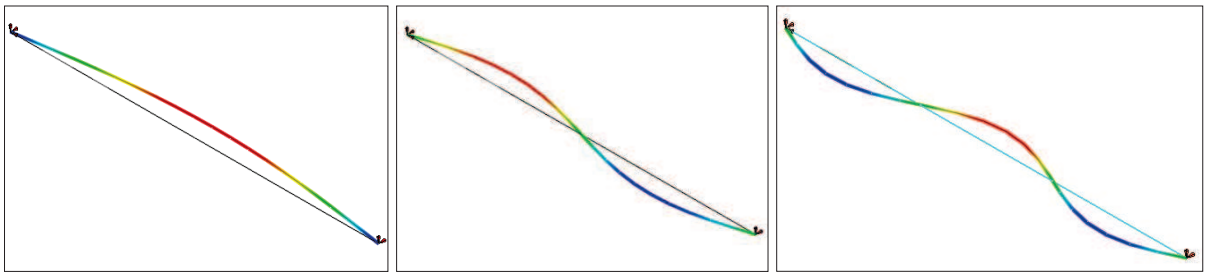

Fig. 66 – Mode shapes obtained with the FEM model for pinned condition.

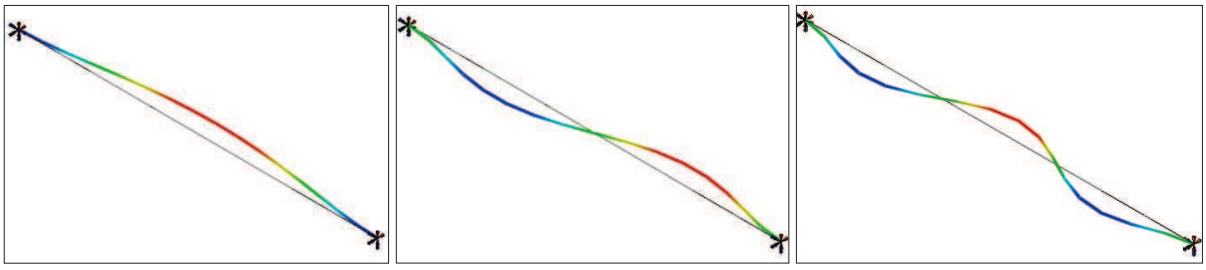

Fig. 67 – Mode shapes obtained with the FEM model for fixed condition.

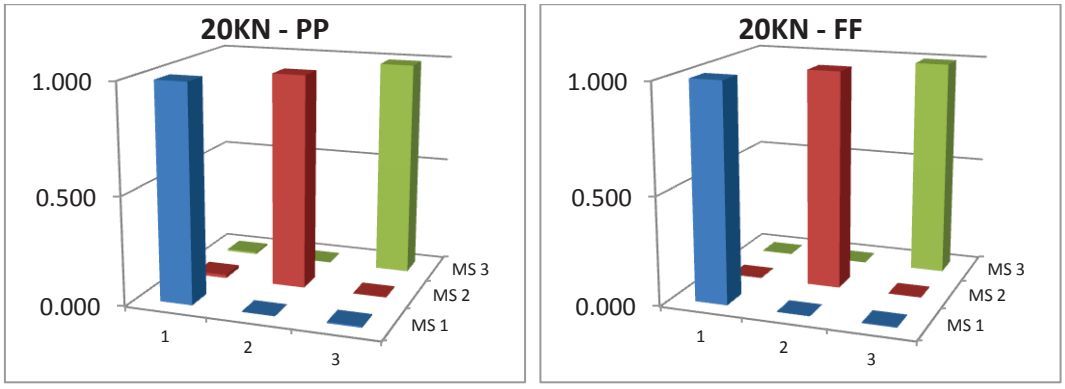

Fig. 68 – MAC correlation between the experimental model and the FEM model for load step 20KN for pinned and clamped boundary condition

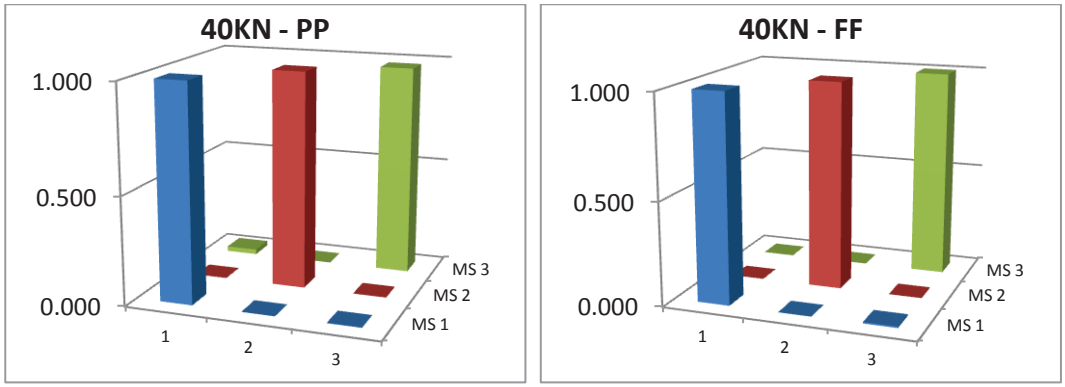

Fig. 69 – MAC correlation between the experimental model and the FEM model for load step 40KN for pinned and clamped boundary condition

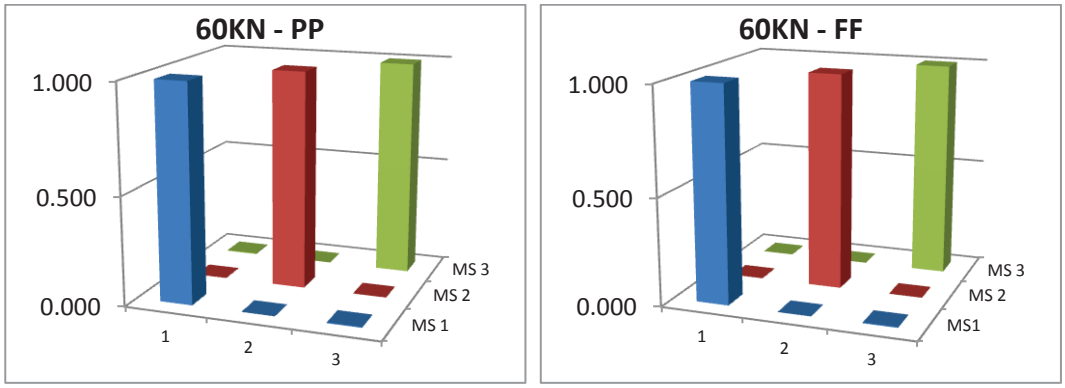

Fig. 70 – MAC correlation between the experimental model and the FEM model for load step 60KN for pinned and clamped boundary condition

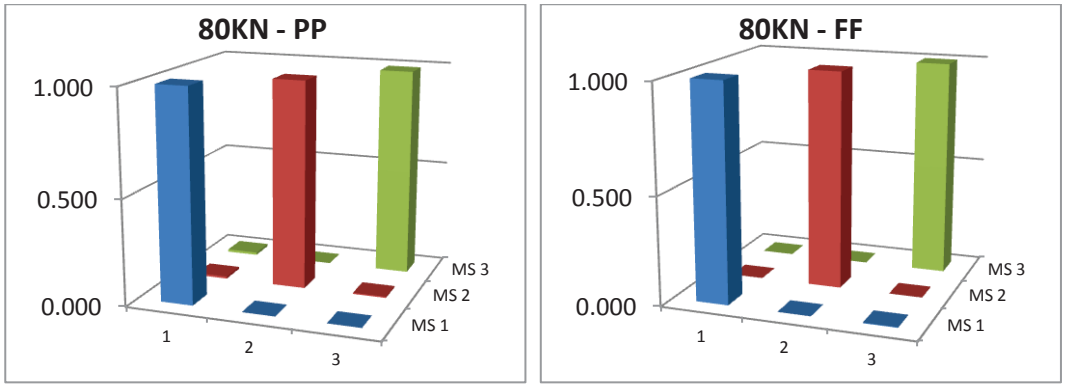

Fig. 71 – MAC correlation between the experimental model and the FEM model for load steps 80KN for pinned and clamped boundary condition

The model used showed great accuracy, considering the correlation between the values obtained with the laboratory acquisition and the ones obtained by the FEM analysis. As a result the FEM model is

reliable and can be used to simulate different state of the ties in order to have a wider spectrum of cases.

Table 20 shows the results from the numerical modeling. The values were obtained making use of the modes shapes gathered from the eigenvalue analysis of the FEM model of the layout of the laboratory test for the extremes conditions. The accuracy and reliability of the model can be seen in the average of the ratio between the estimated load and the real load, which is of 1, and the coefficient of variation of the values is of 1.4%.

Nº of analysis	Identification	Results First Mode [KN]		
		$N_{Tullini}$	Real load Tullini	Error [%]
1	Lab Tull 0KN PP	0.006	0	-
3	Lab Tull 0KN FF	0.056	0	-
5	Lab Tull 10KN PP	10.002	10	0.02%
7	Lab Tull 10KN FF	10.051	10	0.51%
9	Lab Tull 20KN PP	19.873	20	-0.64%
11	Lab Tull 20KN FF	20.826	20	4.13%
13	Lab Tull 40KN PP	40.051	40	0.13%
15	Lab Tull 40KN FF	40.013	40	0.03%
17	Lab Tull 60KN PP	60.064	60	0.11%
19	Lab Tull 60KN FF	60.097	60	0.16%
21	Lab Tull 80KN PP	79.962	80	-0.05%
23	Lab Tull 80KN FF	79.156	80	-1.05%

Table 20 – Results of the analytical model with the mode shapes obtained in the FEM model.

The analytical model of all the cases analyzed with the FEM model, led to the calculation of the variables λ and n involved, which allowed the construction of the curves (see Fig. 72 – Correlation λ vs n for PP and FF condition Fig. 72) for the extremes boundary condition. In contrast with the one obtained from the database (see Section 2.6.1-Fig. 18), with the wire-rod theory, the new curves show a better behavior of the ties, compatible with the Authors' states in its scientific paper (*Tullini,, 2008*), as the tension get higher, the boundary conditions are not longer influent on the results of the estimation.

Moreover the fact that the variable λ is function of the circular frequency, the graph can also be built for higher mode shapes.

The interesting point of this graphic correlation is its utility for already analyzed ties for which only one frequency was acquired, and no mode shape is known. For this cases it can be estimated the axial force with a more accurate result than the one that could be obtained if the wire-rod theory is applied instead. Considering just its geometrical features and the frequency acquired, it can be obtained the values of the axial force through the adimensional axial force *n*.

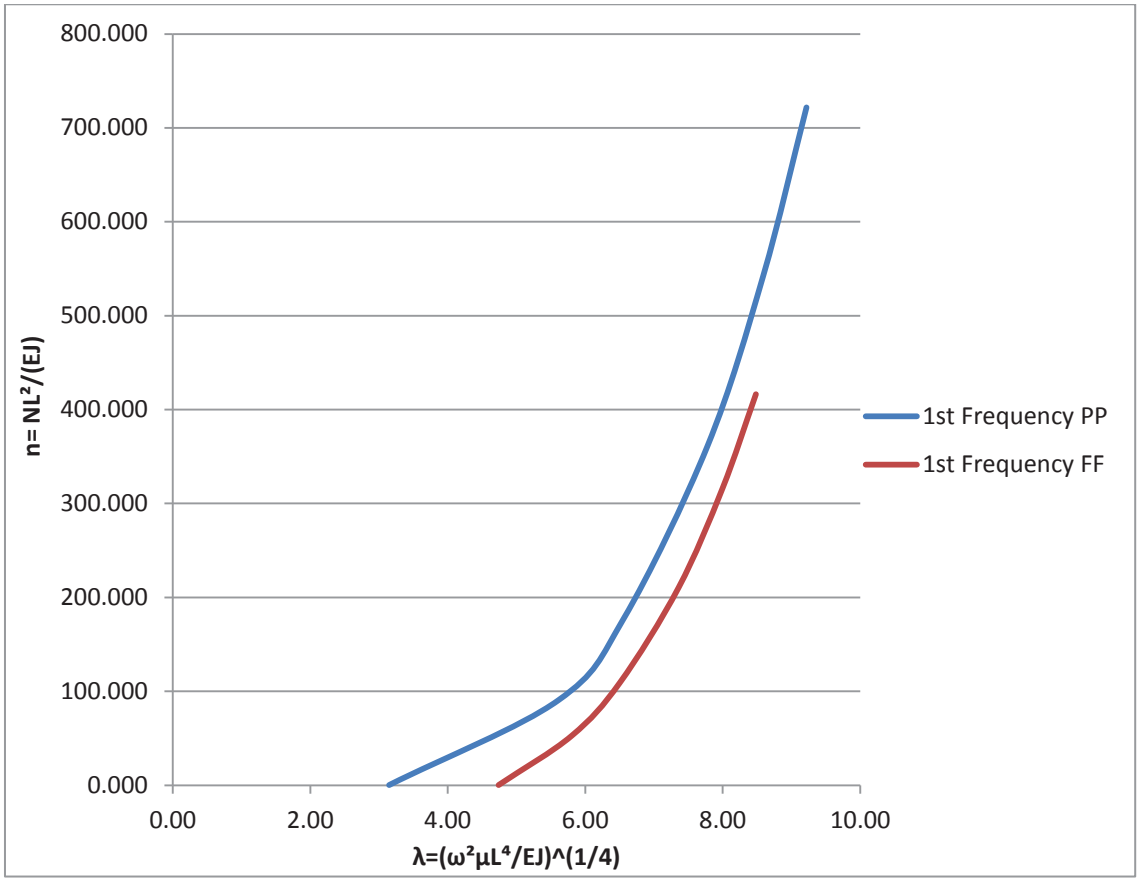

Fig. 72 – Correlation λ vs n for PP and FF condition

Intermediate boundary conditions

The laboratory set up was able to simulate different intermediate boundary conditions, with the complete plate and later with the partial plates. To improve the FEM model, built for the extremes cases PP an FF, the model was upgraded to perform the analysis of a larger spectrum which included the intermediate condition.

This new model, as the one described before, was modelled as a beam with uniform cross-section with an area of 622 mm^2 (rectangular 40.43 x 15.38 mm) and a complete length of 4.82 meters, subjected to a constant axial load in correspondence with each load step, from 20 to 80 KN. As a way to stick to the real set up of the laboratory as much as possible, the threaded bars used to adjust the plates were modelled as springs with the stiffness obtained from the static test carried out on the laboratory (*see Section 5.1*).

Again the density and Young Modulus were assumed 7850 kg/m^3, E= 210.0 Gpa and the Poisson ratio 0.3. The extremes supports of the tie itself and the springs were modelled as pinned, as shown in Fig. 73.

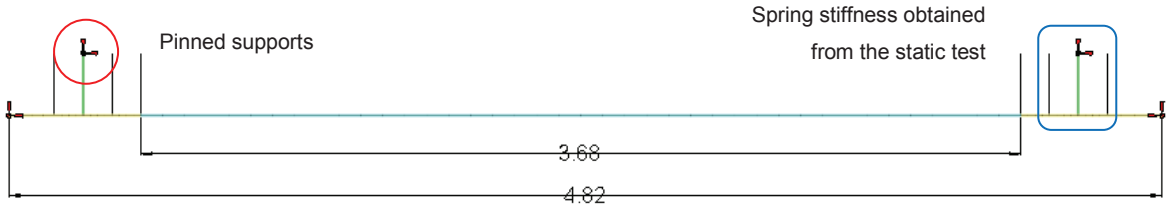

Fig. 73 – FEM model of the layout of the laboratory tests carried out

To determine the reliability of the new model, the stiffness obtained by static method, was set on the springs for each case of intermediate condition, from PIC 1 to PIC 4. The results obtained were correlated with the experimental frequencies and mode shapes obtained after analyzing the information acquired.

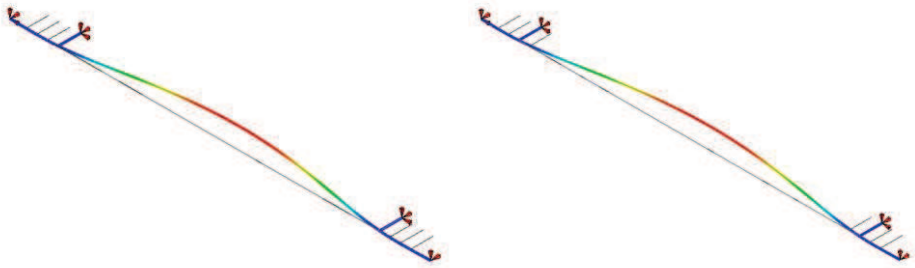

Fig. 74 – First Mode shape corresponding to 20KN and intermediate condition PIC1 and PIC2

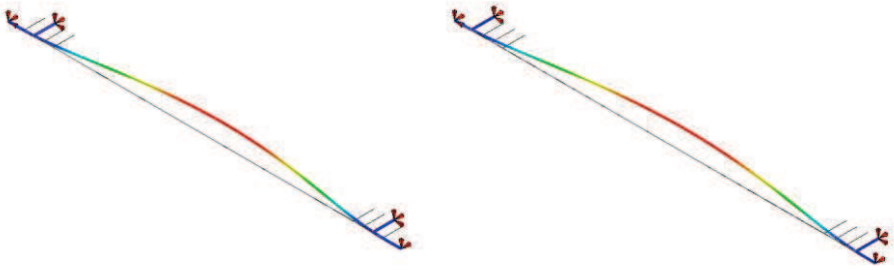

Fig. 75 – First Mode shape corresponding to 20KN and intermediate condition PIC3 and PIC4

The comparison of the first mode shape for different intermediate conditions shows the variation of the rotational stiffness of the supports of the tie. In the first intermediate condition case (PIC1) the results were close to the ones got for the fixed condition, and in the case of PIC4 the result were nearly pinned, although it did not reach the complete pinned condition due to the flexural stiffness given by the beam.

The values estimated for the for the four intermediate condition with partial plates and for the two leoad steps are shown in Table 21. The coefficient of variation to the real load is of 2.1%with a ratio average of 0.99, which establish the good response of the model for different boundary conditions.

Nº of analysis	Identification	Results Third Mode [KN]		
		$N_{Tullini}$ [KN]	Real load Tullini [KN]	Error [%]
25	20KN PIC1	20.112	20	0.56%
27	20KN PIC2	19.520	20	-2.40%
29	20KN PIC3	20.667	20	3.33%
31	20KN PIC4	19.789	20	-1.06%
33	40KN PIC1	40.102	40	0.26%
35	40KN PIC2	39.161	40	-2.10%
37	40KN PIC3	41.030	40	2.58%
39	40KN PIC4	39.465	40	-1.34%

Table 21 – Results of the analytical model with the response of the FEM model for intermediate conditions PIC1 to PIC4 for 20 and 40 KN.

In addition, it was performed a MAC correlation, between the experimental results and the one obtained by performing a FEM analysis, to see the conformity of the results obtained with the model. The correlations are depicted in Fig. 76 and Fig. 77, and the similarity of frequencies are shown in Table 22 and Table 23from these results and the previous one for extremes conditions, it can be concluded that the FEM model is reliable, and the stiffness can be calibrated with the static method so to reduce the impact of the error in the values estimated as much as possible.

In addition a calibrated model would allow the performance of a large number of cases to gather more information on ties and its response to dynamic excitation.

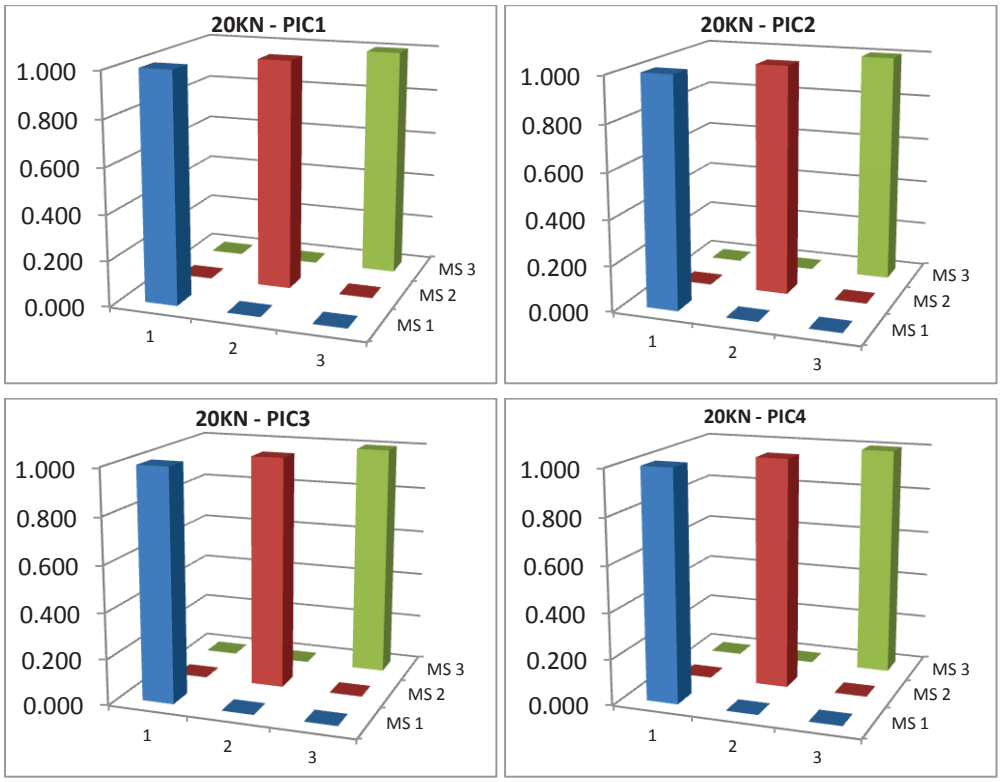

Fig. 76 - MAC correlation between the experimental and FEM model for 20KN

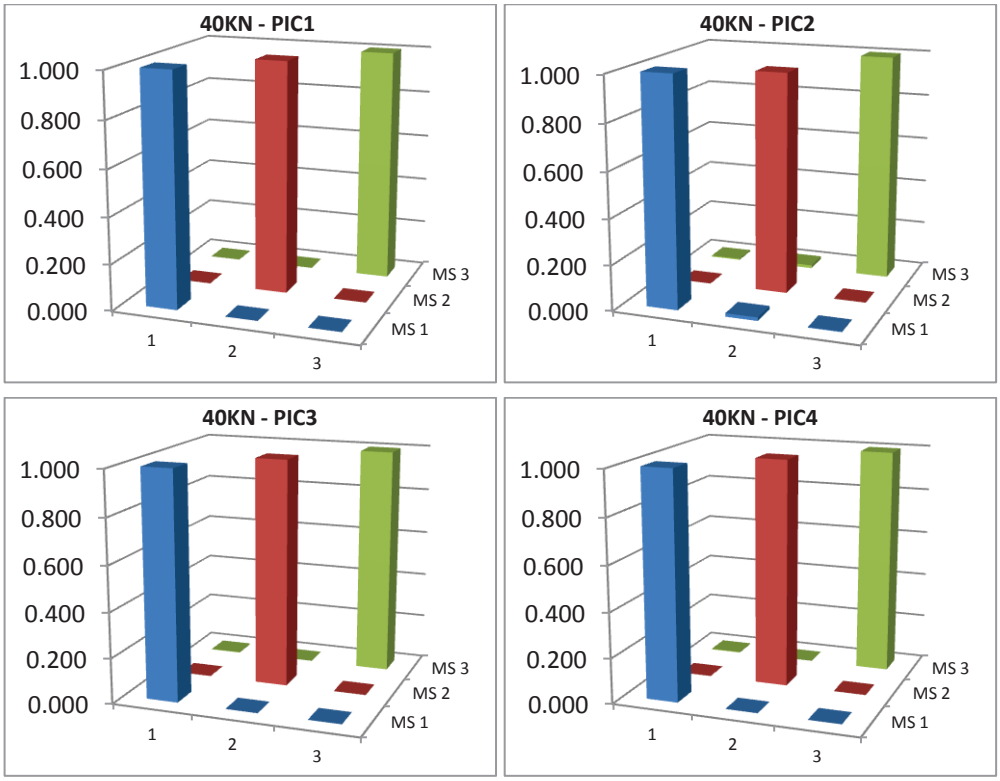

Fig. 77 - MAC correlation between the experimental and FEM model for 40KN

Mode Shape	20KN PIC1		20KN PIC2		20KN PIC3		20KN PIC4	
	$f_{ON\ SITE}$ [Hz]	f_{FEM}[Hz]	$f_{ON\ SITE}$ [Hz]	f_{FEM}[Hz]	$f_{ON\ SITE}$ [Hz]	f_{FEM}[Hz]	$f_{ON\ SITE}$ [Hz]	f_{FEM}[Hz]
1	10.25	10.30	9.77	9.72	9.28	9.00	8.79	8.43
2	22.46	22.66	21.00	21.28	19.90	19.49	18.68	18.12
3	37.60	38.39	34.67	35.89	32.59	32.48	30.40	29.98

Table 22 – Comparison between frequencies gathered onsite and obtained with FEM for 20KN IC

Mode Shape	40KN PIC1		40KN PIC2		40KN PIC3		40KN PIC4	
	$f_{ON\ SITE}$ [Hz]	f_{FEM}[Hz]	$f_{ON\ SITE}$ [Hz]	f_{FEM}[Hz]	$f_{ON\ SITE}$ [Hz]	f_{FEM}[Hz]	$f_{ON\ SITE}$ [Hz]	f_{FEM}[Hz]
1	13.31	13.50	12.57	12.82	12.21	11.84	11.47	11.12
2	27.95	28.50	26.25	27.01	24.78	24.76	23.80	23.15
3	44.92	46.18	41.99	43.63	37.96	39.61	37.35	36.82

Table 23 – Comparison between frequencies gathered onsite and obtained with FEM for 40KN IC

The analysis of the intermediate conditions, made possible to verify, through the correlation of variable of the method developed by Tullini, to that the values of the pair (λ,n) for conditions PP and FF determined the limits for the intermediate conditions. As it is depicted in the Fig. 78, the intermediate conditions studied for the partial steel plates found themselves inside the limits establish by the extremes conditions.

It is of extreme importance to explain that when performing an onsite testing, these limits mean the validity of the results obtained. If the boundary condition cannot be assessed properly, the values should always be contrasted with the results obtained for extremes boundary conditions to determine if the range of results is accurate or the analytical model should be calibrated.

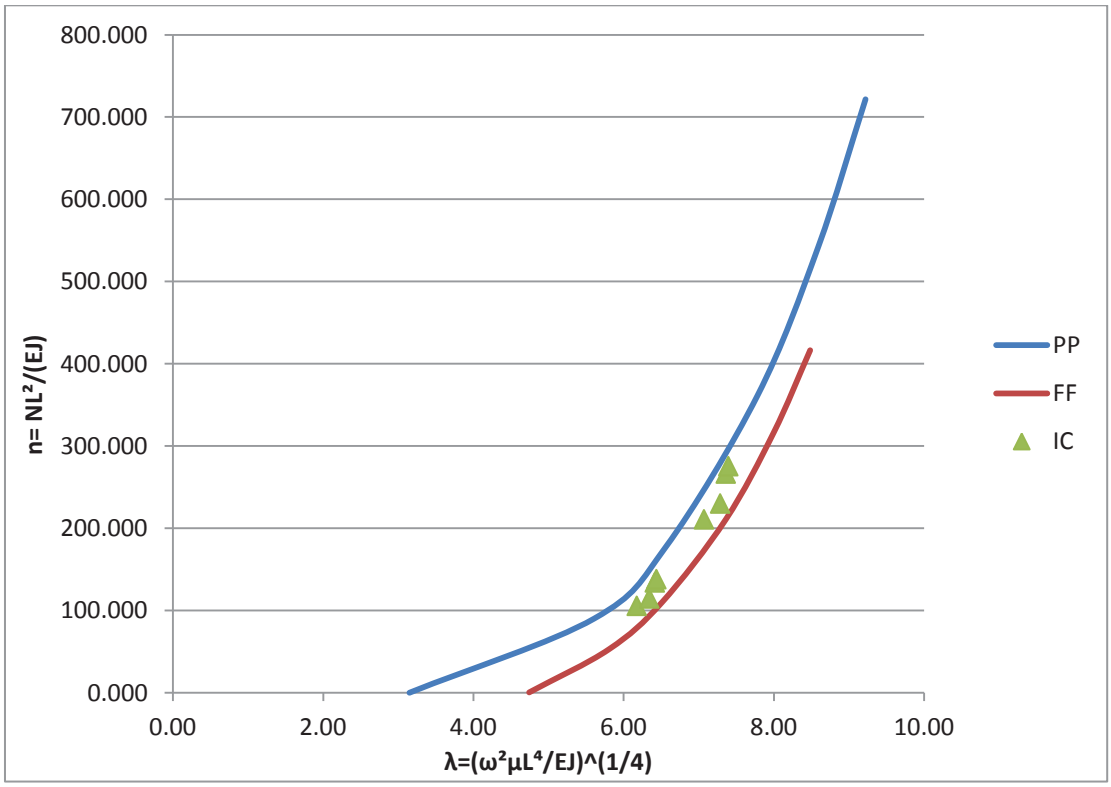

Fig. 78 – λ vs n for the three types of boundary conditions.

5.2.2 Sensitivity analysis

The free length and the position of the accelerometers are two variables that require attention when performing the test on the tie. For this reason a sensitivity test was performed, as a way to detect in a qualitative was the impact of the position of the accelerometers. The sensitivity test was performed in three loads steps, 30, 40 and 60 KN.

Nominal Load	Identification	Position of the accelerometers					Results	
		ACC11	ACC12	ACC13	ACC14	ACC15	$N_{Tullini}$	***Variation***
30	Tull_30KN_PP	-	1.52	2.39	3.31		74.157	***-43.915***
30	TullC_30KN_PP	-	1.2	2.4	3.6	-	30.242	
40	Tull_40KN_PP	-	1.2	2.4	3.6	-	37.133	***4.025***
40	TullNew_40KN_PP	-	1.205	2.41	3.615	-	41.158	
60	Tull_60KN_PP	-	1.2	2.4	3.6	-	57.518	***-4.158***
60	TullNew_60KN_PP	-	1.205	2.41	3.615	-	53.360	

Table 24 – Results of the sensitivity analysis.

In Table 24 are exposed the position of the accelerometers in both cases studies. In the case of the accelerometers located in 1.20m, 2.40m, 3.60m correspond to the middle and quarters of the length for the pinned-pinned condition, the position suggested by the Author in the scientific paper (*Tullini, 2008*), and as it can be seen the values obtained show a great accuracy with the real axial force.

For the cases of the steps 40KN and 60KN, the position of the accelerometers shows a slight difference, of only a couple of centimetres. In the case of 40KN the correction increases the accuracy of the result, as it was said before. Different is the case of load step 60KN where the reduction of the axial force estimated is not due to the position of the accelerometers but due to the lack of coupling of the frequencies of all the accelerometers.

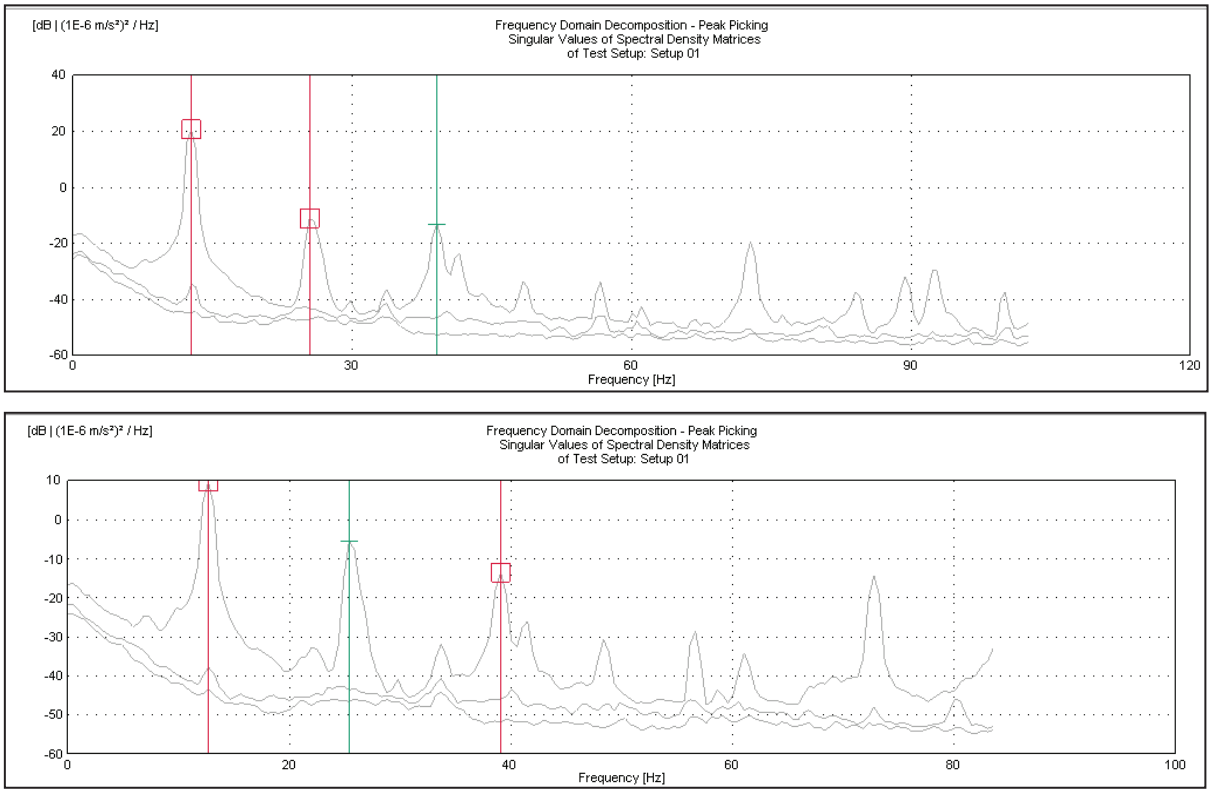

Fig. 79 – Lack of coupling of the three first natural frequency of vibration for loas step 60KN and boundary condition PP.

Finally in the case of the load step 30KN, the difference between the position of the accelerometers is significant larger than in the other cases, more than 30 centimetres. The impact of such variation on the position of the devices is being reflected on the results obtained with the method, the axial load estimated increases rapidly, while the accuracy decreases.

In conclusion, from the qualitative analysis the position of the sensors should be located in the surrounding of the quarters and the middle, allowing only a small margin for the variation of the position.

Further research should be carried out, making use of the FEM model calibrated for the dynamic tests, to determine the percentage of variation with the real load if the positions of the accelerometers are

changed. This parametric study on the position of the accelerometer would demonstrate in a quantitative analysis the real impact on the estimation of the axial force.

5.2.3 Third frequency of vibration

In addition to the analytical model developed with the mode shape of the first frequency of vibration, the method was also performed for the third natural frequency, since the second frequency presented a modal node in the position of the middle accelerometer.

According to the author (*Tullini, 2008*) the symmetry of the tie for the two extremes condition, pinned and fixed, should be reflected in the ratio $v_1 + v_2/v_3$ and the following axial force estimation. During the testing the different boundary conditions were achieved manually, what can induce to a difference between the two extremes stiffness what is transducer as a non symmetrical tie.

In the

Fig. 80 can be seen the comparison between the axial force estimation for the first frequency obtained and the third one. It can be concluded that even though there are two cases where the difference is significant in the remaining cases can be said that the coefficient of variation is of less than 11%, while the ratio is equal to 0.88.

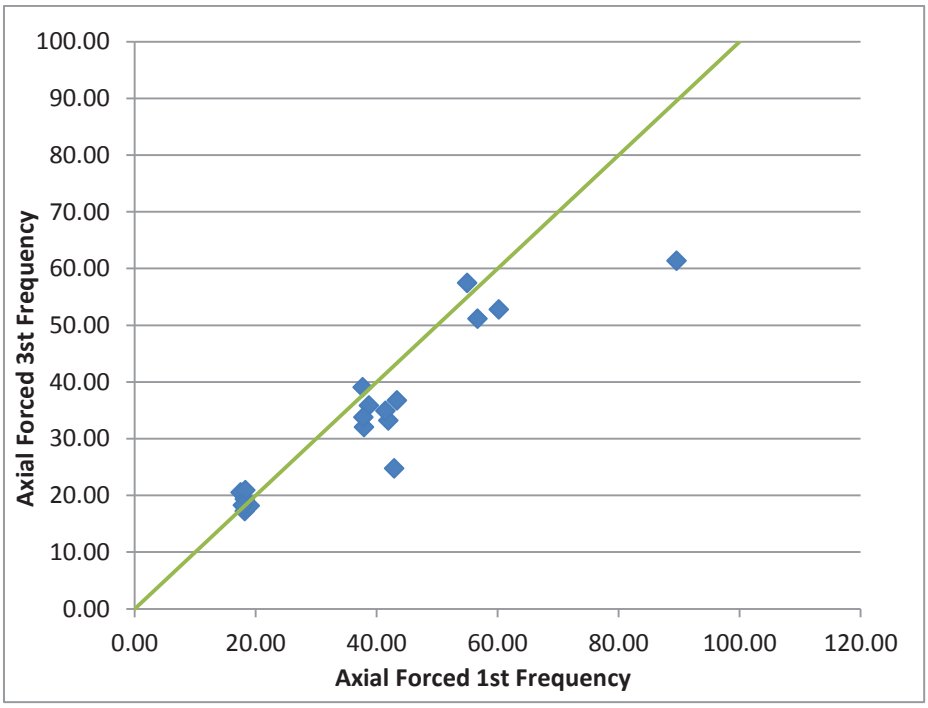

Fig. 80 – Comparison between the Axial force estimation with the first and third frequency.

Nº of analysis	Identification	First mode	Third mode	
		N Tullini	***N Tullini***	Error [%]
1	0KN_PP	1.556	***0.19***	-
2	20KN_PP	20.62	**-**	-
3	20KN_FF	17.51	***20.53***	-1%
4	20KN_IC1	18.20	***19.36***	-8%

5	20KN_IC2	18.29	***20.93***	5%
6	40KN_PP	37.69	***39.07***	-2%
7	40KN_FF	41.93	***33.22***	-17%
8	40KN_IC1	38.72	***35.86***	-10%
9	40KN_IC2	37.78	**-**	-
10	60KN_PP	60.20	***52.80***	-12%
11	TullNew_40KN_PP	42.90	***24.78***	-38%
12	TullNew_60KN_PP	54.96	***57.47***	-4%
13	TullNew_60KN_FF	56.67	***51.17***	-15%
14	TullNew_80KN_PP	89.59	***61.38***	-23%
15	TullNew_80KN_FF	61.32	**-**	-
16	Tull_20KN_PIC1	18.20	***17.25***	-15%
17	Tull_20KN_PIC2	18.39	***17.75***	-12%
18	Tull_20KN_PIC3	19.02	***18.19***	-11%
19	Tull_20KN_PIC4	17.88	***18.28***	-11%
20	Tull_40KN_PIC1	43.35	***36.76***	-9%
21	Tull_40KN_PIC2	41.45	***34.92***	-14%
22	Tull_40KN_PIC3	37.91	***32.05***	-20%
23	Tull_40KN_PIC4	37.81	***33.79***	-16%

Table 25 – Result of the analytical model for the third mode.

The results are promising since the coefficient of variation is low, which would mean that in order to verify the validity of the value of axial force obtained by using the first mode shape, the results can be contrasted with the one obtained with the third mode to determine if the values reach are reliable.

In order to prove the validity of the third mode, the result of the FEM model for the third mode was tested.

Nº of analysis	Identification	Results Third Mode [KN]		
		N tullini	Real load Tull	Error [%]
2	Lab Tull 0KN PP	0.087	0	-
4	Lab Tull 0KN FF	0.155	0	-
6	Lab Tull 10KN PP	10.085	10	0.85%
8	Lab Tull 10KN FF	10.162	10	1.62%
10	Lab Tull 20KN PP	19.842	20	-0.79%
12	Lab Tull 20KN FF	20.938	20	4.69%
14	Lab Tull 40KN PP	40.143	40	0.36%
16	Lab Tull 40KN FF	40.139	40	0.35%
18	Lab Tull 60KN PP	60.091	60	0.15%
20	Lab Tull 60KN FF	60.195	60	0.33%
22	Lab Tull 80KN PP	80.097	80	0.12%
24	Lab Tull 80KN FF	79.213	80	-0.98%

Table 26 – Results from the analytical model with the third mode of the FEM model

In Fig. 81 it is show the comparison of the curves corresponding to the variables (λ,n) for the first and third mode. The curves validate the correlation found with the analytical model, since the curves for both modes present similar behavior. Again if the utility of this curves are thought for already analyzed ties that only have information on one frequency, independent if is the first or the third, the estimation of the axial force can be achieve with a more reliable and suitable method for tie rods than the wire-rod theory.

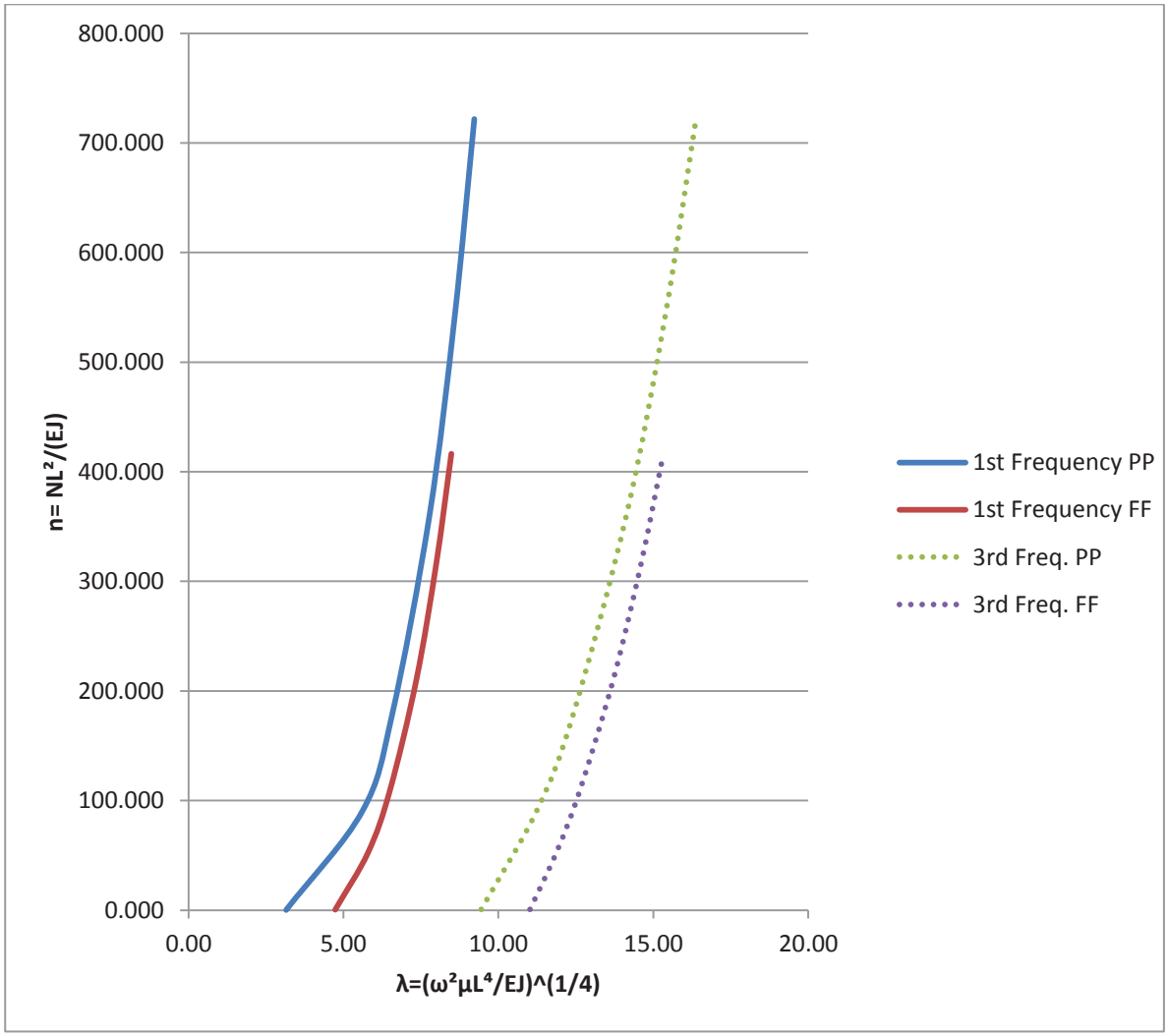

Fig. 81 – λ vs n, comparison for both modes shapes.

6. PROPOSAL AND RECOMMENDATIONS

There are different scenarios in which the need of estimating the tensional state of the tie can be presented. When the estimation demands a high accuracy due to the importance of the elements a combined approach of static and dynamic is highly suggested. However there are cases when the need for an approximate value of the axial force is more than enough.
For these latter cases the performance of a static method that would allow the exact definition of the boundary conditions is not performed due to its complexity and time consumption. And the situation can even be improved with a simpler method.

Bearing in mind this last scenario, the analysis of the results for two different modes shapes, first and third, led to the evaluation of the result considering a hypothetical situation where only two accelerometers were used. The methodology is of great interest since the reduction of one accelerometer would signify a reduction of the time of set up and performance of the test. This economic method is desired for onsite campaigns because of the problems previously explain that are being faced during the measurements.

For this situation, it has to be assumed that the tie is symmetrical, and so are its boundary conditions so the sensor can be located in the middle and in one of the quarters.
To prove the validity of such hypothesis, the information acquired and processed for all the tests carried out on the laboratory were taking into account, being of higher interest the intermediate condition where the symmetry hypothesis is not accurate at all due to the fact that for this situations the plates were fasten and released manually with no control on the force subjected.

The procedure was carried out for the first and third mode shape and for each case it was considered both symmetries, considering the sensors located in the middle and in position v_1 and later in the middle and in position v_3. In total 58 cases were analyzed.
The analytical model was performed for each case considering the symmetry hypothesis and the results were compared with the real load measured during the testing.

ID	Mode Shape	Symmetry	Tullini [KN]	Real Load	Error [%]
Lab 0KN PP	First	v_1	1.09	1.56	-30%
Lab 0KN PP	First	v_3	2.04		31%
Lab 20KN PP	First	v_1	19.04	20.10	-5%
Lab 20KN PP	First	v_3	22.36		11%
Lab 20KN FF	First	v_1	18.13	20.80	-13%
Lab 20KN FF	First	v_3	16.96		-18%
Lab 20KN IC1	First	v_1	19.85	21.06	-6%

Lab 20KN IC1	First	v_3	16.74		-21%
Lab 20KN IC2	First	v_1	19.31	20.01	-3%
Lab 20KN IC2	First	v_3	17.30		-14%
Lab 40KN PP	First	v_1	41.04	40.07	2%
Lab 40KN PP	First	v_3	44.79		12%
Lab 40KN FF	First	v_1	43.42	40.06	8%
Lab 40KN FF	First	v_3	40.48		1%
Lab 40KN IC1	First	v_1	45.60	40.03	14%
Lab 40KN IC1	First	v_3	33.17		-17%
Lab 40KN IC2	First	v_1	40.35	40.21	0.4%
Lab 40KN IC2	First	v_3	35.44		-12%
Lab 60KN PP	First	v_1	53.59	60.03	-11%
Lab 60KN PP	First	v_3	56.36		-6%
Lab 60KN FF	First	v_1	56.36	60.10	-6%
Lab 60KN FF	First	v_3	57.11		-5%
Lab 80KN PP	First	v_1	87.23	80.05	9%
Lab 80KN PP	First	v_3	91.99		15%
Lab 80KN FF	First	v_1	70.92	79.20	-10%
Lab 80KN FF	First	v_3	70.92		-10%

Table 27 – Results of the analytical model with symmetry hypothesis for the loads steps for PP and FF condition and first mode shape.

ID	Mode Shape	Symmetry	Tullini [KN]	Real Load	Error [%]
Lab 20KN PIC1	First	v_1	18.09	20.40	-11%
Lab 20KN PIC1	First	v_3	18.30		-10%
Lab 20KN PIC2	First	v_1	18.19	20.10	-10%
Lab 20KN PIC2	First	v_3	18.58		-8%
Lab 20KN PIC3	First	v_1	18.61	20.48	-9%
Lab 20KN PIC3	First	v_3	19.40		-5%
Lab 20KN PIC4	First	v_1	22.44	20.46	10%
Lab 20KN PIC4	First	v_3	23.82		16%
Lab 40KN PIC1	First	v_1	38.82	40.42	-4%
Lab 40KN PIC1	First	v_3	43.77		8%
Lab 40KN PIC2	First	v_1	41.15	40.40	2%
Lab 40KN PIC2	First	v_3	41.71		3%
Lab 40KN PIC3	First	v_1	37.75	40.25	-6%

Lab 40KN PIC3	First	v_3	37.95		-6%
Lab 40KN PIC4	First	v_1	37.26	40.16	-7%
Lab 40KN PIC4	First	v_3	38.42		-4%
Lab 20KN PIC1	Third	v_1	17.37	20.40	-15%
Lab 20KN PIC1	Third	v_3	17.11		-16%
Lab 20KN PIC2	Third	v_1	17.78	20.10	-12%
Lab 20KN PIC2	Third	v_3	17.72		-12%
Lab 20KN PIC3	Third	v_1	18.08	20.48	-12%
Lab 20KN PIC3	Third	v_3	18.30		-11%
Lab 20KN PIC4	Third	v_1	17.77	20.46	-13%
Lab 20KN PIC4	Third	v_3	17.67		-14%
Lab 40KN PIC1	Third	v_1	37.16	40.42	-8%
Lab 40KN PIC1	Third	v_3	36.36		-10%
Lab 40KN PIC2	Third	v_1	35.28	40.40	-13%
Lab 40KN PIC2	Third	v_3	34.60		-14%
Lab 40KN PIC3	Third	v_1	31.36	40.25	-22%
Lab 40KN PIC3	Third	v_3	32.75		-19%
Lab 40KN PIC4	Third	v_1	33.77	40.16	-16%
Lab 40KN PIC4	Third	v_3	33.83		-16%

Table 28 - Results of the analytical model with symmetry hypothesis for the loads steps for intermediate boundary conditions and first and third mode shape.

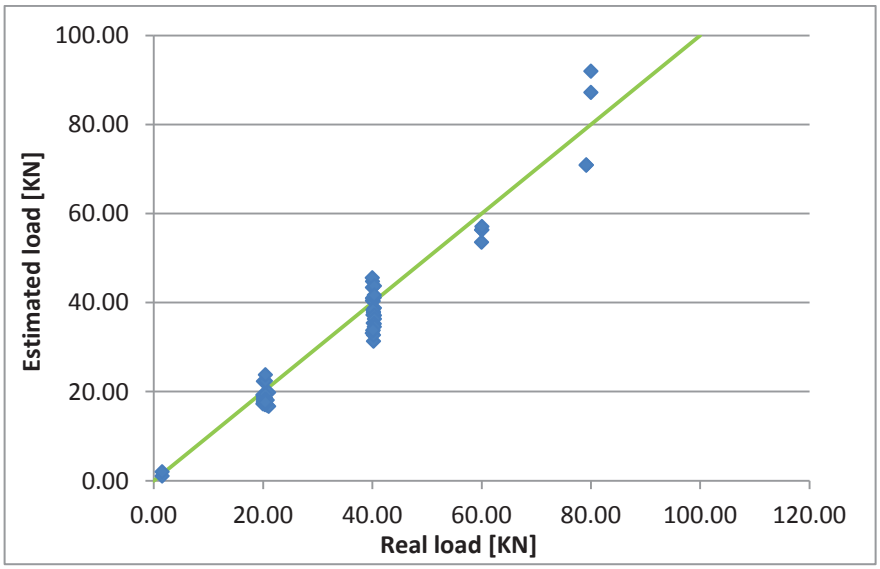

Fig. 82 – Correlation between the real load and the estimation with the symmetry hypothesis

The error between the axial force obtained, assuming a symmetric tie, and the real one measured during the laboratory tests present encouraging results since the coefficient of variation is of less than 12% (see Fig. 82) with an average ratio of 0.94, and in the cases of the intermediate conditions, which are the one most interesting to evaluate, the results for the first mode shape are into the admissible error for onsite campaigns. In the cases of the third mode, the error showed to be higher but should be considered that the error is the cumulative error present on the estimation of the axial force plus the addition of the symmetry condition.

Moreover, to increase the sample of cases were also analyzed the onsite tests carried out in [14], checking the symmetry measured in these real cases. In Fig. 83 are displayed the relation between the two position of the symmetrical accelerometers. The dispersion shown was also reflected in some of the results. However if it is considered that with three accelerometers the result obtained is not accurate and presents some anomalies, it can be considered that the use of only two accelerometers which would signify a reduction of the time consumption and a simpler set up without losing any accuracy at all.

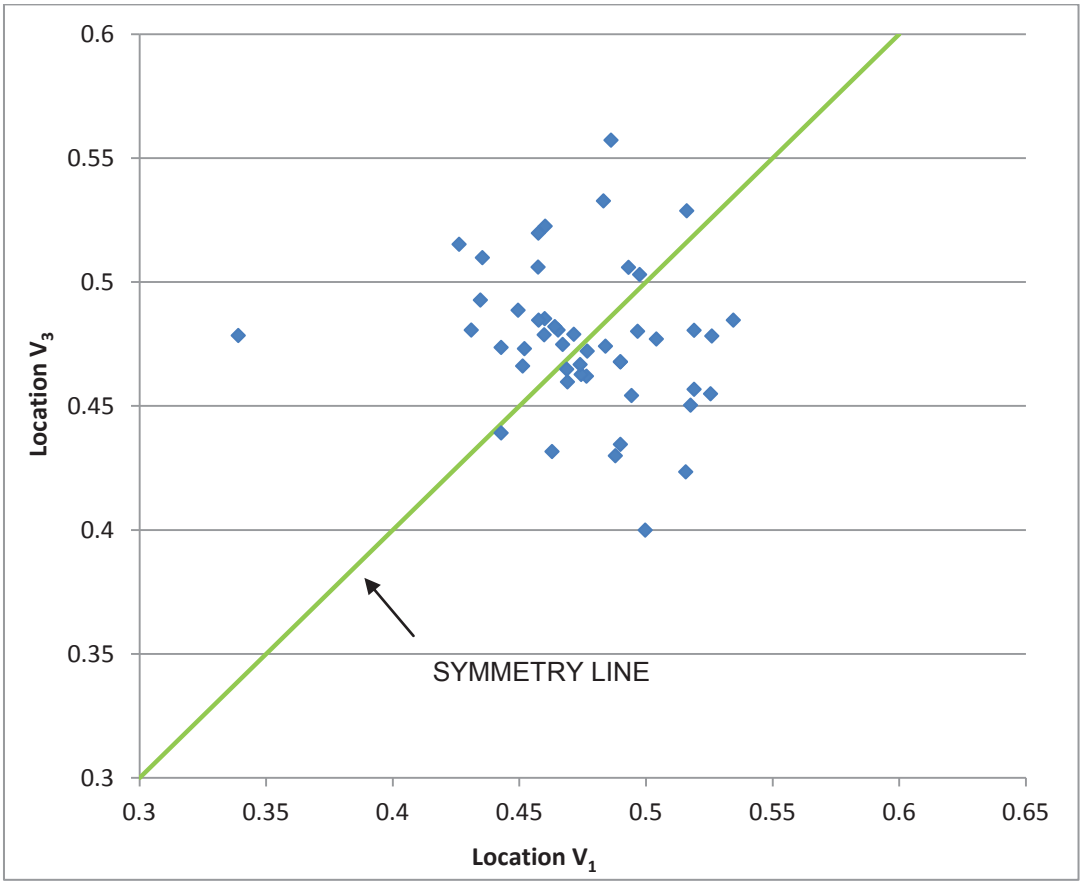

Fig. 83 – Comparison of v1 and v3 for the symmetry hypothesis, case studies [14]

Considering the aforementioned cases and considerations, and bearing in mind the aim of proposing a simpler method that would led to a more expeditious and economic set up and testing for cases were the number of ties to test is high or the location of the ties is not of easy access, the results here obtained showed that the possibility of considering a symmetry hypothesis and reducing the sensor to two is feasible.

In Fig. 84 are exposed, in the seek of comparison, the method analyzed throughout this thesis. The Charts proposed by Luong has a dispersion of results due to the extremes boundary conditions on which is based the theory analyzed.

The dynamic procedure of Tullini and the methodology propose in this chapter showed just slight difference between each other, and can be considered much more accurate than the other method studied. The coefficient of variation of the values obtained with the method of Tullini is of 9% with a average ratio of 0.98, while for the proposed method is of less than 12% with an average ratio of 0.94.

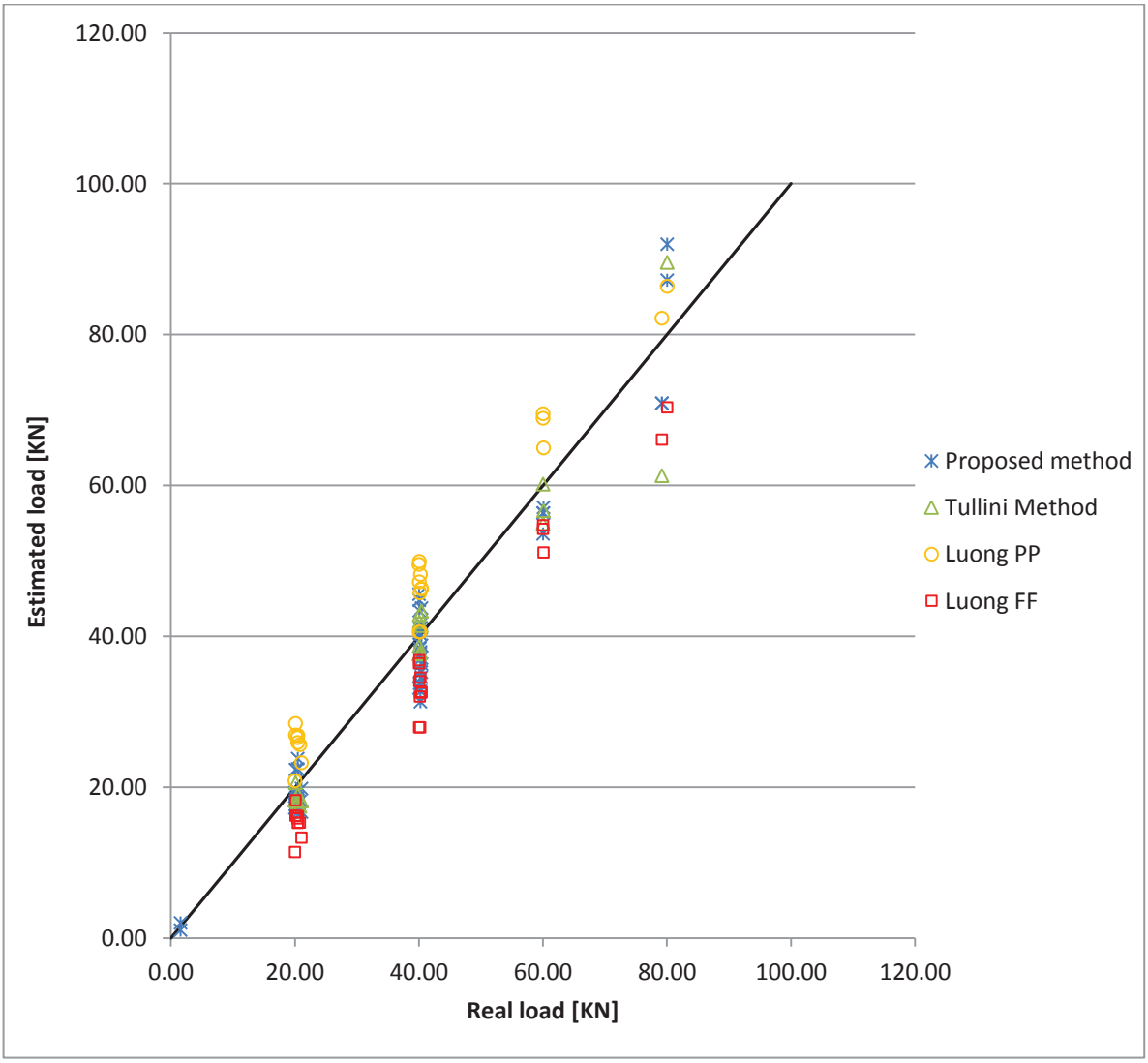

Fig. 84 – Comparison of the dispersion and accuracy between the methodologies.

7. CONCLUSIONS AND FURTHER WORK.

The aim of this thesis was the improvement of the NDT methodology to estimate on site the current axial force of historical ties. The main goal was the testing of an expeditious and reliable method, which would allow a fast set up and acquisition with reliable results.

The studies were carried out in the framework of an ongoing investigation in the University of Padova. Firstly was carried out a compilation of the state of art of the different methodologies, static and dynamic, developed so far. Moreover, the research was based on a database which allows a parametric analysis to design the lab test that it has been performed in the framework of this thesis.

From the literature analyzed, several dynamic methods were tested with examples of already analyzed ties, from the Database [14] built in the early stages of the research with the aim of studying the parameters that were influencing the dynamic response of ties. The conclusion is that the more accurate method was the technique developed by Tullini [9]. The method has the advantage of being simple on its numerical calculation and on its set up to acquire the data. However it has shown some sensitivity regarding the positioning of the sensor, hence regarding the length taken to perform the test.

The sensitivity showed by the method led us to the analysis of the main problems that must be faced when an onsite test has to be carried out. During the laboratory tests these problems: length, boundary condition, position of sensors, was recognized and some of them were solved while others helped to reach some conclusions.

The methodology used to assess the dynamic technique selected was compound of three stages: Experimental campaign (data acquisition and processing) followed by analytical model with which the axial force was estimated, using as input the experimental data, and finally a FEM model calibrated with the real input of the experimental data, and correlated with the numerical model by means of a MAC correlation.

The laboratory raised awareness of the importance of two significant factors: the definition of the boundary conditions, hypothesis that has great impact on the estimation of the axial force and the effective length of the tie, which as a consequence on the position of the sensor to record the response of the tie.

The first issue has to be assessed properly on site in order to reduce the risk of obtained bias results, which would lead to an overestimation of the real value or underestimation of it, according to the end support hypothesis made. However, the static test has proved to be good and calibration method for evaluating of the stiffness of the boundary conditions.

As for the length, measurements were done for different conditions with different lengths and it was qualitatively concluded that even though the use of effective length improves the accuracy of the estimation, the use of the free length induces some errors in the estimation, which are small and acceptable. Even though these error must be borne in mind when assessing a tie.

Other problem that the laboratory tests revealed was regarding the acquisition process; the positioning of the accelerometers depends on the real length considered, and in addition it influences the accuracy of the data acquisition. It was observed during the campaign the uncoupling of the frequency in all the sensors led to a lower accuracy on the estimation of the axial force.
Once the response of the tie was processed the analytical model was performed to estimate the value of the axial force and it was compared with the real one measured during the testing. The method of Tullini, proved to be accurate and reliable with a coefficient of variation of less than 9%.
Finally the last stage was the FEM model, which was calibrated with the experimental results, and tested for static and dynamic behaviour to reach the conclusion of it accuracy and reliability to be used to simulate further cases of load and boundary condition increasing the spectrum of analyzed cases.

The wire-rod theory has been used in the past to estimate the axial force of the tie, and is still being used due to the fact that only requires one accelerometer to determine the first frequency. However such theory is based on the neglect of the flexural stiffness of the tie, which in most of the cases is not viable hypothesis. The later methodologies developed in the last few years presents a more accurate and reliable hypothesis regarding the influence of the stiffness but demands more experimental effort since they require, as the case of Tullini, three sensors to determine the mode shapes and frequencies.
The proposed methodology of Section 6, which is based on the Tullini Methodology, makes use of only two sensors, reducing the experimental effort when contrasted with the method of Tullini.
If it is considered the experimental effort involved in setting a second sensor and its positive impact in the estimation of the axial force, the proposed methodology reveals a better prospective.
Furthermore, if the same considerations are made to compare the set up of Tullini Method and its results with the characteristic of the proposed method, it can be suggested that the reduction of one sensor, with all its implication, and it corresponding small increase of the coefficient of variation, just 3%, would represent a simpler, but still accurate, method to be carried on site.
The major advantage when considering the hypothesis of geometrical symmetry and boundary conditions symmetry is that the problem now is no longer related to the definition of boundary conditions, but to the definition of the effective length that is going to be used. It can be said that the error committed is move from the error of the boundary conditions determination to the assumption of the length and for the latter case the error is much smaller.

Despite the good outcomes got during the laboratory test and the analysis of the methodology proposed, further work should be carried out, in order to test ties with other geometrical characteristics, shape of the cross-section and length. To completely validate the reliability of the method proposed, further research should be carried out on laboratory and by means of FEM analysis, to determine the response of non symmetrical boundary conditions such as pinned-clamped conditions and its sensitivity when condition of large asymmetries has to be tested. For this goal can

be said that during this work the regulation device of the laboratory set up was improved to simulate more boundary conditions. Moreover, the finite element model was calibrated with the experimental data from the static and dynamic method, so its reponse is of high accuracy and reliability, which in addition to the improved set up would allow further work on the symmetry hypothesis of the method proposed.

REFERENCES

1. **Facchini, L.- Galano, L.- Vignoli, A.** *Experimental analysis of two methods for estimating in-situ tensile force in tie-rods.* Florence : s.n., 2003.

2. **Heyman, J.** *The stone skeleton: Structural Engineering of Masonry Architecture.* Cambridge : Cambridge University Press, 1995.

3. **Pisani, M.** *Consolidamneto delle strutture.* Milano : Ulrico Hoepli , 2008.

4. **Astrua, G.** *Manuale completo del capomastro assistente edile.* Milano : Ulrico Hoepli, 1953.

5. **Briccoli Bati, S.- Tonietti, U.** *Experimental Methods for estimating in situ tensile force in tie-rods.* Florence : Journal of Engineering Mechanics, 2001.

6. **Dardano, D.- Miranda J.C.- Persichetti, B.- Valvo, P.** *Un metodo per la determinazione del tiro nelle catene mediante identificazione dinamica.* Pisa : A.I.C.E Consulting S.r.l, 2005.

7. **Lagomarsino, S.- Claderini, C.** *The dynamical identification of the tensile force in ancient tie-rods.* Genova : Elsevier, 2005.

8. **Park, S. , Choi, S et al.** *Identification of the tensile force in high-tension bars using modal sensitivities.* Republic of Korea : Elsevier, 2006.

9. **Tullini, N. - Lauderio, F.** *Dynamic identification of beam axial loads using one flexural mode shape.* Ferrara, Italy : Elsevier, 2008.

10. **Amabili, M.- Carra, S.- Collini,L.- Garziera, R.- Panno, A.** *Estimation of tensile force in tie-rods using a frequency-based identification method.* Parma, Italy : Journal of Sound and Vibration, 2010.

11. **Luong, T.** *Identification of the tensile force in tie-rods using modal analysis tests.* University of Minho, Guimaraes, Portugal : SAHC Master, 2010.

12. **Rebecci, G.- Tullini, N.- Laudiero, F.** *Estimate of the axial force in slender beams with unknown boundary conditions using one flexural mode shape.* Ferrara, Italy : Elsevier, 2013.

13. **Mastrodicasa, S.** *Dissesti statici delle strutture edilizie.* Milano : Ulric Hoepli, 1981.

14. **Mosca, L.** *Metodi Dinamici sperimentali e numerici per la stima dello sforzo assiale in catene esistenti.* Padova, Italy : Università degli Studi di Padova, 2015.

15. **Basto, C.- Kyriakou, M.- Salat, Z.- Zhou H.** *Integrated Project: Castel San Pietro.* Padova : SAHC Master, 2015.

16. **A/S, Structural Vibration Solutions.** ARTeMIS Extractor Manual, Release 4.0.

17. **BV, TNO DIANA.** User's Manual release 9.6 FX+ for DIANA. Delf, The Netherlands : s.n., 2014.

18. **Allemang, R.** *The Modal Assurance Criterion - Twenty years of use and Abuse.* University of Cincinnati, Cincinnati, Ohio : Journal USound and Vibration, 2003.

19. National Instruments Measurement Fundamentals. [Online] 04 November 2014. [Cited: 09 Junio 2015.] http://www.ni.com/white-paper/3642/en/.

20. **Carbonara, G.** *Trattato di restauro architettonico.* Torino : UTET, 1996.

21. **Garziera, L Collini - R.** *A vibration-based method for the evaluation of axial load in tie-rods: two main case studies.* Parma, Italy : University of Parma, Department of Industrial Engineering, 2013.

22. **Bruschi, G - Nardoni, G.** Experimental stress analysis of historical forged tie beams of archaeological museum of Spina in Ferrara, Italy. *Structural Analysis of historical Constructions Vol.1.* London : Taylor & Francis , 2005, pp. 489-497.

23. **Collini, L. Garziera, R.** *A vibration-based method for the evaluation of axial load in tie-rods: Two main case studies.* Ouro Preto, Brazil : Experimental Vibration Analysis for Civil Engineering Structures 2013, 2013.